The visual opsins of the starry flounder (*Platichthys stellatus*), a new model for studying the physiological and molecular basis of fish vision and light sensitivity.

by

Thomas Iwanicki
BSc, University of Victoria, 2013

A Thesis Submitted in Partial Fulfillment
of the Requirements for the Degree of

MASTER OF SCIENCE

in the Department of Biology

Supervisory Committee

The visual opsins of the starry flounder (*Platichthys stellatus*), a new model for studying the physiological and molecular basis of fish vision and light sensitivity.

by

Thomas Iwanicki
BSc, Univeristy of Victoria, 2013

Supervisory Committee

Dr. John S. Taylor, the Department of Biology
Supervisor

Dr. Robert L. Chow, the Department of Biology
Departmental Member

Dr. John F. Dower, the Department of Biology
Departmental Member

Dr. Jürgen Ehlting, the Department of Biology
Departmental Member

Abstract

Supervisory Committee

Dr. John S. Taylor, the Department of Biology
Supervisor

Dr. Robert L. Chow, the Department of Biology
Departmental Member

Dr. John F. Dower, the Department of Biology
Departmental Member

Dr. Jürgen Ehlting, the Department of Biology
Departmental Member

Ray-finned fish from a diversity of distantly related lineages have remarkably large visual opsin repertoires. Starry flounder (*Platichthys stellatus*) development, morphology, life history, and behavior make this species especially suitable for experiments designed to determine why fish have so many opsins. Human and bird colour vision uses three and five opsins, respectively. Fish often have many more opsins. We sequenced an eye transcriptome to determine the starry flounder opsin repertoire, and used high performance liquid chromatography to determine the chromophore content of the retina. We found eight visual opsins that utilize only 11-*cis*-retinal (vitamin A1). This species' entire visual opsin toolkit appears to be functional. The number of distinct cone and rod cell absorbance profiles determined using microspectrophotomery are consistent with the number of visual opsins in the transcriptome. RH2 transcripts were more abundant and SWS1 and SWS2 transcripts were less abundant in the dorsal retina, where cone density was highest, outer segments the longest, and where we observed double cones with outer segments that differed in their wavelength of maximum absorbance. Regions of fish

retinas appear to be specialized and I predict that this fine-tuning is enhanced by photoreceptor plasticity and opsin gene duplication and divergence.

Studies that compare opsin expression patterns among individuals, populations, or species typically assume that the differences observed influence vision. Direct connections between opsin expression and quantitative behaviours are rare. This thesis aimed to test whether varying opsin expression affects vision by modifying opsin expression and characterizing vision in starry flounder. We held starry flounder in aquaria exposed to either broad spectrum sunlight or green-filtered light. We tested vision by quantifying the visually-mediated camouflage response and we measured opsin expression using digital-PCR. Granularity analysis of photographs of the camouflage response revealed higher overall pattern energy at each of the seven spatial frequency bands in fish exposed to broad spectrum sunlight compared to the green-filtered fish. However, no statistical difference in typical measurements of pattern or contrast (e.g., maximum filter size, the standard deviation of pattern energy, and the proportional power) was observed between the two groups. Opsin expression was different between fish held in the green light environment compared to those exposed to broad spectrum light. SWS1 (UV sensitive) and SWS2B (blue sensitive) were significantly down regulated in response to the green light environment. Surprisingly, this difference was lost after only three hours under a white LED light, suggesting rapid changes in opsin expression in response to the light environment. We found tantalizing, albeit not statistically significant evidence that fish with higher expression of UV- and blue-wavelength sensitive opsins could see more contrast in colour on blue-green checkerboards.

Table of Contents

List of Tables

List of Figures

Acknowledgments

I would like to thank my supervisor and mentor, John Taylor, for his enthusiasm, support, and guidance throughout my training. He was always available to provide insight, critique, or just have a conversation about motorcycles. He was my proverbial spring board, propelling me to the next stage in my career, and for that I am eternally grateful. I would also like to thank my committee members, Bob Chow, John Dower, and Jürgen Ehlting, for their valuable insight throughout this process.

I would be remiss not to mention the wide variety of people who contributed, in one way or another, to the final version of this thesis. Science is a collaborative effort, and through the technical skills, philosophical discussions, friendship, and emotional support of so many people, I have achieved so much.

My dearest friends, all of whom have put up with my bad jokes and child-like pranks, and have enriched my life beyond measure: Will, Faron, and Marina Duguid, Cameron Freshwater, James Robinson, Sam Ferguson, Kate Donaleshen, Mauricio Carrasquilla Henao, Jimena Gonzales Lema, Kieran Falk, Lindsey Welgush, and Christopher McMullen.

Other friends and collaborators who have helped me learn new techniques, suss out problems, and/or construct equipment: Iñigo Novales Flamarique, Cliff Haman, John Leblanc, Terrie Finston, Koung Le, Marie Vance, David Minkley, Finn Hamilton, Ben Sutherland, Scott Scholz, Mike Delsey, Ronnie Duke, Gordon Lyall, Norm Johnson, and Dr. Belaid Moa (WestGrid and Compute Canada - Calcul Canada).

Taylor lab mates (past and present): Lara Puetz, Frances Stewart, Emily Morris, Felix Beaudry, Diana Rennison, Chelsea Reimer, Matt Burke, Chase Crisfield, Amy Liu, Althea Wong, Emma Pascoe, Jennifer Borchert, and Andrea Reyes.

The Novales Flamarique, Ehlting, Hintz, Helbing, Howard, Ausio, and Willerth labs generously donated their time and equipment for the different assays I ran.

Finally, a heartfelt thanks to Donna Boyko and Larissa, Shawna, Annie, and Ken Arthur for accepting me into their family, and continually encouraging me as Holly – their beautiful sister and daughter – moves with me to faraway places.

Dedication

I dedicate this thesis to my family: Jen, Dave, Joe, Theresa, Becky, and Amy. Their love and unwavering support has afforded me the privilege to turn my passion for science into a career. And to Holly, the light of my life.

Chapter 1 – General introduction

Background

Motivation for this study

In the closing paragraph of *The Origin of Species*, Darwin (1859) asked the reader to consider a tangled bank:

> *"…clothed with many plants of many kinds, with birds singing on the bushes, with various insects flitting about, and with worms crawling through the damp earth, and to reflect that these elaborately constructed forms, so different from each other, and dependent on each other in so complex a manner, have all been produced by laws acting around us."*

A proverbial symphony of plants and animals, struggling to survive, with evolutionary origins so humble. Darwin's point was that evolution, guided by simple rules, resulted in incredible complexity. Of all the complex sensory systems that evolution has produced, few are more striking than vision. The fundamental molecular unit for vision is the opsin. Opsins are membrane-bound G-protein coupled receptors (GPCRs) that are light sensitive when in complex with their ligand, a vitamin-A derived chromophore (Yokoyama 1997), forming visual pigments (Hárosi 1994). The ability to detect and discriminate among different wavelengths of light depends on the diversity of opsins present in the photoreceptors (rods and cones) of the retina. In humans the *RHO* gene encodes rhodopsin, which is expressed in rods, and *OPN1SW*, *OPN1MW* and *OPN1LW* encode short-wavelength sensitive, middle-wavelength sensitive, and long-wavelength sensitive opsins in cones. Although many other opsins (e.g., melanopsin, neuropsin, teleost multi-

tissue opsin) are expressed in visual tissues (Davies et al., 2015; Beaudry, Iwanicki et al., *submitted*), we use the term 'visual opsin' to refer to the five opsin subfamilies commonly associated with vertebrate rods and cones (i.e., RH1, RH2, LWS, SWS1, and SWS2). Mutations that reduce the number of visual opsins or sequence diversity among opsins leads to colour vision deficiencies (Yokoyama 1997; Jacobs et al., 1996; Jacobs, 2013).

Colour vision is mediated through the opponent process, a theory first proposed by Hering in 1878. In humans, the signals from the cones are binned into three channels (i.e., yellow minus blue, red minus green, and white minus black) and hue is detected by the ratio of the yellow-blue and red-green channels (Hurvich and Jameson, 1957). The red-green channel begins with red and green cones synapsing with red and green-associated bipolar cells, which then synapse with red-green retinal ganglion cells. The blue-yellow pathway begins with red and green cones synapsing to the same bipolar cell (i.e., yellow), and the blue cones synapsing with another bipolar cell (i.e., blue). The blue and yellow bipolar cells then interact with the blue-yellow retinal ganglion cell. The signal-to-noise ratio is increased through lateral inhibition of the bipolar cells by horizontal cells (Gegenfurtner and Sharpe, 2001). Human colour vision is mediated by three opsins, and as described above, possessing fewer than three opsins leads to colour vision deficiencies; the advantages, if any exist, to possessing four or more opsins is not well described.

Teleost fish have, in general, more opsins than other vertebrates (Rennison et al., 2012; Davies et al., 2015). For the visual opsins this is largely the result of lineage-specific tandem duplications (Rennison et al., 2012). The adaptive value of large opsin gene

repertoires is unclear. Improved wavelength discrimination is a possible explanation. Primates, with three cone opsins (trichromatic), have better wavelength discrimination than mammals with two cone opsins (dichromatic) (Melin et al., 2009; Mancuso et al., 2009). White-faced capuchins are either dichromats or trichromats, and trichromats identify conspicuously coloured ripe figs faster than dichromats (Melin et al., 2009). Although the advantage trichromatic capuchins have over dichromats was slight, and dichromatic capuchins appeared to compensate vision with olfaction when identifying the cryptic figs. Sensory plasticity – or compensation – has also been observed in guppies (Chapman et al., 2010). Guppies reared under higher light levels than conspecifics performed better in a visual-only behavioural assay, although the influence of light on opsin expression was not measured. Adding an opsin to dichromatic squirrel monkeys and mice through gene therapy can produce behavioural responses indicative of trichromatic vision (Mancuso et al., 2009; Jacobs et al., 1999; Jacobs et al., 2007). However, chickens have four cone opsins but do not perform any better than humans in wavelength discrimination tests (Olsson et al., 2015). As well, some stomatopod crustaceans have 12 different photoreceptors, but perform poorly in colour discrimination tasks; the difference between two wavelengths had to exceed 12-25 nm before stomatopods could successfully discriminate between them (Thoen et al., 2014). With three cone opsins, humans can discriminate between wavelengths of light that differ by as little as 0.25 nanometers in some cases (Mollon et al., 1990) to a few nanometers in others (Pokorny and Smith, 1970; Zhaoping et al., 2011). Thus, repertoires of more than four opsins, which are common in fish, are not necessarily adaptations for greater wavelength discrimination, and may be used for other types of vision.

The quality of light a fish is exposed to depends on the physical properties of the water (e.g., depth, turbidity) and the light itself (e.g., intensity, hue). Newton (1704) discovered that colour was a physical property of light. Sunlight enters the atmosphere and is subject to Raleigh Scattering (Raleigh, 1871); photons of light strike and scatter off of molecules suspended in the air and water. Small molecules scatter photons with short wavelengths, and that is why the sky appears blue. Large molecules, like water droplets in a cloud, are "spectrally flat" and scatter all wavelengths of light, causing clouds to appear white (Lythgoe, 1979). In the ocean, Raleigh scattering influences the light that is available above (downwelling), horizontally (sidewelling), and below (upwelling) any given position in the water column. Downwelling light is at least three to four times as intense as upwelling or sidewelling light. Furthermore, short wavelengths are more abundant in downwelling light (Figure 1, from Novales Flamarique and Hawryshyn, 1993). Coastal waters are typically more turbid, containing dissolved molecules larger in size compared to the open ocean. This results in coastal waters being more green-shifted than the open ocean. Therefore, different regions of the retina will be exposed to different light spectra depending on line of sight.

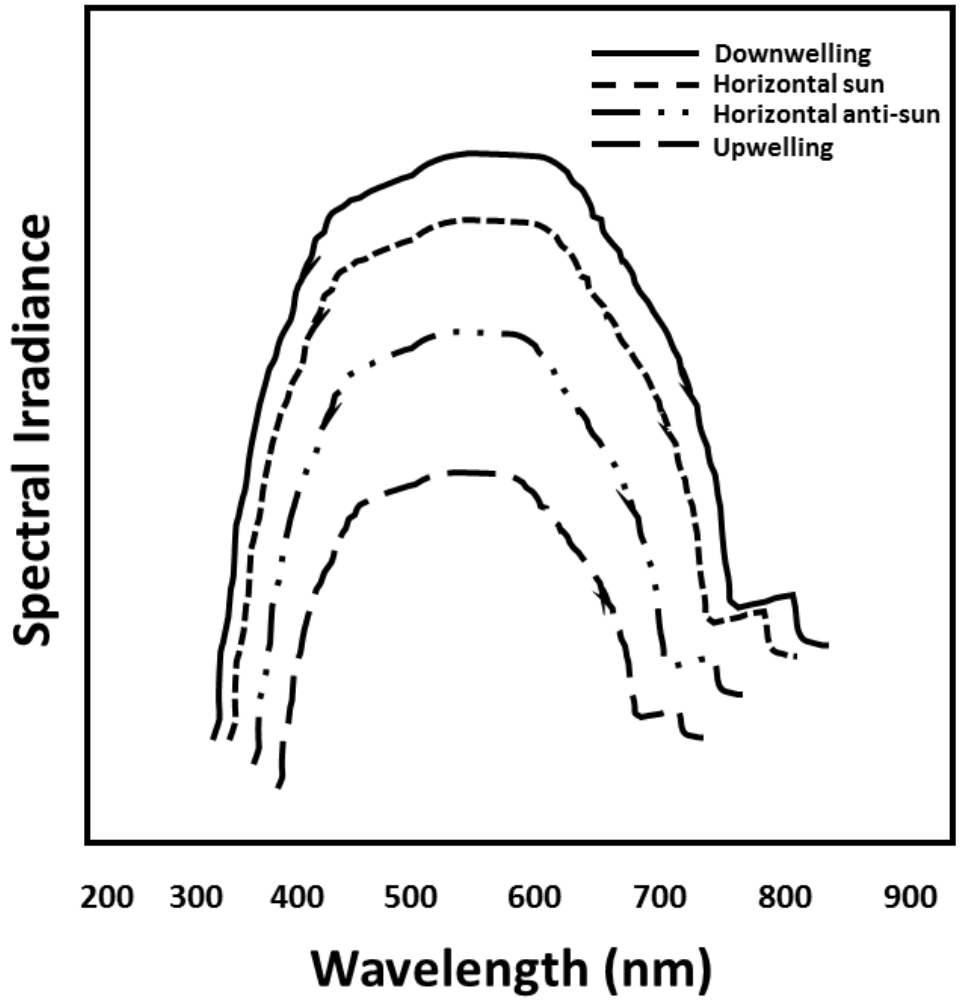

Figure 1: Spectral irradiance profiles of water. Upwelling light corresponds to light travelling from the bottom upwards and downwelling from the surface downwards; horizontal sun is light horizontal to the surface directed away from the sun and horizontal anti-sun is light horizontal to the surface directed towards the sun. (Figure adapted from Novales Flamarique and Hawryshyn 1993).

Spectral tuning of the retina

It is possible that large opsin repertoires convey greater plasticity to optimize vision in different light environments. A subset of a large repertoire may be used in different light

environments or in different regions of the retina. Data from multiple species, including Lake Malawi cichlids (Parry et al., 2005; Dalton et al., 2015), the dusky dottyback (Cortesi et al., 2015), rainbow trout (Cheng and Novales Flamarique, 2007), guppy (Sakai et al., 2016), and bluefin killifish (Fuller and Claricoates, 2011) show differential expression of opsins with varying light environment that presumably enhances some aspect of visual function. As in salmonid fishes (Cheng et al., 2006) and flatfishes (Evans et al., 1993), changes in opsin expression may occur gradually as a function of ontogeny and changing habitats during life history migrations. Pre-metamorphic winter flounder have a cone-only retina. Adult winter flounder, by contrast, have rods, single cones, and double cones. The wavelength of maximum absorbance (λ_{max}) in pre-metamorphic cones differs from the adult cones, indicating a switch in opsin expression following metamorphosis (Evans et al., 1993). Changes in opsin expression may occur rapidly, as observed over a period of days following spectral manipulations in laboratory settings (Fuller and Claricoates, 2011; Dalton et al., 2015).

Opsin expression can further involve differential expression within the retina. For instance, humans and other primates lack S cones in the fovea (Ahnelt et al., 1987; Hagstrom et al., 1998) and mice have opposing ventro-dorsal retinal gradients of S and M opsin expression (Applebury et al., 2000). Fishes, which often experience a photic environment that changes substantially in intensity and spectral distribution with line of sight, often show intra-retinal variation in opsin expression. Red breast cichlid and guppy retinas vary dorso-ventrally. Longer wavelength cones are found dorsally and shorter wavelength cones are found ventrally in both species (Levine et al., 1979; see review: Temple, 2011). Zebrafish shorter-wavelength subtypes of opsin duplicates are expressed

in the central and dorsal retinas, with longer wavelength opsins in the ventral and peripheral retina (Takechi and Kawamura, 2005). Also, four-eyed fish opsin expression varies within the retina; *Rh2-1* is expressed in the ventral retina and *Lws* in the dorsal retina (Owens et al., 2009). Therefore, intra-retinal variation of opsins may tune regions of the retina to the light available from different directions.

Visual opsins may be functional in tissues other than the eye, which may be enhanced by gene duplication and divergence. In humans, the opsins expressed in the retina are also expressed in the epidermis (Tsutsumi et al., 2009) though their role in this tissue is unknown. It may be that trichromatic vision in humans, or vision mediated by even more opsins in some fish, is an opportune side effect of selection for opsin diversity in other tissues. Karatinocytes are epithelial cells that form a primary barrier against UV damage. Rhodopsin is expressed in normal human karatinocytes and mediates the activity of violet light down-regulating the expression of keratinocyte differentiation markers (Kim et al., 2013).

Our lab surveyed the opsin repertoires of Pacific flatfishes and in our initial survey found five visual opsins. Emily Morris, an honour student, measured expression in cDNA derived from ocular tissue and skin from English sole and petrale sole. Intriguingly, RH2 was expressed in skin from the pigmented (dorsal) and unpigmented (ventral) side of the fish (Morris, *Honours thesis 2013*). Further investigations into the broader function of the opsin gene family is warranted.

Starry flounder as a new model for visual ecology

The starry flounder (*Platichthys stellatus*) shares many characteristics with other models, and additional characteristics make it especially suitable for my investigation into why fish have such large opsin repertoires: morphological transformation during development generating right-sided and left-sided morphotypes (Bergstrom 2007), a life history that exposes it to very different spectral environments (Love 2011), and an active camouflage behaviour that provides a quantifiable estimate of visual performance. This species is easily raised in the lab from hatchery-reared brood-stock (Uljin Marine Hatchery, see: Lee et al., 2003), feeding initially on rotifer cultures and transitioning to commercial feed at approximately 2 g body weight. Starry flounder females reach maturity at approximately three years of age (about 300 mm) and can generate enormous numbers of eggs facilitating transgenic manipulations. Furthermore, it is possible to manipulate the light environment during development. At approximately 24 days post-hatching, starry flounder undergo metamorphosis involving the migration of one eye to the contralateral side, and this changes the retina with respect to its ventral and dorsal orientations (Evans and Fernald 1993). The fish retina can be divided into morphological regions (i.e., dorsal, ventral, nasal, and temporal) (Figure 2). If opsins have specialized expression domains in the eye, then we predict that expression will change spatially during eye migration.

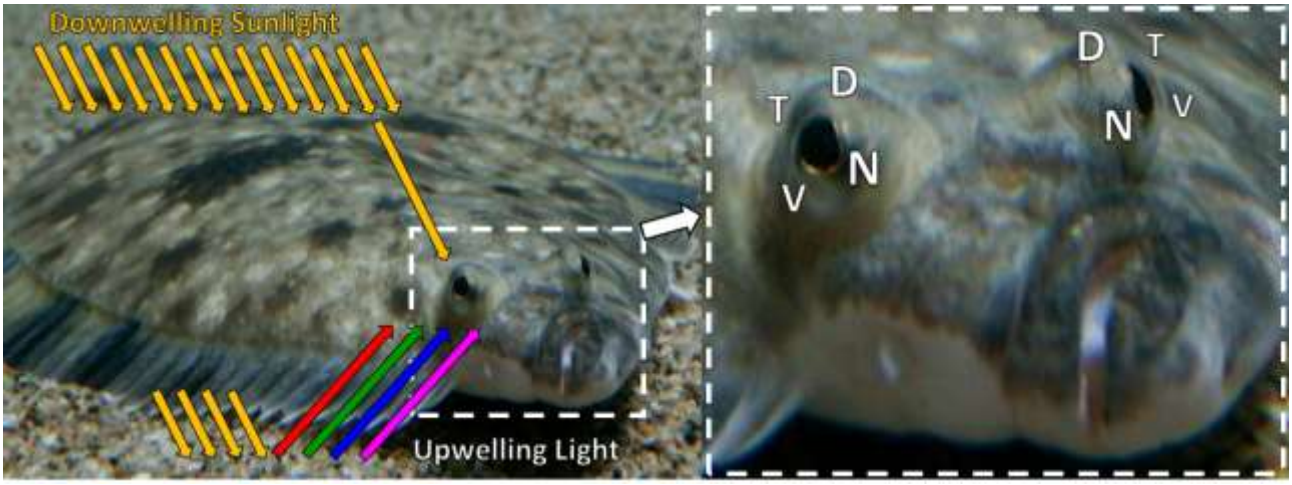

Figure 2: Regions of the starry flounder retina are exposed to different to different light (e.g., downwelling vs. upwelling, left image). The retina is divided into dorsal (**D**), nasal (**N**), ventral (**V**), and temporal (**T**) regions (right image), with the ventral retina exposed to more downwelling light, and the dorsal retina exposed to more upwelling light.

In addition, starry founder have a convenient within species control: While metamorphosis usually leads to right-eyed flatfish (e.g., family Pleuronectidae) or left-eyed flatfish (e.g., family Bothidae), in starry flounder populations from the Pacific Northwest, approximately 50% are dextral (right-eyed) and 50% are sinistral (left eyed). The unusual adult morphology also facilitates testing extra-ocular explanations for the large visual opsin repertoire. Light sensitivity in skin, for example, can be investigated by comparing opsin expression on the ocular and blind sides of the sinistral and dextral morphotypes. Due to the light filtering properties of water, different bodies of water, and even different regions within a body of water, can have very different light profiles (Figure 3). Larval flatfish occupy the light-abundant pelagic zone, and as they mature they descend into a luminosity- and wavelength-restricted spectral environment (Love 2011) making it easy to test hypotheses about changes in opsin expression and the spectral environment in wild-caught fish. Several flatfish species are capable of visually-

mediated active camouflage (Ramachandran et al., 1996). We qualitatively observed this ability in starry flounder collected by beach seine from Willows Beach, Victoria. As mentioned above, this ability provides a rare opportunity to correlate variation in opsin expression with visual performance.

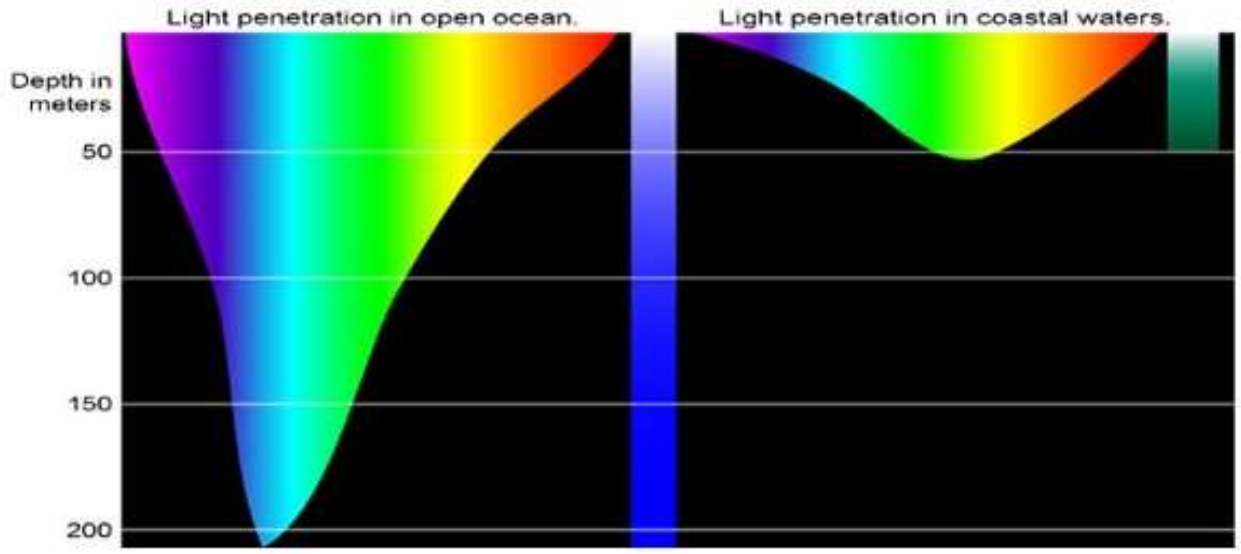

Figure 3: The light filtering properties of the open ocean (left) and turbid, coastal waters (right). Image courtesy of NOAA.

Research objectives

The goal of this research was to test hypotheses addressing the question: why do fish have so many opsins? Inspired in part by Woese (2004), this thesis was designed to pursue science holistically from the outset. Woese argued that biology viewed through a fundamental reductionist lens was an incomplete view, and that 21st century biology's greatest challenge would be to synthesize molecular biology, evolutionary biology, and ecology. To that end, we identified flatfish as an excellent taxonomic group, and the starry flounder as a useful study species. By exploiting the starry flounder's active camouflage, we can study light sensitivity from molecules to animal behaviour.

Chapter 2 outlines the starry flounder visual opsin repertoire, visual pigments, and photoreceptor cells. A whole eye transcriptome was sequenced to discover the full-length coding sequence for all the starry flounder's visual opsins. Fish are known to use two chromophores, vitamin A1 (11-*cis*-retinal) and vitamin A2 (11-*cis*-dehydroretinal). The chromophore usage can influence the wavelength sensitivity of the opsin-chromophore complex, in some cases by as much as 58 nm (Hárosi, 1994). We used high performance liquid chromatography to measure the chromophores present in the juvenile starry flounder retina. We measured *in situ* wavelength of maximum absorbance for the opsin-chromophore complexes using microspectrophotometry (MSP). We measured whole eye and intra-retinal opsin expression in wild-caught starry flounder using digital-PCR. Finally, we used light microscopy to measure the topology of the starry flounder retina (e.g., cone density, outer segment length, mosaic domains).

In the experiment described in chapter 3 we held starry flounder in either broad spectrum or green-filtered light environments for seven weeks. We predicted that opsin expression would change in response to the light, and that those changes would impact vision. Vision was measured using starry flounder's visually-mediated active camouflage response in a controlled behavioural arena. The hypotheses developed are below:

$H1_o$: Opsin expression **is not** different in starry flounder held for seven weeks in broad spectrum light compared to green-filtered light.

$H1_a$: Opsin expression **is** different in starry flounder held for seven weeks in broad spectrum light compared to green-filtered light.

$H2_o$: Camouflage response **is not** different in starry flounder held for seven weeks in broad spectrum light compared to green-filtered light.

$H2_a$: Camouflage response **is** different in starry flounder held for seven weeks in broad spectrum light compared to green-filtered light.

If **$H1_o$** and **$H2_o$** are rejected, then using mixed effects modelling:

$H3_o$: Camouflage response in starry flounder **does not** vary with opsin expression.

$H3_a$: Camouflage response in starry flounder **does** vary with opsin expression.

Chapter 2 – Characterization of the starry flounder visual system: opsins, chromophores, and histology

Note: the data in this chapter has been prepared in a manuscript to be submitted to the Journal of Comparative Neurology. Reference: ***Iwanicki, T.****, Novales Flamarique, I., Ausió, J., Morris, E., Taylor, J.S. "Fine-tuning light sensitivity in the starry flounder (Platichthys stellatus) retina: regional variation in photoreceptor cell morphology and opsin gene expression."*

Introduction

Investigations into flatfish opsin repertoires have yielded large variability in the number and types of opsin genes, from five in winter flounder, *Pleuronectes americanus*, (Mader and Cameron, 2004) and Atlantic halibut, *Hippoglossus hippoglossus,* (Helvik et al., 2001a) to eight in barfin flounder, *Verasper moserii*, (Kasagi et al., 2015) and nine in turbot, *Scophthalmus maximus* (Figueras et al., 2016). Expression studies corroborated with topographical measurements of the retina (i.e., photoreceptor morphology, cone density, mosaic pattern) have been limited, however, to Atlantic flatfish species (Helvik et al., 2001b) such that the number of opsins and their distribution within the retina of Pacific taxa are unknown. Here, we identified the opsin repertoire and its retinal expression in the starry flounder, *Platichthys stellatus*, a Pacific flatfish species. This was accompanied by a topographical analysis of photoreceptors and *in situ* measurements of their visual pigments, which permitted correlation of opsin expression with specific photoreceptor types. Because differences in visual pigment absorbance can be due to chromophore variation rather than differential opsin expression (Hárosi 1991; Novales

Flamarique et al., 2013), we also measured retinal chromophore content. Together, our results depict a chromatically complex retina with topographical adaptations for multiple visual tasks.

Materials and Methods

Fish collection and preparation

Fish were collected by beach seine between 10:00 – 12:00 in November 2014 and May 2015 at Willows Beach, Victoria, British Columbia, Canada. The seine net was deployed from a small aluminum boat at a depth of approximately 3 m, or by hand at around 2 m depth. Starry flounder collected in November 2014 (n =5, TL = 96±19 mm, mass = 13±5.5 g) were euthanized by an overdose of MS-222 and immediately frozen in liquid nitrogen. They were then stored at -80^{o}C. Starry flounder collected in May 2015 (n = 25) were transported to the Outdoor Aquatics Unit at the University of Victoria, and held under ambient light in a tank with recirculating 12^{o}C seawater. Sampling and husbandry was approved by the University of Victoria Animal Care Committee (protocol # 2015-005(1) and 2015-003(1)) which abides by regulations set by the Canadian Council for Animal Care.

Histology

Wild-caught starry flounder were held for up to one week under ambient sunlight at the Outdoor Aquatics Unit, University of Victoria. After a fish was euthanized, the eyes were extracted, lenses removed, and each eyecup immersed in primary fixative (2.5% glutaraldehyde, 1% paraformaldehyde in 0.08 M PBS, pH = 7.4) in a separate vial

labelled for the migrated or non-migrated eye. After overnight fixation at 4ºC, the retina was extracted from each eyecup, rinsed in 0.08 M PBS, and cut into four quarters as depicted in Figure 4. After a brief wash in distilled water, the tissue was dehydrated through a series of solutions of increasing ethanol concentration, infiltrated with mixtures of propylene oxide and EPON resin, and embedded in 100% EPON resin. Retinal blocks were cut tangentially or radially, in 2 µm steps, to reveal the cone mosaic and length of photoreceptors, respectively. Digital images of sections were acquired with an E-600 Nikon microscope equipped with a DXM-100 digital camera. These micrographs were analyzed for cone ellipsoid surface area of single and double cones and their outer segment lengths (n=20 measures per cone type for each retinal sector) using Simple PCI software (Nikon). Because we consistently noticed two different cone size groups in the dorso-temporal quadrant, we describe these two groups separately. For each retinal quadrant, the density of cones was counted over a 0.08 mm^2 area of tangential section showing the cone mosaic at the level where the double cone ellipsoids were widest. From these measures, cone packing was computed as the sum of the product of cone density and mean surface area for single and double cones divided by the retinal area analyzed, and expressed as a percentage. Statistical analyses for differences in cone density, packing, and outer segment length between retinal sectors was performed using a one-way ANOVA with post-hoc grouping tests (NSK, Tukey HSD) and evaluated at $\alpha = 0.05$ level of significance.

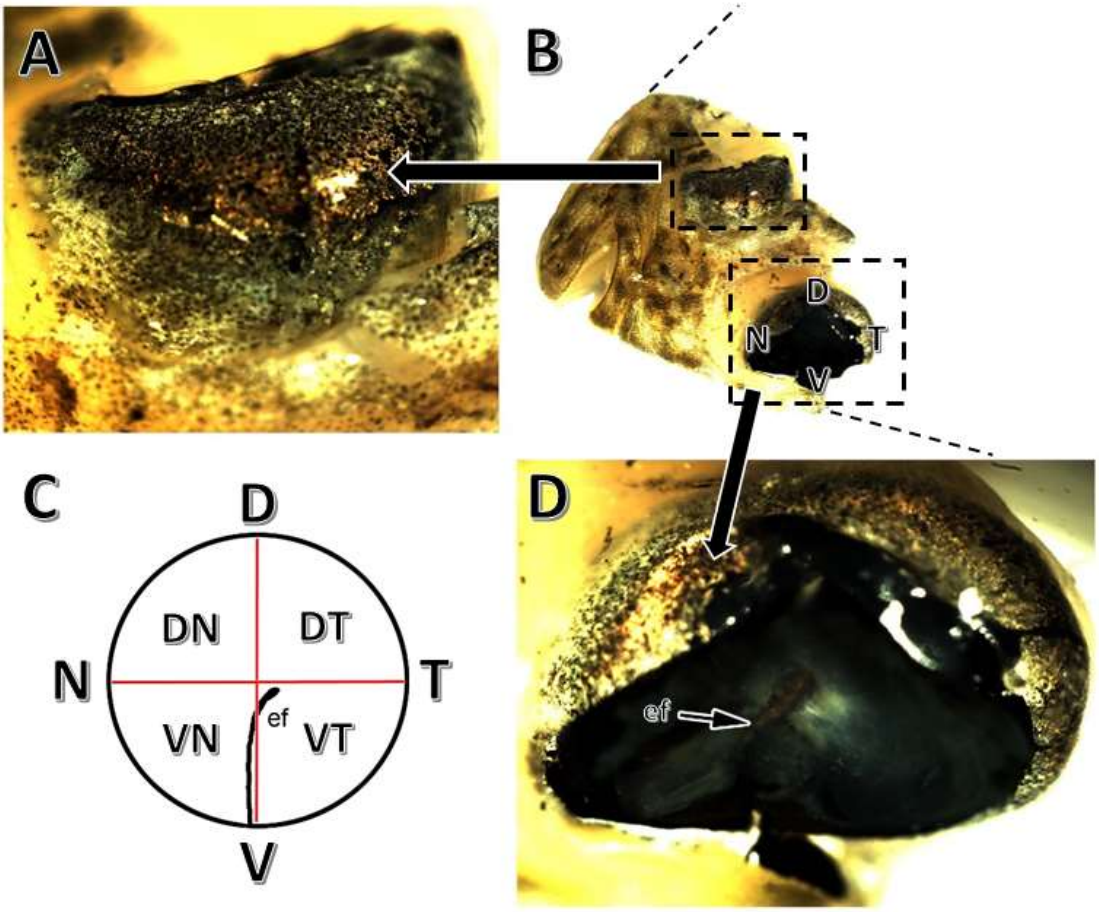

Figure 4: Eyes of a dextral juvenile starry flounder and retinal diagram. B: Photograph of portion of a starry flounder head showing the asymmetrical distribution of eyes (the lenses have been removed). Retina abbreviations: T, temporal; D, dorsal; N, nasal; V, ventral. B,C: Higher magnification of the migrated (D) and non-migrated (A) eye. The embryonic fissure (ef) is indicated on the exposed retina of the migrated eye. C: Diagram of retina showing quarter cuts (red) and the location of the embryonic fissure. Abbreviations: DN, dorso-nasal; DT, dorso-temporal; VN, ventro-nasal; VT, ventro-temporal.

RNA Isolation and RNA-Seq

Whole eyes (n = 4) were removed and homogenized in TriZol (Life Technologies). Samples were immediately processed using a column-based AurumTM Total RNA Fatty

and Fibrous Tissue Pack (BioRad). Isolation of total RNA followed the manufacturer's recommended protocol, which included an on-column DNase I step, to ensure any contaminating DNA was removed. Total RNA was quantified using Qubit® RNA Broad Range Assay Kit (Life Technologies). One µg of RNA from each sample was reverse-transcribed using iScript™ cDNA Synthesis Kit (BioRad).

RNA isolated from starry flounder eyes was mRNA purified using Thermo Scientific MagJET mRNA Enrichment Kit as per the manufacturer's recommended protocol. Library preparation was performed using NEBNext Ultra RNA Library Prep Kit for Illumina. Following mRNA fragmentation, first strand cDNA synthesis, and second strand cDNA synthesis, Thermo Scientific GeneJET NGS Cleanup Kit was used to remove all non-cDNA components. Blunt ends were generated and single A overhangs were added. Looped Y adaptors with T overhangs were ligated to the cDNA fragments at the single A overhang. The adaptor loops were cut at the uracil site using USER Enzyme, which exposed the adaptor's free ends on all cDNA fragments containing sites for PCR amplification. Size selection for fragments approximately 400 bp was completed using MagJET NGS Cleanup and Size Selection Kit, protocol C. PCR library enrichment was run using NEBNext Q5 Hot Start HiFi PCR Master Mix and NEBNext Multiplex Oligos for Illumina (Index Primers Set 2). Excess primers and nucleotides were removed using Thermo Scientific GeneJET NGS Cleanup Kit. The final pooled library was quantified using Qubit® DNA Broad Range Assay Kit (Life Technologies) and visualized using Agilent 2100 Bioanalyzer. The molarity in nM was estimated using the following formula: (Qubit concentration

(ng•ul^{-1})) / ((660g•mol^{-1}) × (average size of library (bp)) × 106). The pooled library was diluted to 4 nM and sequenced on an Illumina MiSeq using a MiSeq v2 500 Cycles Reagent Kit. One percent PhiX control was added to the pooled library. RNA-Seq generated 22 million paired-end reads that were assembled, using the Trinity package (version 2.0.6) with default settings, into 250,000 transcripts.

Phylogenetic analyses

We surveyed the transcriptome using tBlastn (protein query sequences aligned to hits from the transcript database). Query sequences for this search included visual and non-visual opsins from guppy, zebrafish, gar, frog and human. A phylogenetic analysis was run to sort starry flounder opsin transcripts into visual opsin clades. The tree was built using the Neighbor-Joining method (Saitou and Nei, 1987) with a bootstrap reanalysis (500 replicates) (Felsenstein, 1985). Evolutionary distances were inferred using the p-distance method (Nei and Kumar, 2000) and are in the units of the number of base differences per site. The analysis involved 60 nucleotide sequences, including starry flounder transcripts and sequences obtained from the NCBI nucleotide database. All codon positions were included. There were a total of 1233 positions in the final dataset, aligned manually in BioEdit, and using the entire coding sequence for all genes used. Evolutionary analyses were conducted in MEGA6 (Tamura et al., 2013).

High performance liquid chromatography

We used High Performance Liquid Chromatography (HPLC) to measure the presence of vitamin-A derived chromophores: retinal (A1) and dehydroretinal (A2) (Hasegawa,

2005; Kondrashev et al., 2012). Retinas from an individual (starry flounder: n = 3, mass = 7.6±2.3 g, TL = 8.1±0.9 cm; rainbow trout parr: n = 3, mass = 8.6±1.9 g, FL = 9.1±0.6 cm) were extracted and placed in a 1.5 ml tube. These were immersed in liquid Nitrogen and stored at -80^{o}C until processing. Retinas (or 100 µl of the standard solution) were homogenized in 60 µl containing 1.92 mol·L-1 hydroxylamine sulfate (neutralized with 1 N KOH) and 300 µl methanol using sonication. The homogenate was cooled on ice for 5 minutes, after which 300 µl dichloromethane and 150 µl ddH_2O were added and the mixture shaken vigorously. Then, 600 µl of n-hexane were added. The samples remained on ice throughout this extraction process. The mixture was centrifuged at 1000·g for 5 minutes at 4^{o}C. The dichloromethane/hexane (top) layer was removed and placed in a 1.5 ml tube, then the dichloromethane and hexane extraction was repeated on the remaining lower layer. The second extract was combined with the first and evaporated under vacuum for about 1 hour. The dried extract (typically a slightly yellow residue) was dissolved in 100 µl n-hexane for HPLC analysis using a Beckman-Coulter System Gold with mobile phase containing 7% ether, 0.075% ethanol in n-hexane, operating at a flow rate of 0.8 ml·min^{-1} and equipped with a 5 µm YMC-Pack Silica 2.1x250 mm column (YMC America). In addition, a commercial all-trans-retinal (A1) (Sigma, Product number: R2500) standard was prepared by dissolving 2.5 mg of retinal in 600 µl methanol. Absorbance at 360 nm and 400 nm were monitored, and identification of retinal A1 and A2 oximes were based on retention time according to the retinal standard (Hasegawa, 2005; Kondrashev et al., 2012).

Microspectrophotometry

Individual fish were dark adapted for 3-4 hr. Following this adaptation period, a fish was euthanized, one eye enucleated, and the retina removed under infrared illumination (n = 3). Pieces of retina were teased apart and prepared for viewing with a dichroic microspectrophotometer (DMSP) as per previous studies (Novales Flamarique and Hárosi 2000; Cheng et al., 2006). The DMSP is a computer-controlled, wavelength-scanning, single-beam photometer that simultaneously records average and polarized transmitted light fluxes through microscopic samples (Hárosi 1987; Novales Flamarique and Hárosi 2000). The DMSP was equipped with ultrafluar (Zeiss) objectives: 32/0.4 for the condenser and 100/1.20 for the objective. With the aid of reference measurements recorded through cell-free areas of the slide, individual photoreceptor outer segments were illuminated sideways with a measuring beam of rectangular cross section of ca. 2 x 0.6 µm. Absolute absorbance spectra were computed in 2 nm increments between 320 nm and 650 nm from the obtained transmittances. The solid spectra (fits) were derived from experimental data by Fourier filtering (Hárosi 1987).

Digital PCR

Digital-PCR (dPCR) was used to assess whole retina expression levels (n = 5, both eyes, totalling 10 retinas) and expression level variation within the retina (n = 3, one eye per individual bisected along the midline separating the ventral and dorsal halves of the retina). With dPCR the number of wells on a 20,000-well chip showing template amplification is used to determine target cDNA abundance in the sample. Sample concentrations are adjusted to ensure that the estimated copies per microliter fall within

the digital range of the 3D system (i.e., 200 – 2000 copies•µl-1). cDNA template varied from 0.1 to 100 ng per chip. Opsin expression was normalized, using the alpha subunit of transducin (*Gnat2*), the G-protein activated by cone opsins, as the denominator (Dalton et al., 2015). dPCR was run on QuantStudio® 3D Digital PCR System (Life Technologies) using locus-specific primers and TaqMan probes (Table 1). Opsins were multiplexed using FAM (emission = 517 nm) and VIC (emission = 551 nm) reporter dyes. cDNA, primers (900 nM each), probes (250 nM), and master mix were applied to a QuantStudio® 3D Digital PCR 20K v2 Chip, loaded with immersion oil to prevent evaporation, and sealed. After equilibrating at room temperature for 15 minutes, PCR was performed on a ProFlex™ 2x Flat PCR System (step 1: 94^{o}C × 30 sec; step 2: 55^{o}C × 2 min, 94^{o}C × 30 sec (39 cycles); step 3: 55^{o}C × 2 min, 10^{o}C hold). Chips were read using the QuantStudio® 3D Digital PCR instrument. The expression in migrated and non-migrated eyes was assessed using a two-way ANOVA. Overall relative expression was tested using a student's t-test. Patterns in intra-retinal variation were tested using a paired student's t-test. All statistical tests were evaluated at $\alpha = 0.05$ level of significance.

Table 1: Primers and TaqMan probes used for starry flounder digital-PCR

Gene	Oligo	Sequence (5' to 3')
Lws	*Forward*	AACTCCGTCACCCACTGAAC
	Reverse	TCTCCCAGGAGATGATGGAC
	Probe	**FAM**-TTCTGGGACACCCGATGTGCA-QSY
Sws1	*Forward*	TGTTCTCAGTGAGCCAGGTG
	Reverse	GGCTCCGAATGGTTTACAGA
	Probe	**FAM**-TGGAATCTGCCATGGGCTCGA-QSY
Sws2B	*Forward*	GCTCTTTCACCTGCTTCTACTG
	Reverse	CTATGGCATGGCTGGATTTG
	Probe	**FAM**-TACAGCGACTGTTGGTGGAATGGTCAG-QSY
Rh1	*Forward*	CTTGGCTGCAACCTAGAAGG
	Reverse	CCCTCAGGGATGTAACGAGA
	Probe	**FAM**-TTTGCAGCCTCTGCTTGCGC-QSY
Rh2A-1	*Forward*	CGTCCACTTCTTCCTTCCAG
	Reverse	AAGACCATCAGGACGCACAT
	Probe	**VIC**-GGTGCTGACAGTCAAAGCTGCTGC-QSY
Rh2A-2	*Forward*	ACGGCTCCTGTCTTCACAAT
	Reverse	AGCTACCAGGAAGCCAATGA
	Probe	**VIC**-CATTCTGACAGTCAAAGCCGCTGC-QSY
Sws2A-1	*Forward*	GTGACACTTGGTGGGATGGT
	Reverse	CATCCGAACAGAGGTGGAGT
	Probe	**VIC**-GGCTTGTCATCTGCAAGCCATTAGGT-QSY
Sws2A-2	*Forward*	GCATCAACACCCTGACCATT
	Reverse	ACCATACCTCCGAGTGTTGC
	Probe	**VIC**-TGGTGAATTTGGCTGTGGCGA-QSY
Efa-1	*Forward*	ACACTGCTAGAAGCCCTGGA
	Reverse	GAGCATACCGGGCTTAATGA
	Probe	**FAM**-TGCCCCTGCAGGACGTCTACAA-QSY
Gnat2	*Forward*	AGCCAGATTACCTCCCCACT
	Reverse	GGTCACACCCTCGAAACAGT
	Probe	**VIC**-TGTGCTGCGTTCCCGAGTCAA-QSY

Results

Cone photoreceptor types and their distributions

Following metamorphosis, the eyes of the starry flounder become bilaterally asymmetric due to migration of one of the eyes onto the opposite side of the head (Figure 4B). This arrangement results in a field of view that is shifted upward for the migrated eye in comparison with that of the non-migrated eye. Nonetheless, because eye migration does not involve eye rotation (Bao et al., 2011), the relative orientation of the retina

remains the same between eyes such that dorsal, ventral, nasal, and temporal regions of the retina view the inferior, superior, posterior and anterior parts of the visual field, respectively, albeit at different angles (Figure 4A,D). As in other fishes, including those in the families Salmonidae (Cheng and Novales Flamarique, 2007) and Engraulidae (Novales Flamarique, 2011), the embryonic fissure in starry flounder extends from the ventral periphery toward the temporal retina abutting near the optic nerve head (Figure 4D). This morphological landmark was used to divide the retina into quarters and to assess the topographical distribution of cone photoreceptors (Figure 4C).

The starry flounder had double and single cones (Figure 5). The double cones consisted of two cells apposed sharing a double membrane partition. At the level of the inner segment ellipsoid, double cones exhibited an elliptical cross section whereas single cones were circular (Figure 5A). Double and single cones formed lattice-like arrangements termed mosaics, the basic unit of which consisted of four double cones forming a square with a single, centre cone located in the middle of the square (Figure 5A). At the level of the inner segment ellipsoid, cones from the lower half of the retina (Figure 5A,B) had greater surface area than cones from the upper half of the retina (Figure 5D-F). In the dorso-temporal retina, however, cones located closer to the mid retina (Figure 5C) resembled those from the lower retina (Figure 5A,B) whereas cones positioned more dorsally (Figure 5D) resembled those from the dorso-nasal retina (Figure 5E-F). Such a difference in cone dimensions within the dorso-temporal quadrant was evident from micrographs expanding the mid to dorsal retina (Figure 6A).

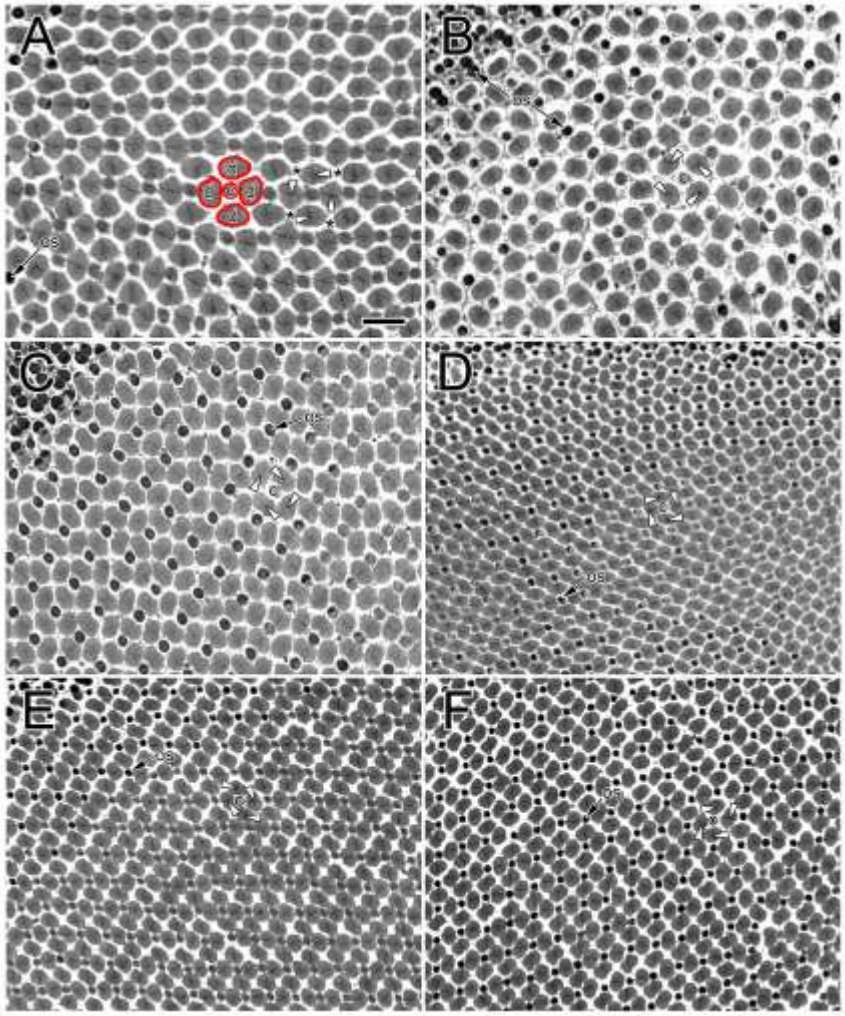

Figure 5: Micrographs of tangential sections from the retina of juvenile starry flounder. A,B: Cone distributions from the ventro-temporal (A) and the ventro-nasal (B) retina. The cones are arranged in a square mosaic, the unit of which (depicted in red) consists of four double cones (d) making the sides of the square and a single, central cone (c) in the middle of the square. Partitions separating the members of some double cones are indicated with a white arrowhead. The black asterisks indicate corner positions of the unit square mosaic, which are devoid of single cones. The outer segments (os) of some cones are visible in these sections, they stain darker than the inner segments. C,D: Cone distributions from the dorso-temporal retina show larger cones closer to the ventral retina (C) and smaller cones dorsally (D). E,F: Cone distributions from the dorso-nasal retina originating from either eye of a fish. The micrograph on the left (E) shows, primarily, single cone inner segments whereas the one on the right (F) shows predominantly single cone outer segments. The cone distributions were consistent within and between fish for equivalent retinal sectors. Scale bar (in A) = 10 µm, applies to all panels.

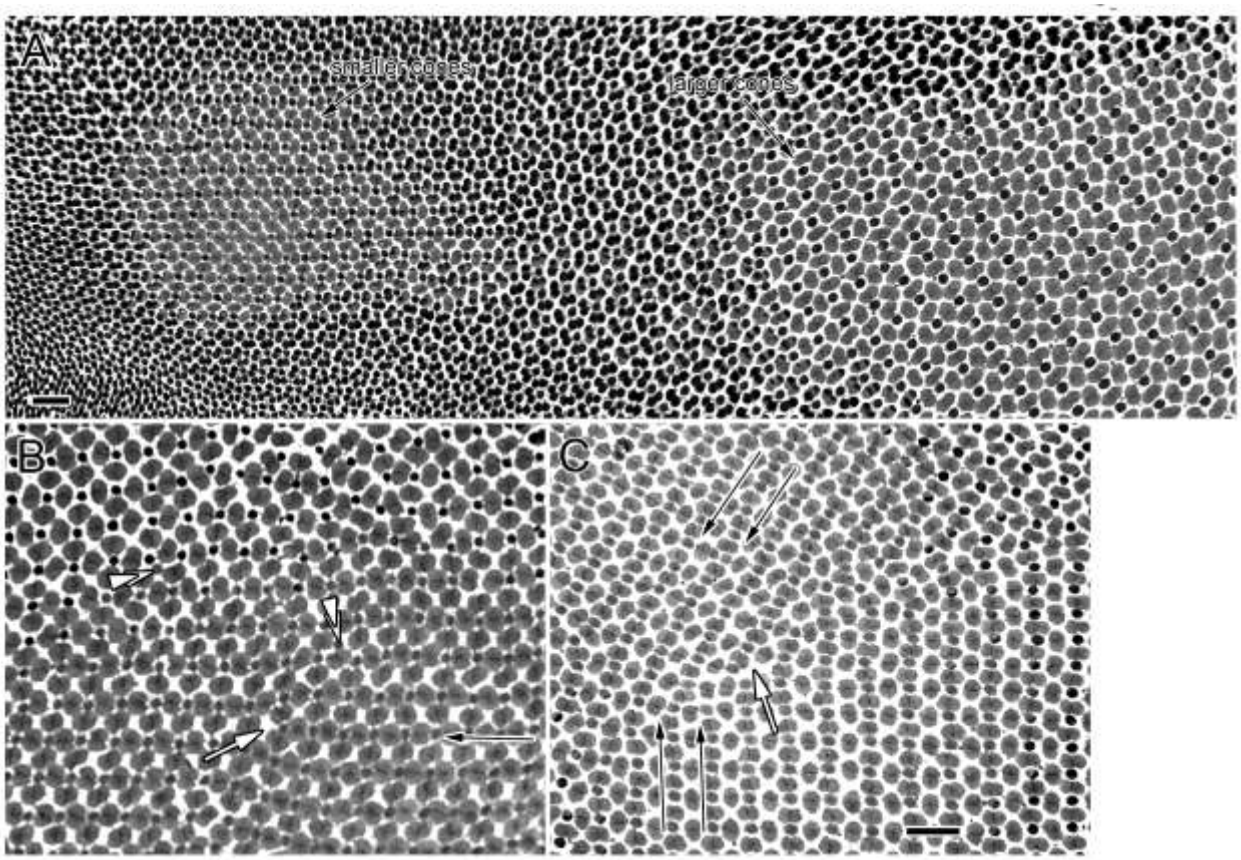

Figure 6: Micrographs of tangential sections from the dorsal retina of juvenile starry flounder. A: Section from the dorso-temporal retina illustrating the two sizes of cones present in this region of the retina. B,C: Sections from the dorso-nasal retina illustrating instances of single corner cones (double white arrowheads) (B), and missing double cones (white arrow) at the site of row termination (black arrow points to ending row in B) or at the boundary of two mosaic domains with different orientations (black arrows point to rows oriented at 45º to each other in C). Scale bar (in A, C) = 10 µm; (B) and (C) share the same magnification. Abbreviations and symbols as per **Figure 5**.

In addition to the regular square mosaic unit with a single centre cone at its centre, rare instances of single corner cones were observed in the dorso-nasal retina (Figure 6B). These cones, which are ubiquitous in the retinas of many fishes at the juvenile stages (see references in Hárosi and Novales Flamarique, 2012), were located at the corners of the

square unit, facing the membrane partitions of surrounding double cones. In addition to these extra single cones, the dorso-nasal retina was characterized by the odd, missing double cone in areas of row congruence (Figure 6B) and convergence of mosaic regions with different orientations (Figure 6C).

The differences in cone ellipsoid dimensions as a function of retinal location were also apparent in radial sections (Figure 7). These micrographs further revealed that the outer segments of cones in the upper retina (especially in the dorso-nasal region, Figure 7E,F) were, on average, 2.3 times longer (n = 3) than those in the lower half of the retina (Figure 7A,B). Cone outer segments stained darker than those of rods, which were located closer to the sclera, within the retinal pigment epithelium (Figure 7A,B,D). The darker stain of cone outer segments was also visible in tangential sections and contrasted with the reduced staining of inner segments (Figure 5A-D).

A statistical analysis from the eyes of three starry flounder (Figure 8A-F) showed that cone densities in the dorso-nasal and upper dorso-temporal retina were similar and significantly greater than those in the remainder of the retina, by an average factor of 2.4 ($F = 53.1$ and 19.9 for the left and right eye, respectively, $p<0.0001$; Figure 8G,H). The same statistical trend was found for cone outer segment length ($F = 85.5$; $p< 0.0001$; Figure 8**G**). In contrast, cone packing, i.e., the area of retina occupied by cones, was not significantly different between sectors and ranged from 45% to 67% ($F=3.3$, $p =0.06$ and $F=2.9$, $p= 0.07$ for left and right eye, respectively; Figure 8A-F). The latter finding results from an inverse relationship between cone ellipsoid surface area and density such that, theoretically, the same amount of light would be intercepted across the retina, were the light field homogeneous.

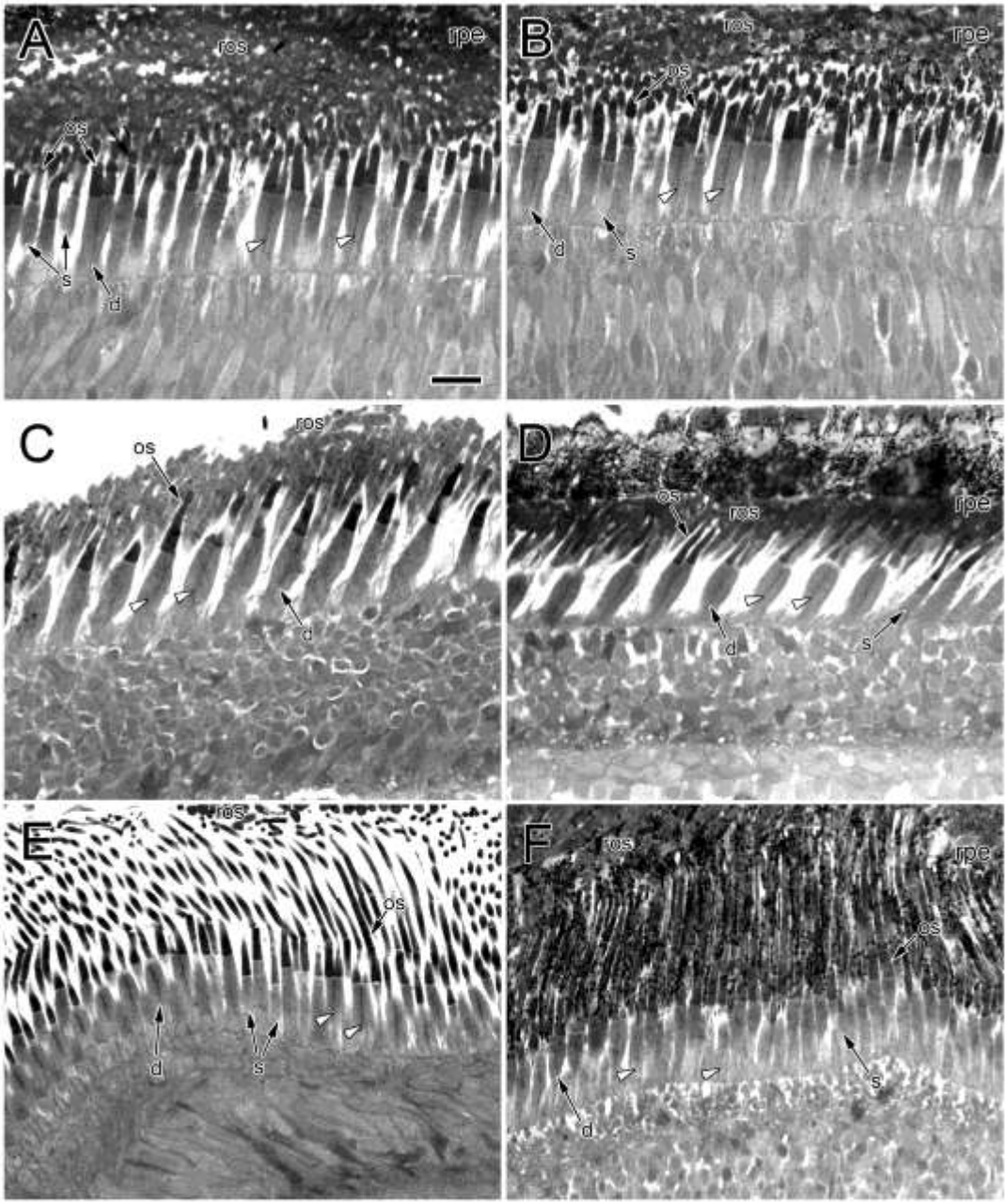

Figure 7: Micrographs of radial sections from the retina of juvenile starry flounder. A,B: Double and single (s) cones from the ventro-temporal (A) and the ventro-nasal (B) retina. C,D: Cones from the lower dorso-temporal retina (C) and from an area located further dorsally (D). The cones are wider but shorter and have shorter outer segments in the lower compared to the upper dorso-temporal retina. E,F: Cones from the dorso-nasal retina of two fish. Scale bar (in A) = 10 µm, applies to all panels. Abbreviations: ros, rod outer segment; rpe, retinal pigment epithelium. Other abbreviations and symbols as per **Figure 5**.

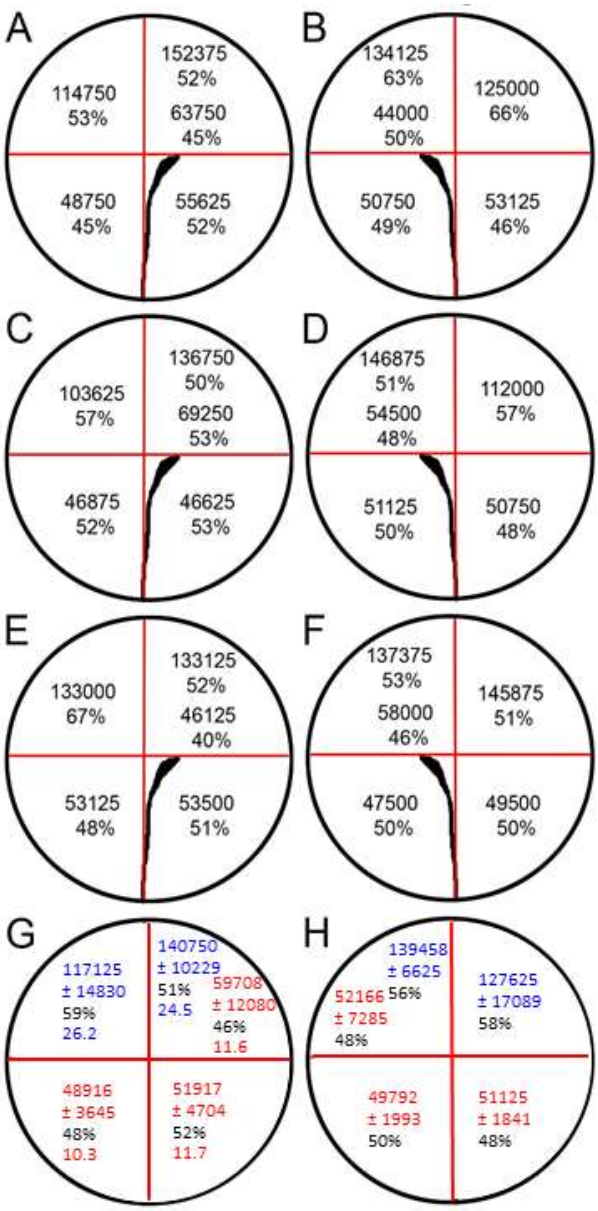

Figure 8: Diagrams illustrating topographic maps of cone densities and packing from the retinas of three fish. A-F: Topographic maps for three pairs of eyes. In each quadrant, cone density (total number of cones per mm2) is the top number and cone packing (percentage of the photoreceptor layer surface occupied by cones) is the bottom number. For dorso-temporal quadrants, two sets of numbers are presented corresponding to the two populations of cones that were consistently found. G,H: Topographic maps showing mean statistics from the three sets of eyes in A-F. Mean cone outer segment length (in µm) appears as a third, bottom number in each set in G. In these summary diagrams, standard deviation of mean cone density are shown. Also, means within a given category that are significantly different from each other have different colours.

Opsin repertoire

Eight visual opsins were sequenced from starry flounder, one representative from the LWS, SWS1 and RH1 visual opsin subfamilies, two from the RH2 subfamily, and three from the SWS2 subfamily (Figure 9). The barfin flounder, a Pacific flatfish of the same family, Pleuronectidae, possesses RH2 paralogs: two functional RH2A's and an RH2B pseudogene. We found no evidence of an RH2B ortholog in the starry flounder eye transcriptome. We did, however, find two RH2A paralogs; the RH2 duplicates (*Rh2A1* and *Rh2A2*) have orthologs in Turbot (*Scophthalmus maximus*) indicating that they were generated early during Pleuronectiformes evolution (Rennison et al., 2012). SWS2 was also duplicated early in Acanthopterygii evolution generating SWS2A and SWS2B. In percomorph fish SWS2A duplicated generating additional paralogs, *Sws2A1* and *Sws2A2* (Cortesi et al., 2015). Starry flounder amino acid sequences differed from barfin flounder at several positions in the retinal binding pocket and at key tuning sites in all opsin orthologs (see Appendix B: Figure 27-31). Our initial RT-PCR experiments showed that all visual opsins were expressed in the eyes of fish caught at Willows Beach (n=5). This was confirmed by RNA-Seq, which generated 22 million paired-end reads that were assembled, using the Trinity package, into 250,000 transcripts. This high number of transcripts indicates that assembly requires fine-tuning, however, we were able to recover full-length transcripts of the eight visual opsins uncovered in our initial PCR-based survey, and no additional visual opsin genes.

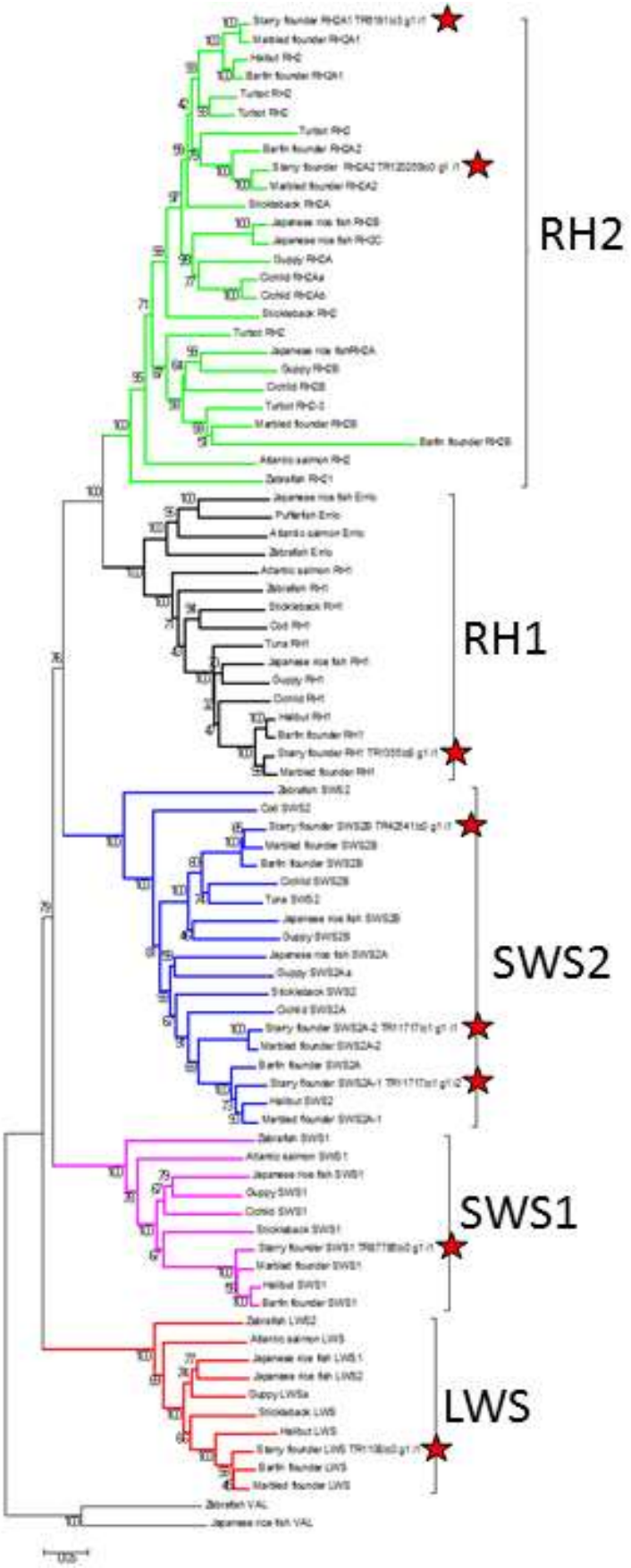

Figure 9: Phylogenetic analysis of starry flounder opsins and other teleost opsins. The evolutionary history was inferred using the Neighbor-Joining method. The evolutionary distances were computed using the p-distance method and are in the units of the number of base differences per site. Evolutionary analyses were conducted in MEGA6.

Retinal chromophore content

Retinal extracts from juvenile starry flounder analyzed by HPLC resulted in absorbance profiles characterized by a main peak at 10 minutes and a secondary peak at 23.3 minutes retention time (Figure 10A). Likewise, the all-trans A1 retinal standard produced a main peak corresponding to all-trans-retinal oxime (A1) at 10 minutes, and a secondary peak corresponding to anti-all-trans-retinal oxime at 23.3 minutes retention time (Figure 10B). As such the starry flounder retina contained all-trans A1 retinal chromophore exclusively. By comparison, the rainbow trout juvenile at the parr stage (Cheng et al., 2007), which is known to use vitamin A1 and A2-based chromophores in the retina (Hawryshyn and Hárosi, 1994) showed two peaks: the A1 peak at 10 minutes, and the A2 and anti-A2 peaks at 11 and approximately 25 minutes retention times, respectively (Figure 10C). Although a peak at approximately 11.5 minutes is visible in the starry flounder retina extracts, that is not to be confused with vitamin A2. The retinal extracts are a complex mixture of aldehydes and lipids that co-precipiate with retinal, and will result in unknown peaks on the chromatogram. Retinal will appear as a distinct oxime and *anti*-oxime peak. The *anti*-oxime peak corresponding to vitamin A2 is absent in the starry flounder. Notably, there is a “shoulder” in the A2-peak in rainbow trout, and we predict that this shoulder corresponds to the unknown peak observed in the starry flounder chromatograms.

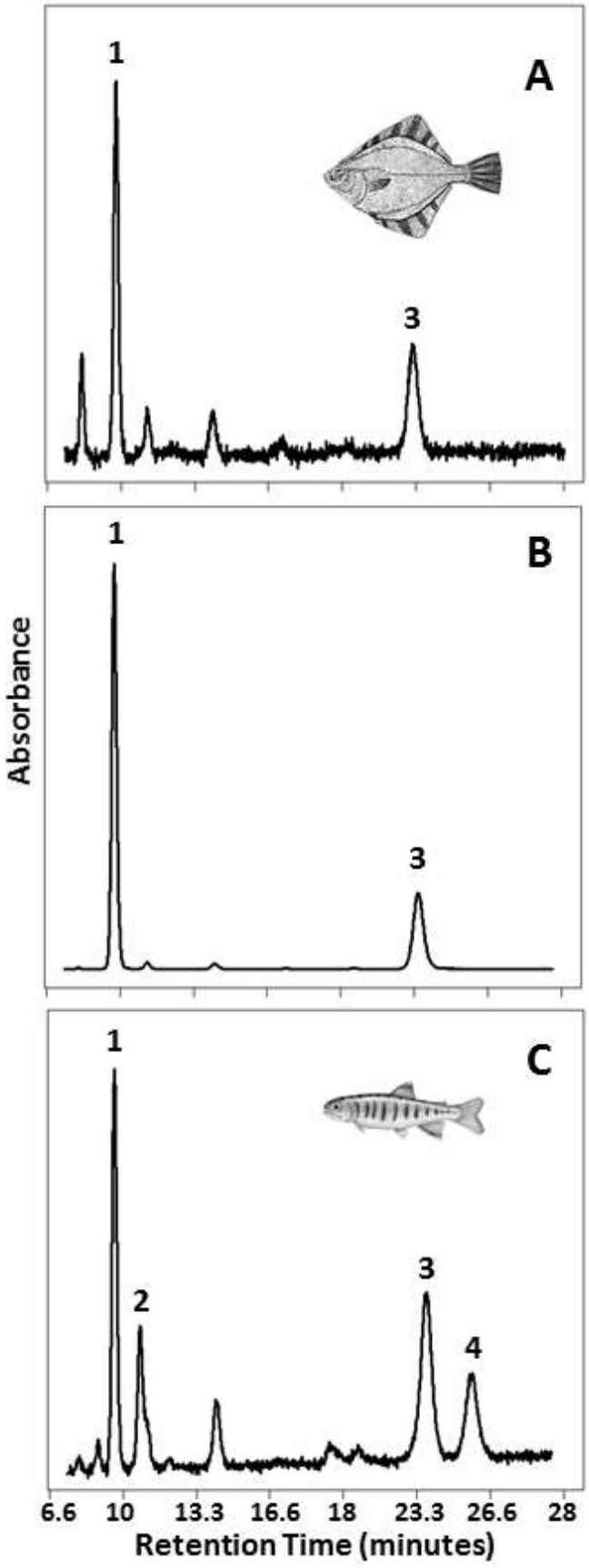

Figure 10: Representative HPLC-derived absorbance profiles of (A) juvenile starry flounder retina extract, (B) all-trans-retinal standard, and (C) rainbow trout parr retina extract. Peaks correspond to vitamin A-derived chromophores, (1) all-trans-retinal (A1), (2) all-trans-dehydroretinal (A2), (3) anti-all-trans-retinal, and (4) anti-all-trans-dehydroretinal.

Visual pigments

Absorbance measurements from the outer segment of individual photoreceptors from three fish revealed seven cone pigments and one rod pigment (Figure 11). These comprised one ultraviolet (UV) pigment, three different short wavelength (S) pigments, two middle wavelength (M) and one long wavelength (L) pigments, and the rod visual pigment. Their wavelengths of maximum absorbance (λ_{max}) ± SD were: UV (369 ± 6 nm, n=8), S (415 nm, n=2; 437 ± 7 nm, n=7; 456 ± 5 nm, n=10), M (527 ± 5 nm, n=14; 545 ± 6 nm, n=11), L (557 ± 9 nm, n=6), and rod (507 ± 4 nm, n=18). The UV and S visual pigments were found in the single cones whereas the M and L visual pigments were found in the double cones. Among the double cones measured, some contained the same visual pigment in each member and were equal M_{527}/M_{527} pairs and others contained a different visual pigment between members and were chiefly unequal M_{527}/M_{545} and a few M_{527}/L_{557} pairs. The unequal double cones were associated with cells having long outer segments (> 15 µm) or small ellipsoid cross sectional areas, corresponding primarily to cones in the dorsal retina (Figure 5, Figure 6). Equal (M_{527}/ M_{527}) double cones were commonly associated with smaller outer segments (< 15 µm) or with cells having mid to large ellipsoids, corresponding primarily to those in the ventral retina (Figure 5, Figure 6).

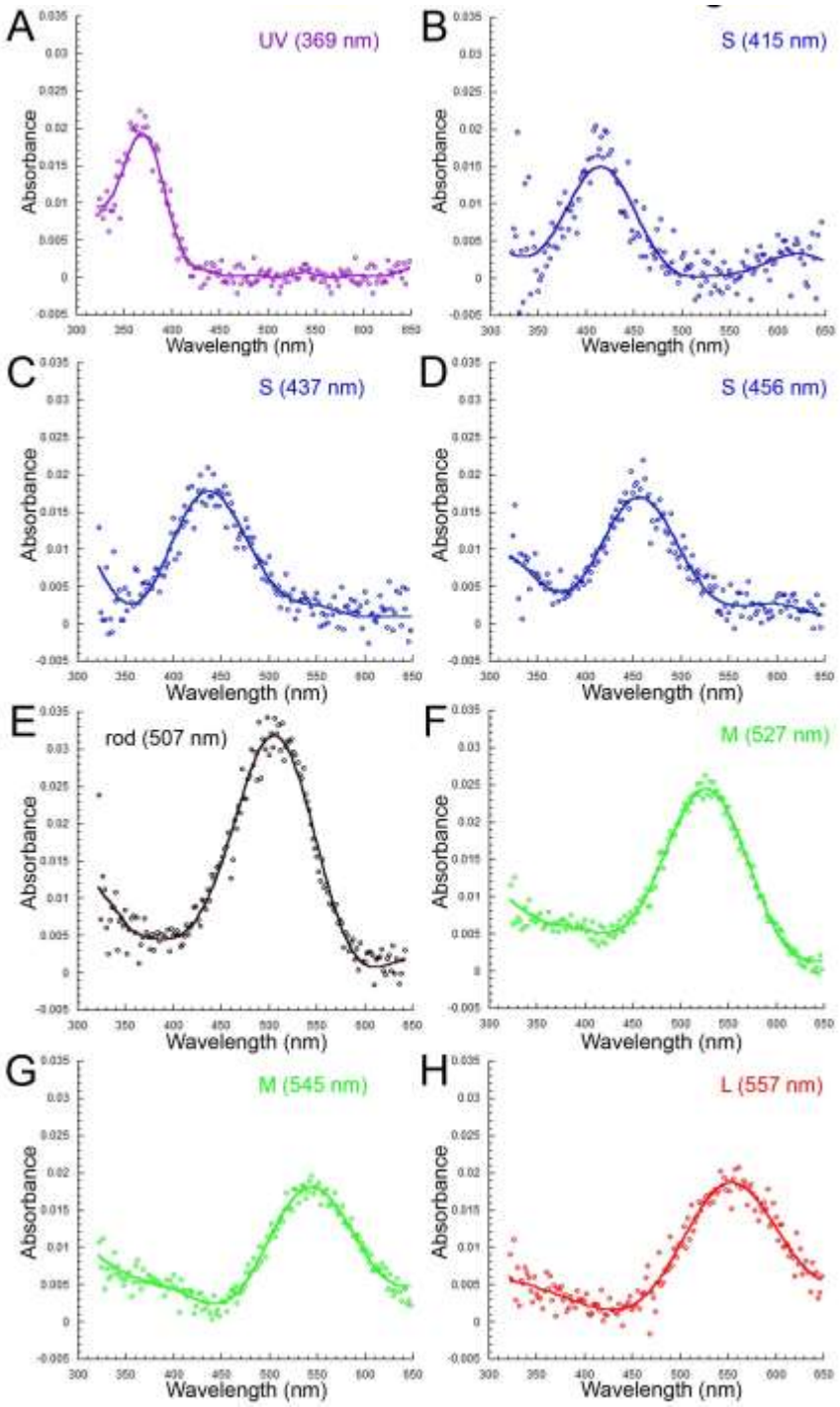

Figure 11: Mean absorbance spectra of visual pigments from the retina of starry flounder (from n=3 fish). Seven cone visual pigments and one rod visual pigment were found: one ultraviolet (UV) (A), three types of short-wavelength (S) (B-D), one rod (E), two middle wavelength (M) (F,G), and one long wavelength (L) (H). The maximum wavelength of absorbance (λmax) of each visual pigment is indicated on the corresponding panel.

Opsin expression

The majority of the total opsin mRNA in starry flounder retinas from individuals collected in approximately one meter of water consisted of *Rh2A1*, *Rh1*, and *Lws*, with *Sws2A2* and *Sws2A1* being expressed at intermediate levels, and *Rh2A2*, *Sws1*, and *Sws2B* being expressed the least (Table 2, Figure 12). Opsin expression was similar between both eyes (two-way ANOVA, $F = 0.953$, $p = 0.333$). The ventral retina had higher levels of *Rh1*, *Sws1*, *Sws2A1*, and *Sws2A2* transcripts than the dorsal retina, whereas the opposite trend was true for *Rh2A1* and *Rh2A2* transcripts (Figure 13). The ratio of dorsal to ventral transcript expression was greater for *Rh2A2* than *Rh2A1* (student's paired t-test, $t = 4.4882$, $p = 0.04623$).

Table 2: Transcripts identified from the RNA-Seq Trinity assembly for starry flounder whole eyes. Eight visual opsins and *Gnat2* expression, as measured by fragments per thousand base pairs mapped (FPKM), is shown. Isoforms of *Rh2A2* and *Sws2B* had 261 bp and 111 bp of identical nucleotide overlap, respectively.

Opsin	**Transcript ID (with isoforms)**	**Length**	**Effective Length**	**Expected Count**	**TPM**	**FPKM**
Rh1	TR1355|c8_g1_i1	1506	1170.49	49037	9226.37	17943.87
Rh2A1	TR6191|c3_g1_i1	1687	1351.49	8070	1315.03	2557.53
Lws	TR1108|c0_g1_i1	1536	1200.49	2107	386.53	751.74
Gnat2	TR61391|c5_g2_i1 TR61391|c5_g2_i2	2692	2357.02	2962	276.75	538.24
Sws2A2	TR11717|c1_g1_i1	1414	1078.49	906	185.01	359.81
Sws2A1	TR11717|c1_g1_i2	1409	1073.49	212	43.49	84.59
Rh2A2	TR9572|c1_g1_i1 TR100663|c0_g1_i1	1033 522	697.49 217.07	69 11	21.79 11.16	42.37 21.7
Sws1	TR87786|c0_g1_i1	1179	843.49	71	18.54	36.05
Sws2B	TR42541|c0_g1_i1 TR50392|c0_g1_i1	977 1286	641.49 950.49	54 16	18.54 3.71	36.05 7.21

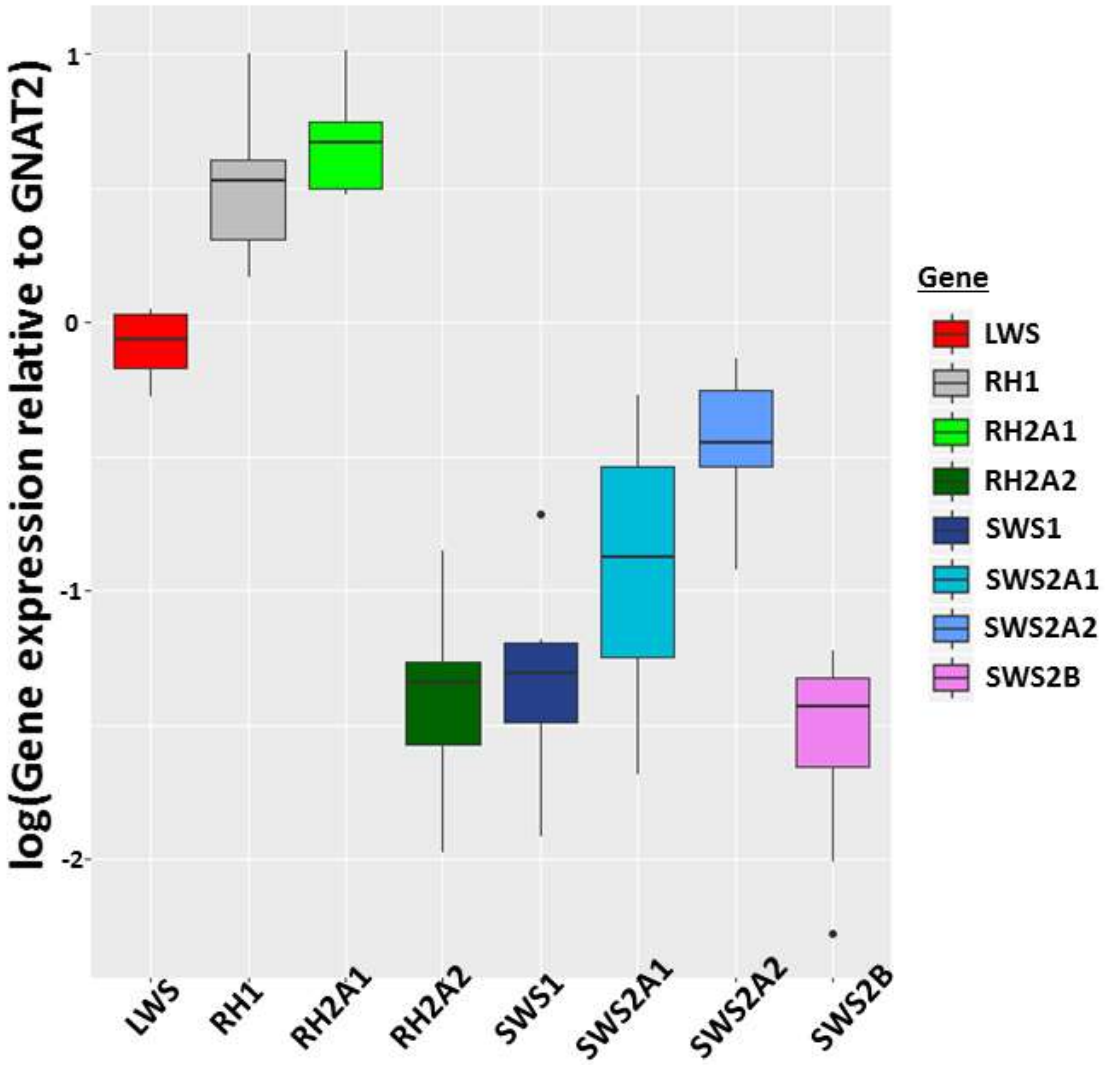

Figure 12: Log transformed opsin expression normalized to *Gnat2* (see: Dalton et al., 2015), quantified using digital-PCR from starry flounder whole eyes (n = 5).

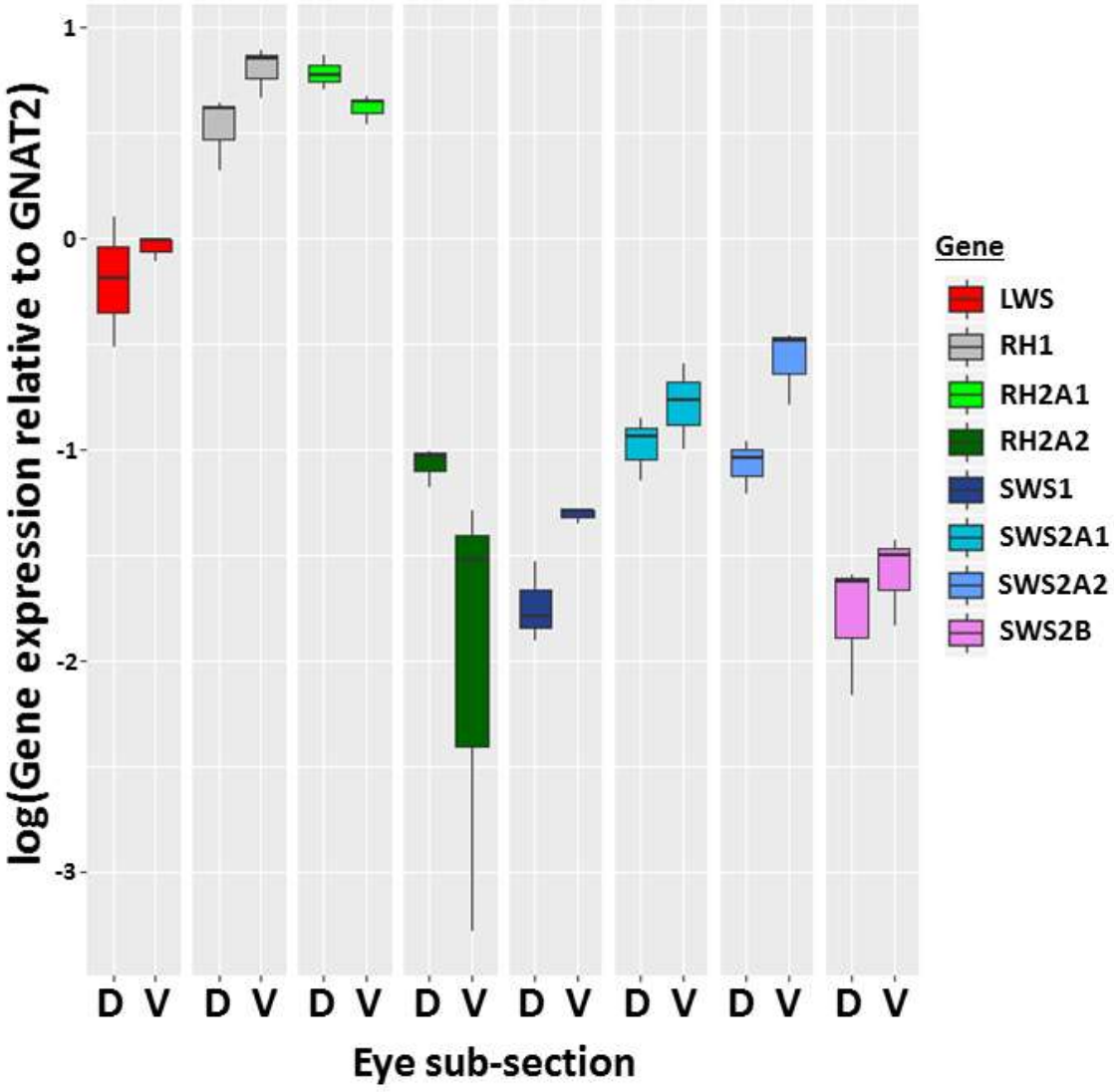

Figure 13: Log transformed opsin expression (panels = visual opsin gene normalized to *Gnat2*) quantified using digital-PCR from starry flounder dorsal (D) and ventral (V) retinas (n = 3).

Discussion

Visual opsin repertoire and visual pigments

The juvenile starry flounder has a large number of visual opsin genes, each with orthologs in other, closely related species. Starry flounder opsins are related to one another in a manner consistent with the known evolutionary relationships among opsin subfamilies. RH2A paralogs are present in two families of Pleuronectiformes (i.e., Scophthalmidae and Pleuronectidae), suggesting a pleuronectid-specific RH2A duplication event (Rennison et al., 2012). In addition, we found SWS2A paralogs from a percomorph-specific duplication event first reported by Cortesi et al. (2015). The rather large number of sequences from each clade, including the flatfish-specific paralogs, meant that we were able to identify clade-specific amino acid substitutions. Although associating amino acid sequence variation with differential wavelength sensitivity is reliable for only a few positions in the sequence (Yokoyama and Radlwimmer, 1998) the observation that some clade-specific substitutions occurred in the retinal binding pocket and key tuning sites suggests that the variation observed influences visual function.

The goal of the RNA-Seq experiment was to obtain full-length coding sequences for the visual opsins. Phylogenetic analysis was used to assign these transcripts into their respective gene family. P-distance was used to infer the evolutionary relationships among sequences, and simply measures the proportion of nucleotide differences between two sequences, and trees were built using the Neighbor-Joining method (Saitou and Nei, 1987). This method assumes a constant mutation rate and equal base frequency, and does

not correct for multiple substitutions at the same site or mutation rate biases. More complex evolutionary models may be employed that consider molecular phenomena not accounted for here, for example, transitions and transversions (Kimura, 1980) and base frequencies that deviate from 0.25 (Felsenstein, 1981).

The number of visual pigments detected using MSP corresponded well to the opsin repertoire and showed that these opsins were functional in the retina. In comparison with barfin flounder (*Verasper moserii*), also in the Pleuronectidae family, and with seven (one fewer SWS2) visual pigment types (Kasagi et al. 2015), the starry flounder peak absorbances differed slightly. Kasagi et al. (2015) reconstituted opsin photopigments and measured *Sws1* (λ_{max} = 336.8±0.9 nm), *Sws2A* (λ_{max} = 482.3±2.2 nm), *Sws2B* (λ_{max} = 415.8±2.0 nm), *Rh2A1* (λ_{max} = 505.9±6.5 nm), *Rh2A2* (λ_{max} = 489.5±2.5 nm), *Lws* (λ_{max} = 551.9±6.7 nm), and *Rh1* (λ_{max} = 494.1±2.0 nm). Thus, the starry flounder visual pigments absorbed at longer wavelengths than the corresponding barfin flounder reconstituted pigments. Parry et al. (2005) found slight differences between cichlid λ_{max} measurements derived from *in vitro* opsin reconstitution experiments and *in vivo* photoreceptors measured by microspectrophotometry. Kasagi et al. (2015) did not reconstitute both SWS2A paralogs, their *Sws2A* data is based on the *Sws2A1* ortholog. Amino acid differences in the retinal binding pocket and at key tuning sites between starry flounder and barfin flounder orthologs may explain the absorbance differences.

The absorbance of a visual pigment is determined by the combination of its opsin and chromophore (Hárosi 1994). Fish are known to utilize two vitamin-A derived chromophores, 11-cis-retinal (A1) and 11-cis-dehydroretinal (A2) (Isayama and Makino, 2012). Any opsin coupled to a vitamin A2-based chromophore will exhibit an absorbance

with greater λ_{max} than the same opsin coupled to a vitamin A1-based chromophore. Such shifts in absorbance can be quite pronounced, reaching ~ 65 nm for the L visual pigment in some fishes (Hárosi, 1994). Although computed λ_{max} shifts based on mathematical models (Hárosi, 1994) could not account for the variation in S visual pigments measured, this was not the case for the M and L visual pigments. For instance, assuming that the 527 nm λ_{max} measured was the result of an RH2 opsin couple to a vitamin A1 chromophore, the predicted λ_{max} for this opsin coupled to a vitamin A2 chromophore is 567 nm. Thus, the λ_{max} of the M visual pigments and that of the L visual pigment could be explained by different amounts of vitamin A1- and A2-based chromophores present in the outer segments of the cones measured. To disambiguate between sources of the absorbance measured, we assessed chromophore content by High Performance Liquid Chromatography (HPLC), and found only vitamin A1 in the juvenile starry flounder retina.

Retinal specializations for benthic existence in shallow waters

Fish retinas are exposed to different light depending on the direction from which it came (e.g., downwelling and upwelling light). Variation in opsin expression can facilitate visual adaptations, or spectral tuning, to the light environment. Large repertoires can act like a generalist's toolkit, with opsins sensitive to a wide range of wavelengths, from which specialization to particular light environments can be made. Differences in opsin expression among sympatric populations and species of Lake Victoria cichlids has been proposed as a driver of speciation (Seehausen et al., 2008). In wild-caught Lake Malawi cichlids, *Lws* and *Rh2Aα* are co-expressed in double cones of the ventral retina.

However, when 3 day post-fertilization cichlids were illuminated from below for six months, co-expression occurred in the dorsal and ventral retina (Dalton et al., 2015). Intra-retinal variation is prevalent among fishes, as seen in red breast cichlids, guppy (Levine et al., 1979), zebrafish (Takechi and Kawamura, 2005), archerfish (Temple et al., 2010), and four-eyed fish (Owens et al., 2009). Starry flounder are no exception. Juvenile starry flounder retinas have greater RH2 transcripts and fewer RH1, SWS1, and SWS2 transcripts in the dorsal retina. This regional spectral tuning of opsin expression may represent an adaptation of the visual system to benthic life in shallow coastal waters.

Juvenile starry flounders of the size examined in this research are commonly found in sandy and gravel beaches of moderate depth (1-20 m) where the light environment varies substantially in spectrum and intensity with line of sight (Novales Flamarique and Hawryshyn 1993, 1997). In particular, downwelling light is at least three to four times more intense than sidewelling light and will comprise UV wavelengths (< 400 nm), which may or may not be present in sidewelling and upwelling illumination, depending on depth. The overall spectrum of light in these coastal waters peaks between 520-540 nm (Novales Flamarique and Hawryshyn, 1993).

In such a diverse light environment, and given its demersal life style following metamorphosis, the starry flounder has evolved a highly specialized retina. The region of greater cone density expands from the dorso-nasal to the upper dorso-temporal retina, looking downward and posteriorly from both eyes, but also horizontally from the migrated eye (Figure 4). Because this region was associated with a full repertoire of visual pigments and the presence of unequal M_{527}/M_{545} and M_{527}/L_{557} double cones and rare instances of single corner cones, it likely subserves high resolution colour vision.

The long outer segments of cones in this region of the retina further suggests that sensitivity to light is strongest here, in accordance with the lower intensity of the upwelling and side-welling spectra that it receives. There are at least two functional reasons why this specialized area may have evolved. First, like other flatfishes (Fujimoto et al., 1991), starry flounder employ active camouflage for crypsis and, at shallow depths, the substrate will vary both in colour and texture. A high resolution and colour vision area could mediate camouflage by precisely detecting the size of substrate components and their colour in a complex environment. Double cones can contribute to background matching (Loew and Lythgoe, 1978) and wavelength discrimination (Pignatelli et al., 2010). Second, the minute zooplankton that the juvenile feeds upon are known to reflect or absorb wavelengths that are different from the background, enhancing their contrast to an animal with a high resolution colour vision system that, in addition, comprises UV cones (Novales Flamarique, 2013, 2016). Starry flounder of the approximately the same size studied here were found to forage primarily on amphipods, mostly from the genus *Gammarus* and *Corophium* (Orcutt, 1950). These amphipods are primarily benthic dwelling, and *Corophium* in particular, inhabit sandy burrows in the substrate (Barnard et al., 1988).

The various mosaic domains found in the dorso-nasal retina could further mediate different visual tasks. For instance, if the double cones act as a waveguide to detect the polarization of light. These waveguides could direct light to the UV receptors in either the horizontal or vertical plane, as seen in rainbow trout (Hawryshyn, 2000, Novales Flamarique et al., 2008). Distinct horizontal and vertical channels could be used to analyze the polarized light field in natural waters and to sense polarization contrast of

targets, such as zooplankton (Novales Flamarique et al., 1998; Novales Flamarique and Browman, 2001).

The lower half of the retina is well suited to view silhouettes of objects on a high intensity background. This area was associated with equal (M_{527}/M_{527}) double cones and higher expression of short wavelength opsins, indicating a predominance of UV and S cones in comparison with the dorsal retina. The emphasis on expression of M, UV and S visual pigments, whose combined sensitivity range would span the spectrum of wavelengths transmitted in the water column (Novales Flamarique and Hawryshyn, 1993), is optimally suited for luminosity-based detection of dark silhouettes on a bright background. The ventral retina could therefore be used to detect predators that attack from above. Other species whose juveniles also inhabit these waters, like the salmonid fishes, have M cones with λ_{max} that also match the peak wavelengths transmitted (Cheng and Novales Flamarique, 2007). These cones are the primary contributors to the OFF retinal response, i.e., the response to decrements of light (Novales Flamarique and Wachowiak, 2015), as occurs when predators block the downwelling light. We therefore predict that the M_{527}/M_{527} cones will also drive the OFF response in juvenile starry flounder. The dominance of UV and S cones in this region of the retina, coupled with the demersal life style of juvenile starry flounder, may reflect a retinal specialization for feeding on benthopelagic zooplankton, which are known to reflect UV and short wavelength light (Novales Flamarique, 2013, 2016). Reflections in the UV are particularly enhanced with increased angle of incidence on the zooplankton (Gur et al., 2015), which would be the optical scenario when perceiving reflections from zooplankton above them, as is the case when this fish strikes its prey (Bergstrom and Palmer, 2007).

To test this hypothesis, one could compare behavioural observations of starry flounder feeding on UV scattering mysid shrimp and opaque (UV absorbing) amphipods. Alternatively, one could quantify strike frequency, angle, and success directed at mysid shrimp in controlled UV-rich and UV-absent light environments (Leech and Johnsen, 2006). Zebrafish UV cones enhanced the foraging performance (e.g., strike distance and angle). Wild-type zebrafish and mutants with diminished UV cone populations were observed foraging in either broad spectrum light, or under UV-absent conditions. The wild-type zebrafish performed significantly better under broad spectrum light, but there was not difference between the wild-type and mutants under UV-absent light conditions (Novales Flamarique, 2016).

Studies on the adults of other flatfishes have generally reported smaller cones in the dorsal versus the ventral retina, though a statistical analysis of cone densities was never conducted (Engström and Ahlbert, 1963; Evans and Fernald, 1993). Longer outer segments have also been observed in the dorsal retina of some adult European flatfishes (Engström and Ahlbert, 1963). These observations are consistent with the general trends found in our study. Investigations of opsin expression and visual pigment absorbance in the retina of the winter flounder, *Pseudopleuronectes americanus*, (Evans et al., 1993; Hoke et al., 2006) and of opsin expression in the retina of the Atlantic halibut, *Hippoglossus hippoglossus* (Helvik et al., 2001), have shown the presence of equal (M_{527}/M_{527}) and unequal (M_{527}/M_{545} and M_{527}/L_{557}) double cones in these species as well. In contrast to our findings, however, equal double cones were only found, by microspectrophotometry, in the dorsal retina of the adult winter flounder (Evans et al., 1993). The adult fish examined in their study were 7-10 times larger than the juveniles

reported in this study, and it is possible that novel opsin expression patterns, as occurs throughout metamorphosis (Evans et al., 1993; Hoke et al., 2006), persist into the reproductive adult stage. Future research with different size animals should answer this question.

The large opsin repertoire in starry flounder facilitates regional specialization of the retina. Opsin expression appears to be driving the major histological and biochemical differences we observe between the dorsal and ventral halves of the retina. We predict that this fine-tuning is enhanced by photoreceptor plasticity and opsin gene duplication and divergence.

Contributions by collaborators

The histology and microspectrophotometry (MSP) described in this chapter was performed by Dr. Iñigo Novales Flamarique. Dr. Novales Flamarique performed the majority of sectioning, imaging and statistical analyses of the starry flounder retina topography, however, Tom Iwanicki did assist Dr. Novales Flamarique with tissue collections, fixation, and some sectioning. Tom Iwanicki and Dr. Novales Flamarique collected the MSP data together at Simon Fraser University. We feel the data play an important role in the narrative and so they were included in this chapter. All other experiments (e.g., RNA-Seq, digital-PCR, phylogenetics) were conducted by Tom Iwanicki, with guidance provided by Dr. John Taylor.

Chapter 3 – Light induced changes in opsin expression and its influence on visual ability estimated using a camouflage-based behavioural assay

Introduction

Chapter 2 revealed that juvenile starry flounder have a regionally specialized retina, characterized by varying cone densities, outer segment size, pigment localization, and opsin expression between the dorsal and ventral halves. We speculate that this intra-retinal variation is adaptive, and has enhanced opsin gene diversity and divergence post-gene duplication. To test the hypothesis that changes in opsin expression reflect 'spectral tuning' of the retina, we aimed to induce changes in expression by holding starry flounder in different light environments, and if changes occurred, test if there is an impact on visual performance.

Sensory Ecology studies the mechanisms at the periphery, processing, higher-order functions, and ecological relevance of the sensory systems in animals (Stevens, 2013). Two animals can be virtually touching but worlds apart in terms of sensory ability. Ambon damselfish (*Pomacentrus amboinensis*) use UV-reflective facial patterns to identify conspecifics (Siebeck et al., 2010), a signal unavailable to the human observer. Vision offers an excellent avenue from which sensory ecological hypotheses can be tested. The fundamental molecular unit for vision is the opsin. Teleost fish possess a remarkably large number of visual opsins when compared to other vertebrates (Rennison et al., 2012; Davies et al., 2015). Guppies (Rennison et al., 2011) and zebrafish (Davies et al., 2015) have ten, and starry flounder have eight visual opsins (see chapter 2). Humans

and birds, by contrast, possess only four and five visual opsins, respectively (Olsson et al., 2015), while most mammals only have three (Jacobs, 2009).

The function and evolution of large opsin repertoires is uncertain. Population- and species-level comparisons of opsin expression have tested the sensory bias hypothesis. In Lake Victoria cichlids, variation in *Lws* expression with depth may drive speciation (Terai et al., 2006; Seehausen et al., 2008). However, Smith et al. (2011) found significant differences in cichlid opsin expression that did not correspond to predicted visual performance models. Intra-specific opsin expression was different between shallow and deep water fish, as well as among fish from different populations sharing similar ambient light environments. Under the models, these differences were not adaptive to *in situ* light measurements of the local environment (Smith et al., 2011). Variation in opsin expression among different populations of guppies may be functional in light of sexual selection (Sandkam et al., 2015). Although the evidence the expression in females correlates to male nuptial colouration, there is a disconnect between opsin expression and mate choice. Rarely have studies demonstrated a direct connection between opsin expression and its impact on variation in vision.

This study builds on behavioural experiments on a diversity of species. Karl von Frisch's grey card experiment provided the first empirical evidence that honey bees see colour (Frisch, 1950). Beckmann et al. (2015) tested negative phototaxis in Onychophora (velvet worms) using LEDs with different wavelengths and intensities. This species avoids 465 nm light, consistent with electrophysiological recordings that indicated their single visual pigment was most sensitive at 474 nm. Smith et al. (2012) measured opsin expression in Lake Malawi Cichlids reared in different light environments and tested the

optomotor response. They discovered that LWS expression varied with light environment, and that variation was found to account for approximately 20% of the observed variance in optomotor response. Sakai et al. (2016) recently found that variation in LWS expression in guppies were related to behaviour in a visual performance assay. Out of nine cone opsins, guppies raised under orange light had higher *Lws-3* expression and had significantly higher visual sensitivity to 600 nm light measured using an optomotor behavioural assay.

Animal colouration is remarkably diverse and serves a variety of functions. Thayer (1909) introduced the concept of disruptive colouration, masquerade, and countershading, and argued that all colouration served some form of camouflage. Cott (1940), equipped with empirical evidence, expanded our understanding of the ecological function of animal colouration to include advertisement, in the form of aposematic signals and sexual signals during courtship, and disguise, in the form of Batesian mimicry (Bates, 1862) and Müllerian mimicry (Müller, 1878). Most animals change colour slowly or have stable colouration that arises during development. Other animals are capable of rapid colour change, or adaptive camouflage, that can be used to inform aspects of the animal's visual performance (Sumner, 1911; Stevens and Merilaita, 2009; Stuart-Fox and Moussalli, 2009).

In a pilot study, we photographed a starry flounder on a grey, black-white, and red-green substrate. This pilot study revealed the starry flounder's rapidly adaptive camouflage (Figure 14). To evaluate visual performance we exploited the camouflage response. Adaptive camouflage in Pleuronectiformes had been described as early as Sumner's 1911 monographs, which found that turbot (*Rhomboidichthys podas* and

Lophopsetta maculata), summer flounder (*Paralichthys dentatus*), and winter flounder (*Pseudopleuronectes americanus*) are capable of adaptive camouflage over a period of days (Sumner, 1911). Juvenile plaice (*Pleuronectes platessa*) camouflage was tested on a uniform substrate, black and white gravel, and natural gravel, and a stable body pattern was achieved within 15 minutes of being exposed (Kelman, 2006). Adaptive camouflage response in fish is visually mediated. When vision is deprived, although pigment changes can still occur, fish do not adaptively camouflage to the substrate upon which they find themselves (Pouchet, 1876; Sumner, 1911).

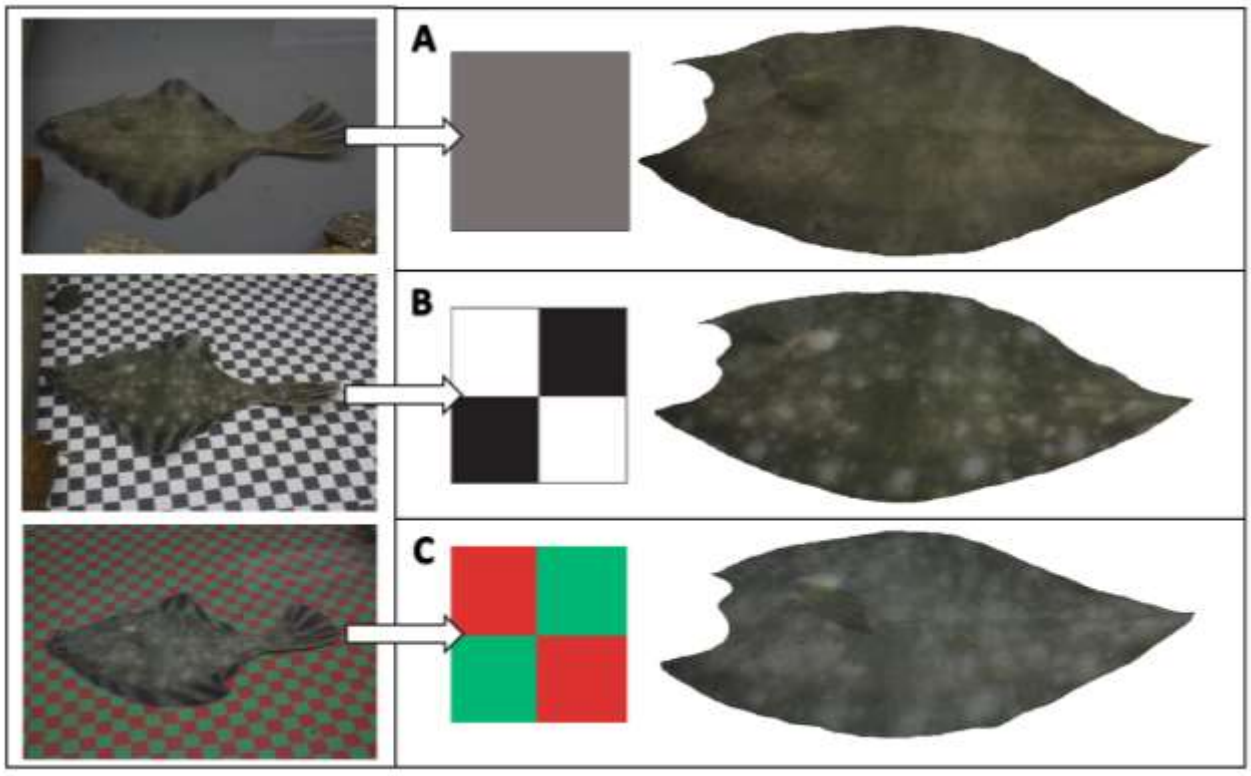

Figure 14: Pilot study of an individual starry flounder's camouflage response to three different substrates; (A): grey, (B) black-white, (C) red-green. Changes were observed within seconds, and the pattern was stable within minutes.

Barbosa et al. (2008), using a behavioural assay similar to Sumner (1911), found that cuttlefish display three basic camouflage patterns (i.e., uniform, mottle, or disruptive). Curiously, the cuttlefish only possess a single visual opsin. Peacock flounder (family: Bothidae) displayed only two basic camouflage patterns (i.e., uniform or mottle) in a field study investigating their substrate preference in the wild (Tyrie et al., 2015), and unfortunately the peacock flounders opsins and visual pigments have not been measured.

Previous studies have relied on qualitative measurements of pattern. We wanted to obtain objective measurements of the starry flounder camouflage response. Troscianko and Stevens (2015) designed the Image Calibration and Analysis Toolbox software used to measure colour and pattern. The toolbox has a plugin for pattern analysis based on Fast Fourier bandpass filtering, similar to that used in Tyrie et al. (2015) and Spottiswoode and Stevens (2010). Images are filtered at eight different spatial frequency bands, and the power (intensity of light) that remains after filtering is measured. From that analysis, four camouflage indices are derived to quantify different aspects of an image's pattern into a single unit. The 'standard deviation of power' measures the amount of contrast in an image. The 'standard deviation of luminance' measures the amount of contrast in an image when modelled using human vision. The 'maximum frequency band' represents the frequency band with the highest power, in other words, the band corresponding to the dominant marking size in an image. Finally, 'proportion of power within the maximum frequency band' quantifies how important the maximum frequency band is to the overall pattern of an image.

The aim of this study was to test the hypothesis that light environment can induce changes in opsin expression, and if so, does opsin expression vary with camouflage

response. A paucity of data has connected varying opsin expression and visual performance. Through measuring gene expression and exploiting the starry flounder's camouflage response as a measure of visual performance, we aim to test hypotheses about the function of large opsin repertoires in fish.

Methods

Fish Collection and Light Environment

Fish were collected by beach seine at low tide between 10:00 – 12:00 AM in May 2015 at Willows Beach, Victoria, British Columbia, Canada. The seine net was deployed from a small aluminum boat at a depth of approximately 3 m, or by hand at around 2 m depth. Sixteen starry flounder were transported to the Outdoor Aquatics Unit at the University of Victoria, and held under ambient light in 12^{o}C recirculating seawater. All sampling was approved by the University of Victoria Animal Care Committee (protocol # 2015-005(1) and 2015-003(1)) which abides by regulations set by the Canadian Council for Animal Care. Starry flounder (TL = 172±28mm, m = 74.8±37.8g) were randomly distributed into their experimental enclosures on July 22, 2015. The light environments were comprised of four fully enclosed tanks (*lwh* = 49"×19"×25") on a stand-alone 12^{o}C recirculating sea-water system (Figure 15). The tanks were partitioned by opaque plastic in the middle and each half was randomly assigned either broad spectrum (Roscolux #3410) or green-filtered light treatment (Roscolux #90) (Figure 16). Starry flounder were placed in pairs into 8 enclosures and held in the light environment for seven weeks. During that time they were fed krill at 1% body weight per day, adjusted weekly at an estimated 2% specific growth rate. Feeding occurred once daily through a 2-cm hole in

the lid that was otherwise sealed by a black rubber stopper to inhibit non-filtered light from entering the tanks.

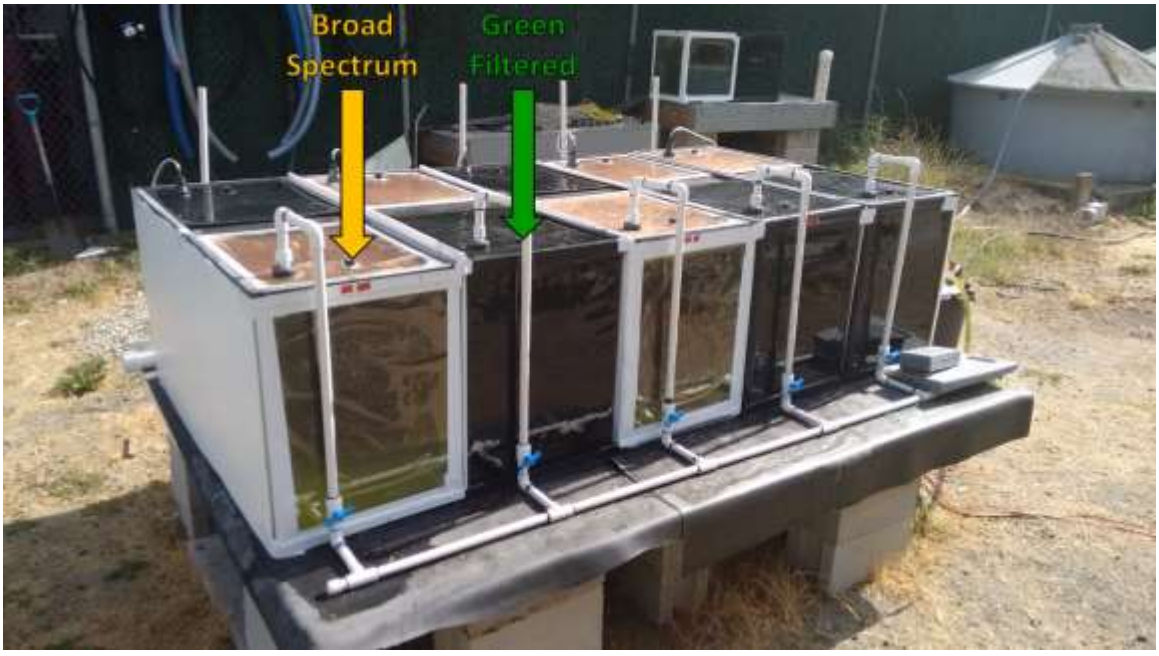

Figure 15: The standalone seawater system, housed at the University of Victoria's Outdoor Aquatics Unit, with their respective theatrical gels (e.g., broad spectrum sunlight, Roscolux #3410 and green filtered light, Roscolux #90).

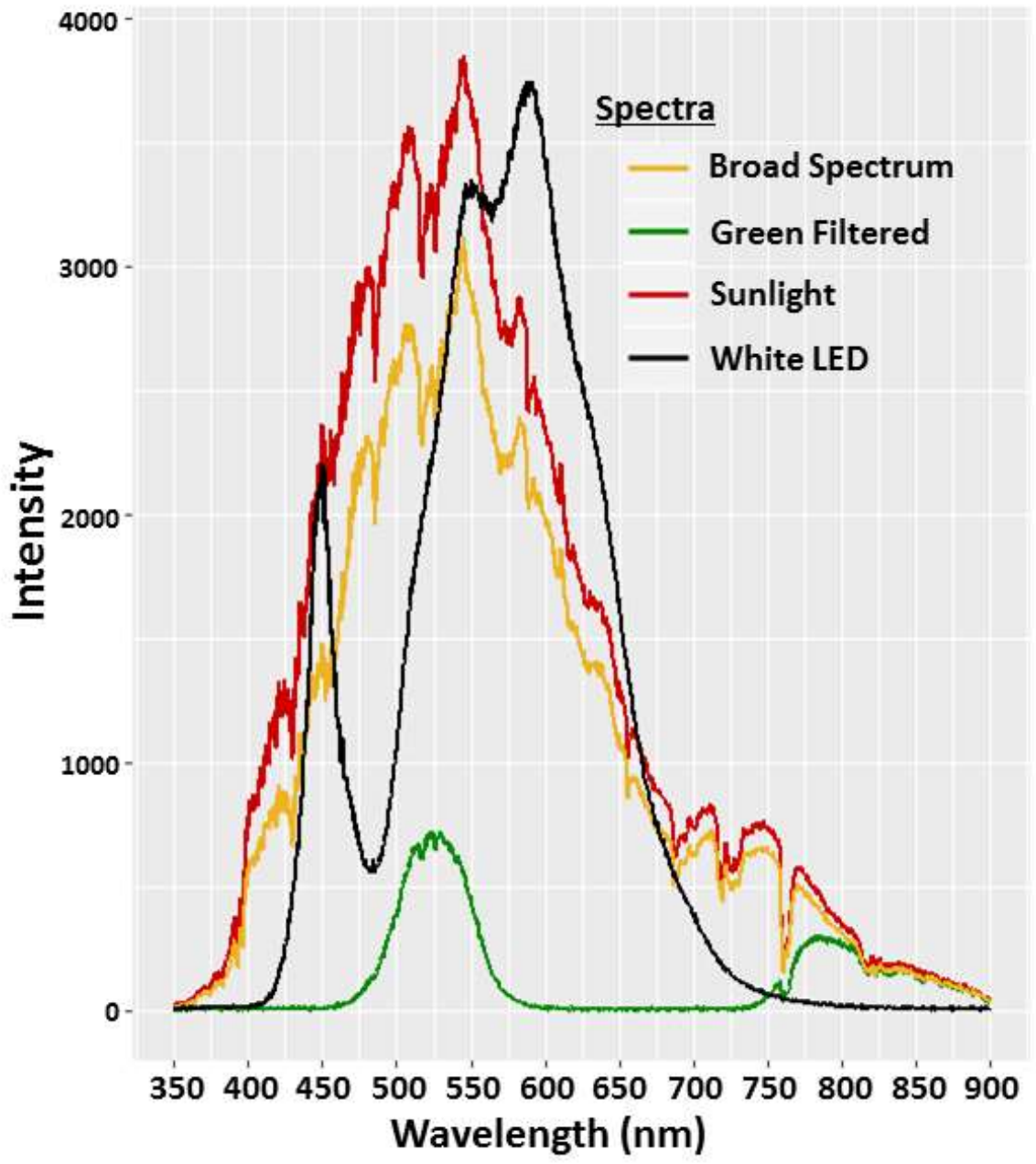

Figure 16: Spectra measured from the sun (red), Roscolux #3410 (yellow), Roscolux #90 (green), and XLamp Neutral White 4000K LEDs (black) used during the camouflage experiment. Spectra were measured through glass and generated using a USB2000 Spectrophotometer (OceanOptics Inc.) and the absorbance software in OOOIBase.

Behavioural Assay

The behavioural assay was conducted in a dark room with a sea-tray table containing 12^{o}C seawater on a recirculating system. The arena was comprised of a 30 cm diameter, 50 cm tall plastic tube with four XLamp Neutral White 4000K LEDs (Cree, Inc.) mounted on top of the tube in pairs at opposite ends (Figure 16, Figure 17). Neutral white foam core was used to reflect light into the arena to reduce hotspots and shadows. Laminated substrates were inserted vertically on the inside of the tube, and positioned on top of a matching 50cm^2 substrate. The substrates were designed in Adobe Photoshop CS6 on an Apple iMac running OS X v10.8x. The colour space used was CMYK US Web Coated SWOP v2. The printer was an Epson Stylus Pro 9890 with Epson UltraChrome K3® Ink package, and substrates were printed on Epson Premium Luster Photo Paper (206). Substrate pigments were selected with the saturation resulting in equal percent-reflectance of photons for all colours. Equal reflectance of photons resulted in total light intensity being equal for all colourful checkers, limiting the spectral signal from the checkerboards to hue (or wavelength), and excluding contrast as an explanation for a camouflage response (if observed). Percent-reflectance was calculated using an USB2000 Spectrophotometer (OceanOptics Inc.) and the reflectance software in OOOIBase. The checkerboards were designed to illicit a camouflage response, and we do not predict that starry flounder are capable of accurately matching the substrates provided. Photos of fish were captured using a Nikon D3100 Digital SLR camera and an AF Nikkor 50mm 1:1.4D lens. The camera settings remained constant for the duration of the experiment (aperture = F5.6, shutter speed = 1/5”, ISO = 200, exposure compensation

= +0.7). The camera was mounted on a tripod approximately 1.5 meters above the behavioural arena.

Figure 17: Photos of the behavioural arena used during the starry flounder camouflage assay. An example of one individual camouflaging on a black-and-white substrate is shown (right). Photo credit: James Robinson.

Beginning on September 9, 2015, two fish from a randomly selected enclosure were used on each of eight days. Fish were chosen by balanced design, alternating between broad-spectrum and green-filtered enclosure daily. One fish was selected (by coin toss) for the behavioural trial and transferred to the experimental arena. Fish were acclimated to the arena for 30 minutes before the five substrate assay was run. The other fish was euthanized and dissected to provide baseline expression, unaffected by the bright white lighting in the behavioural experiment. All behavioural trials began at 9:00AM to control for the effects of circadian rhythms. Fish were exposed to five substrates in the following order at intervals of 30 minutes: grey, blue-green, blue-red, red-green, and black-white. Photos were captured at intervals of 30 seconds.

Image Analysis

Images were captured in RAW file format. Multispectral images were generated and analyzed using the Image Calibration and Analysis Toolbox (Troscianko and Stevens, 2015). All images were calibrated to a standard (PTFE sheet) to control for variation in light reflecting off the different substrates. Fish camouflage response was characterized from a cropped image. Cropping was performed by and assistant, Amy Liu, who was not aware of the study design and which light environment the fish originated from. Image cropping followed a standard protocol, in short: a polygon representing the region of interest (ROI) was created starting at the base of the anal fin near the caudal peduncle. Points of the polygon were selected at the base of every third ray of the anal fin extending anterior the caudal fin. The pelvic fin, operculum, head, and pectoral fin were excluded from the polygon. The polygon extended posterior along the base of the dorsal fin (points at every third ray) back to the caudal peduncle and the polygon was closed off completing the ROI (Figure 18).

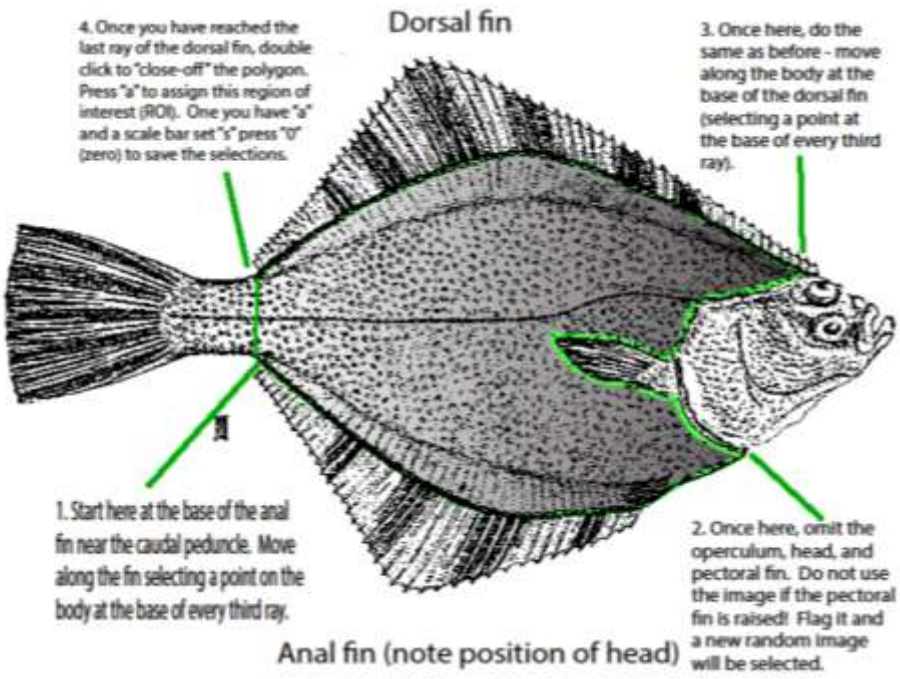

Figure 18: Region of interest (RIO) schematic for starry flounder camouflage analysis.

Granularity analysis similar to that used to quantify cuttlefish camouflage (Barbosa et al., 2008) and avian egg pattern (Spottiswoode and Stevens, 2010) was used. In short, cropped images were filtered at seven spatial frequency bands, or bandpass filters (i.e., 2, 4, 6, 8, 16, 32, 64, 128 pixels). The relative pixel energy and sum of squares per band was calculated. The band that provided the highest energy corresponds to the camouflage response (i.e., mottle, uniform, or disruptive). Image analysis was also performed on three different substrate types collected at low tide from Willows Beach, BC.

Two-way repeated measures ANOVA was run in R version 3.2.4 using the "nlme" package and Tukey multiple comparisons was run using the "multcomp" package. Analyses were based on four indices of camouflage (i.e., standard deviation of power, standard deviation of luminance, maximum frequency, and proportion power) (see: Spottiswoode and Stevens, 2010) from a total of eight fish, held for seven weeks in either

broad spectrum sunlight or green filtered light, on five chromatically different substrates. The four models run were: camouflage ~ light environment + substrate + light environment × substrate + (1|individual) + ε (see the complete R code in Appendix B).

RNA isolation and digital PCR

Eyes from the fish euthanized before the behavioural trial (i.e., baseline fish not exposed to the LED light in the behavioural assay) and those euthanized after the behavioural assay, were cut at the optic nerve and a razor blade was used to cut each eye in half. The lens was removed and the retina extracted. Retinas were frozen in liquid Nitrogen and stored at -80^{o}C. Retinas were homogenized in TriZol (Invitrogen) with zirconia beads using a mini beadbeater (BioSpec products) for 30 seconds. RNA was isolated following the manufacturer's protocol, with slight modification. The RNA pellet was washed twice (rather than once) with >75% ethanol. Contaminating DNA was digested using RNase-free DNase I (ThemoFisher Scientific, EN0521). Total RNA was quantified using Qubit® RNA Broad Range Assay Kit (ThemoFisher Scientific, Q10210). 1 µg of RNA from each sample was reverse-transcribed in 40 µl using iScript™ cDNA Synthesis Kit (BioRad).

With dPCR the number of wells on a 20,000-well chip showing template amplification, measured using locus-specific primers and Taq-Man probes (Life Technologies), is used to determine target cDNA abundance in the sample. Sample concentrations are adjusted to ensure that the estimated copies per microliter fall within the digital range of the 3D system (i.e., 200 – 2000 copies•µl-1). cDNA template varied from 0.1 to 100 ng per chip. Opsin expression was normalized, using the alpha subunit of transducin (*Gnat2*), the G-

protein activated by cone opsins, as the denominator (Dalton et al., 2015). dPCR was run on QuantStudio® 3D Digital PCR System (Life Technologies) using locus-specific primers and TaqMan probes (Table 1). Opsins were multiplexed using FAM and VIC reporter dyes. cDNA, primers, probes, and master mix were loaded onto a QuantStudio® 3D Digital PCR 20K v2 Chip, loaded with immersion oil to prevent evaporation, and sealed. After equilibrating at room temperature for 15 minutes, PCR was performed on a ProFlex™ 2x Flat PCR System (step 1: 94^{o}C × 30 sec; step 2: 55^{o}C × 2 min, 94^{o}C × 30 sec (39 cycles); step 3: 55^{o}C × 2 min, 10^{o}C hold). Chips were read using the QuantStudio® 3D Digital PCR instrument. Patterns in expression were tested using a paired student's t-test. All statistical tests were evaluated at $\alpha = 0.05$ level of significance.

Results

Experimental animals

Final fish total length (TL) and mass were not significantly different between treatments (broad spectrum: TL = 182.50±27.76 mm and mass = 78.87±33.60 g; green filtered: TL = 173.50±31.74 mm and mass = 72.70±38.23g; student's t-test, TL: t = 0.60375, p = 0.5558 and mass: t = 0.3426, p = 0.7371). There was no statistical difference in TL and mass of baseline fish (i.e., those immediately euthanized) and fish exposed to the behavioural assay (i.e., fish exposed to bright white LED for 3 hours) (baseline: TL = 165.20±24.20 mm and mass = 61.60±29 g; time 3 hours: TL = 190.80±29.42 mm and mass = 89.97±36.20 g; TL: t = -1.8925, p = 0.08006 and mass: t = -1.7296, p = 0.1067). Fish were weighed and measured before being introduced to the tanks. There was no significant difference between growth in TL (broad spectrum: ΔTL = 7.5±5.9 mm; green-

filtered: ΔTL = 4±7.2 mm) or mass (broad spectrum: Δmass = 1.2±9.3 g; green-filtered: Δmass = 0.9±9.2 g) based on light environment.

Image analysis

Four camouflage indices were measured: i) standard deviation of power, ii) standard deviation of luminance, iii) maximum frequency band, and iv) the proportion of power from the maximum spatial frequency band. Each index measures a different aspect of an image's pattern. The standard deviation of power and standard deviation of luminance measures the overall contrast within an image, the former is the objective contrast, and the latter measures contrast when modelled to human vision. The maximum frequency band measures the spatial frequency that best resembles the pattern contained within an image. Finally, the proportion of power from the maximum spatial frequency band measures how important that particular band is to the overall pattern.

The three substrate types typically found at Willows Beach, BC ranged from fine sand to large pebbles. The substrates are shown in Figure 19 and were analyzed to demonstrate the image analysis. The maximum frequency bands for fine, mottled, and disruptive sand were 8, 16, and 128 pixels, respectively. The standard deviation of power (fine: 172; mottled: 229; and disruptive: 501), luminance standard deviation (fine: 3364; mottled: 6659; and disruptive: 9673) varied consistent with expectations; the proportion of power (fine: 0.239; mottled: 0.197; and disruptive: 0.284) informs us of how important the maximum frequency band is to the overall pattern of the sand.

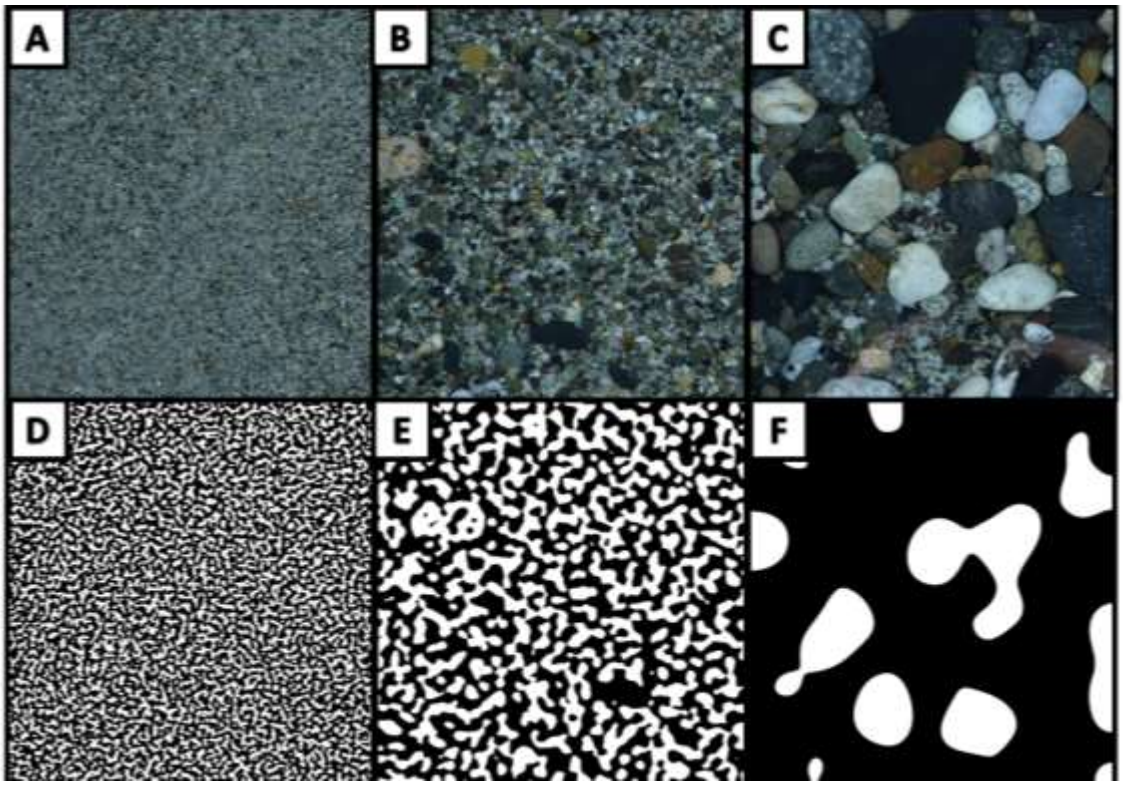

Figure 19: Substrate types from Willows Beach, BC. Fine (A), mottled (B), and disruptive (C) sand typically found at the site of starry flounder collection. The corresponding maximum spatial frequency band for each below (fine, 8 pixels, (D); mottled, 16 pixels (E); disruptive, 128 pixels (F)).

Results of the two-way repeated measures ANOVA model on the camouflage standard deviation of power from eight starry flounder on five different substrates indicated that the main effect (e.g., substrate) was significantly associated with the camouflage index ($F = 6.777$, $p = 0.0008$). The effects of light environment and the interaction between substrate and light environment did not significantly influence camouflage ($F = 2.43959$, $p = 0.1693$ and $F = 0.49367$, $p = 0.7404$, respectively). Tukey multiple comparisons indicated that the broad spectrum camouflage on the black-white substrate was significantly different than almost all other camouflage responses (broad spectrum, black-white versus: broad spectrum, grey substrate ($z = 3.122$, $p = 0.0522$), blue-red ($z = 3.606$,

p = 0.0108), red-green (z = 3.313, p = 0.0289); green-filtered, grey substrate (z = 3.544, p = 0.0135), blue-green (z = 3.578, p = 0.0118), blue-red (z = 3.313, p = 0.0256), red-green (z = 3.247, p = 0.0359)) (Figure 20).

Results of the model on the camouflage standard deviation of luminance indicated that the main effect (e.g., substrate) was significantly associated with the camouflage index (F = 4.552, p = 0.0071). The effects of light environment approached significance (F = 5.767, p = 0.0532) and the interaction between substrate and light environment did not significantly influence camouflage (F = 1.209, p = 0.3327). Tukey multiple comparisons indicated that the broad spectrum camouflage on the black-white substrate was significantly different than broad spectrum, blue-red substrate (z = 3.135, p = 0.0493) and green-filtered, grey (z = 3.506, p = 0.015), blue-green (z = 3.876, p < 0.01), blue-red (z = 3.338, p = 0.0264). Green-filtered, black-white was significantly different than green-filtered, blue-green (z = 3.3132, p = 0.0498). The difference between light environments on the blue-green substrate approached significance (z = -3.110, p = 0.0536) (Figure 21).

Results of the model on the camouflage maximum spatial frequency band indicated that the main effects (i.e., light environment and substrate) and the interaction between them was not significantly associated with the camouflage index (F = 2.538119, p = 0.1622, F = 1.981, p = 0.1297, and F = 1.805, p = 0.1608, respectively) (Figure 22). Results of the model on the proportion of power from the camouflage maximum spatial frequency band indicated that the main effects (i.e., light environment and substrate) and the interaction between them was not significantly associated with the camouflage index (F = 0.005, p = 0.9476, F = 1.939, p = 0.1365, and F = 0.264, p = 0.8981, respectively) (Figure 23). The granularity curves (see: Barbosa et al., 2008 and Tyrie et al., 2015)

qualitatively demonstrates that starry flounder held in broad spectrum light had an overall brighter appearance across the seven spatial frequency bands compared to the green-filtered (Figure 24).

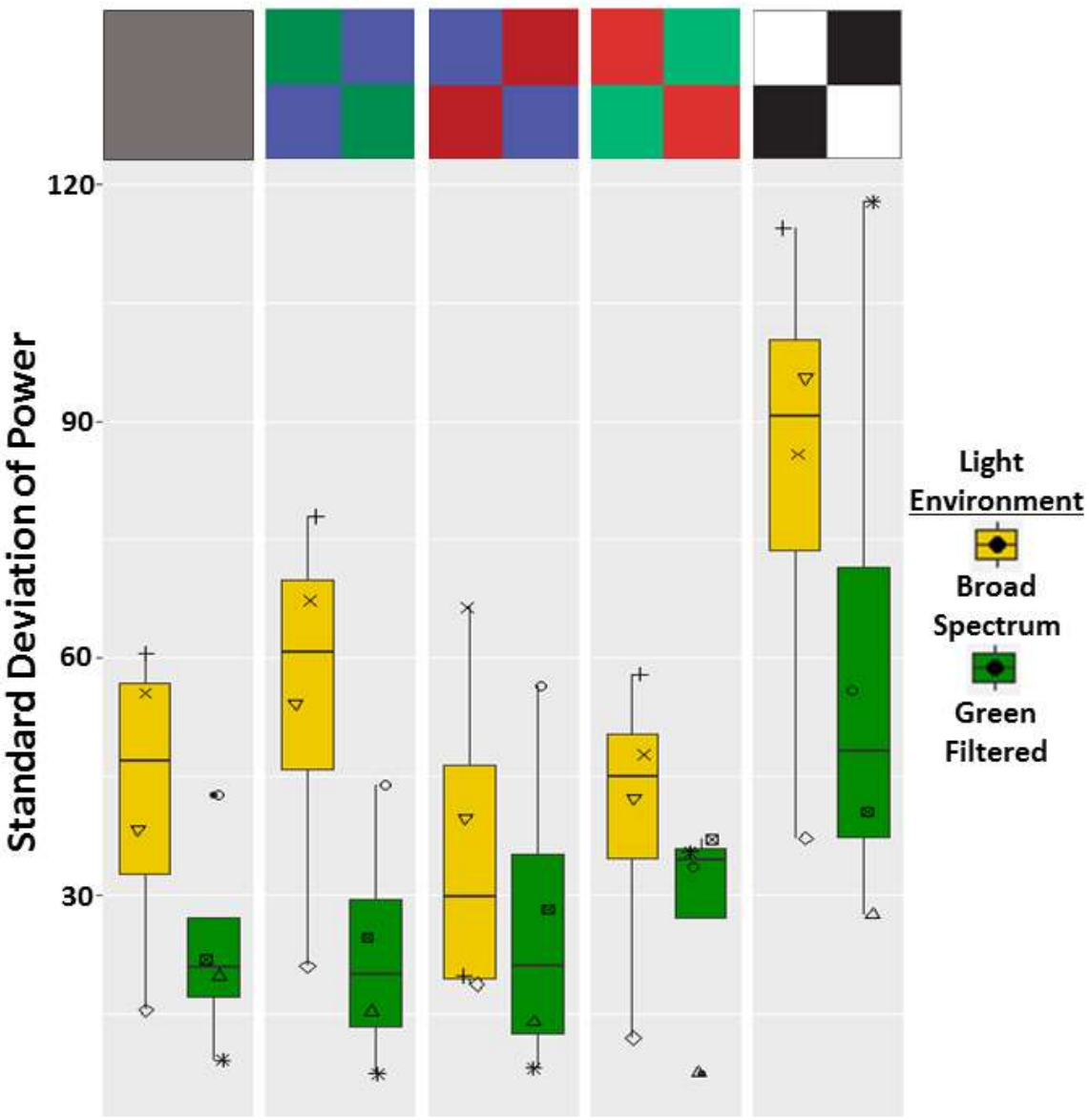

Figure 20: Standard deviation of power across seven spatial frequency bands (granularity analysis) of starry flounder (n = 8, shapes represent individuals) camouflaging in response to five

different checkerboards (top of each panel). Fish were held in either a broad-spectrum (yellow bars) or green-filtered light (green bars) environment for seven weeks.

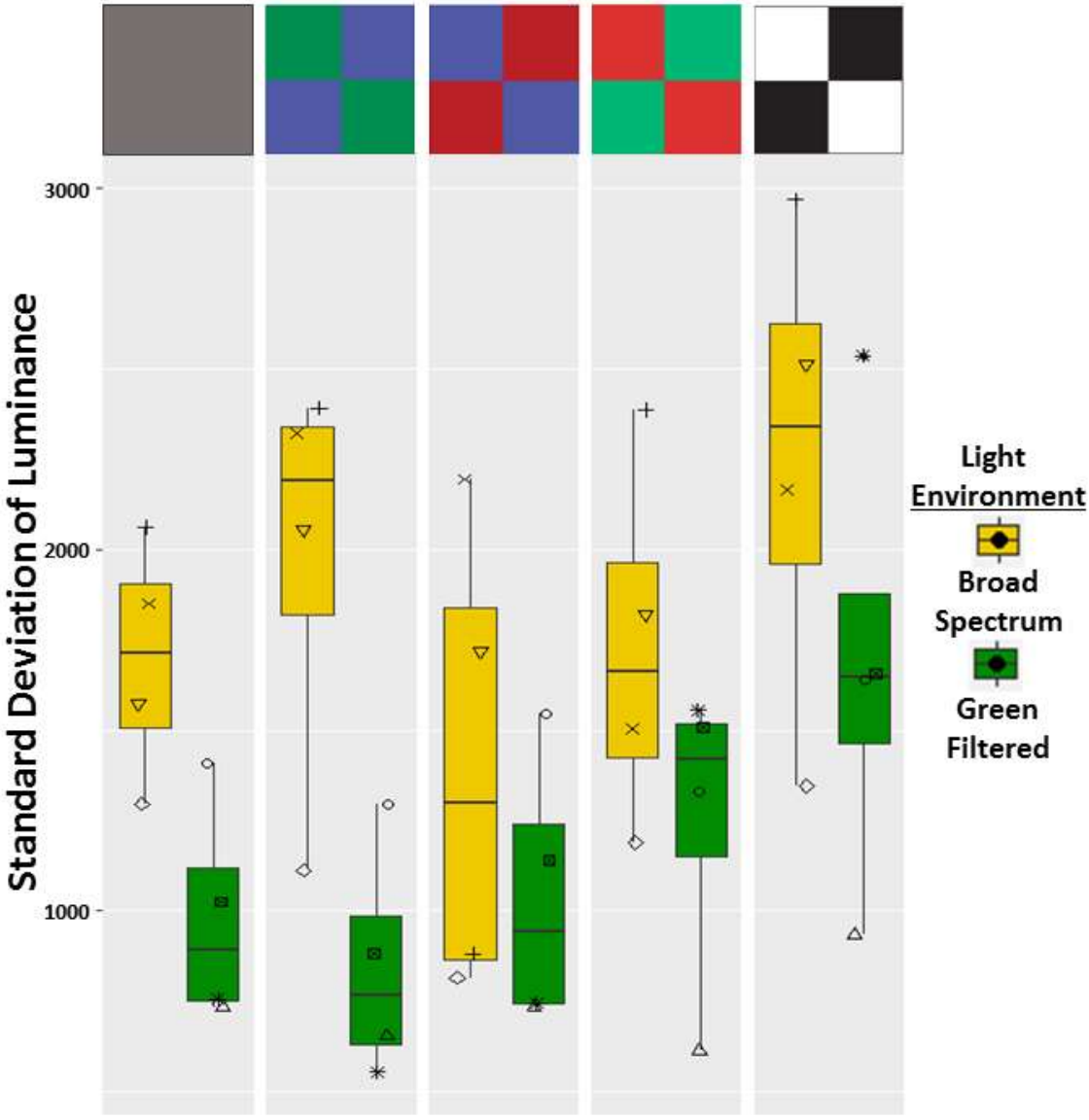

Figure 21: Standard deviation of luminance across seven spatial frequency bands (granularity analysis) of starry flounder (n = 8, shapes represent individuals) camouflaging in response five different checkerboards (top of each panel). Fish were held in either a broad-spectrum (yellow bars) or green-filtered light (green bars) environment for seven weeks.

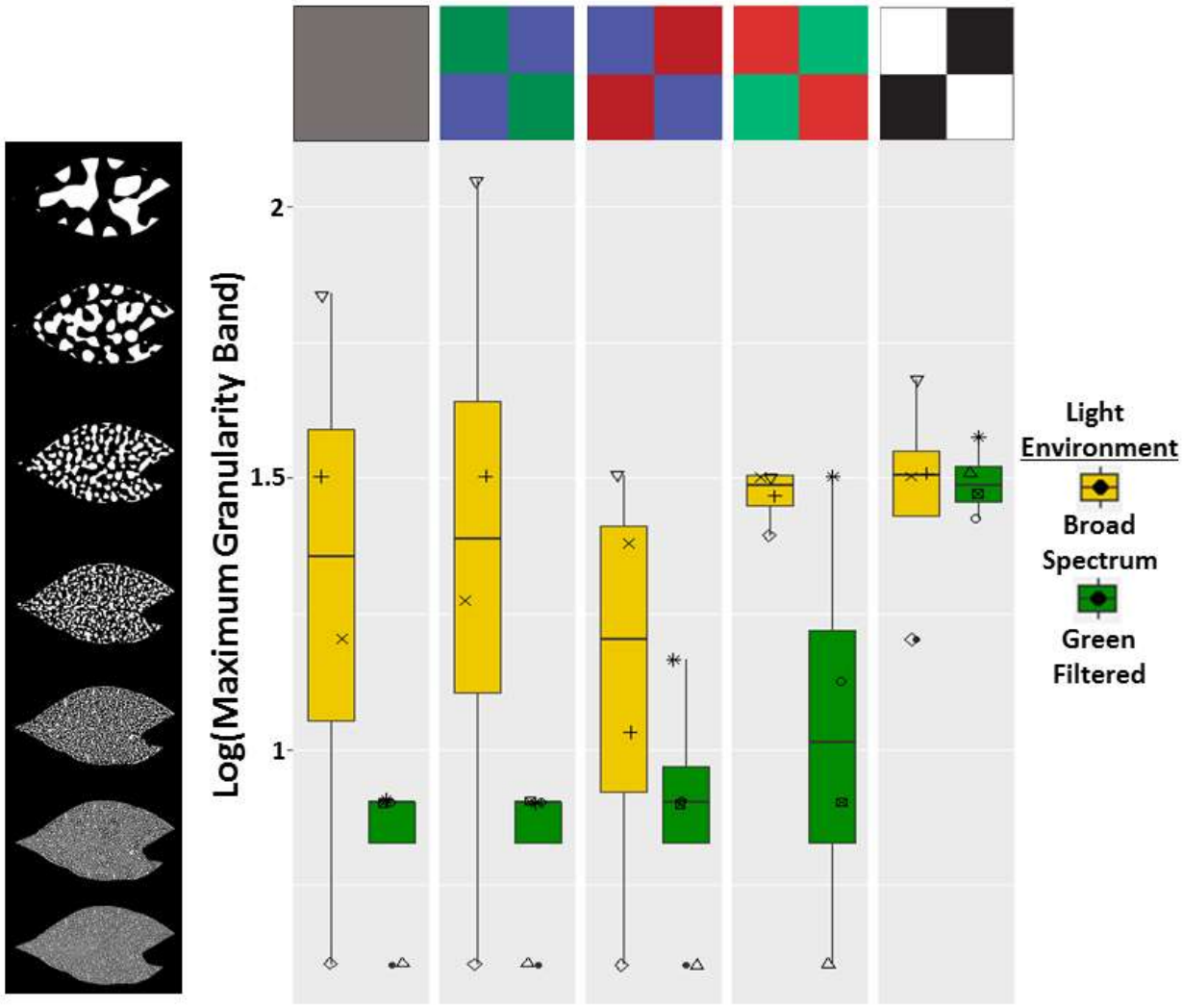

Figure 22: The spatial frequency with the highest power (granularity analysis) of starry flounder (n = 8, shapes represent individuals) camouflaging in response to five different checkerboards (top of each panel). Fish were held in either a broad-spectrum (yellow bars) or green-filtered light (green bars) environment for seven weeks. Left, y-axis shows energy maps generated for a cropped starry flounder ROI corresponding to each frequency band.

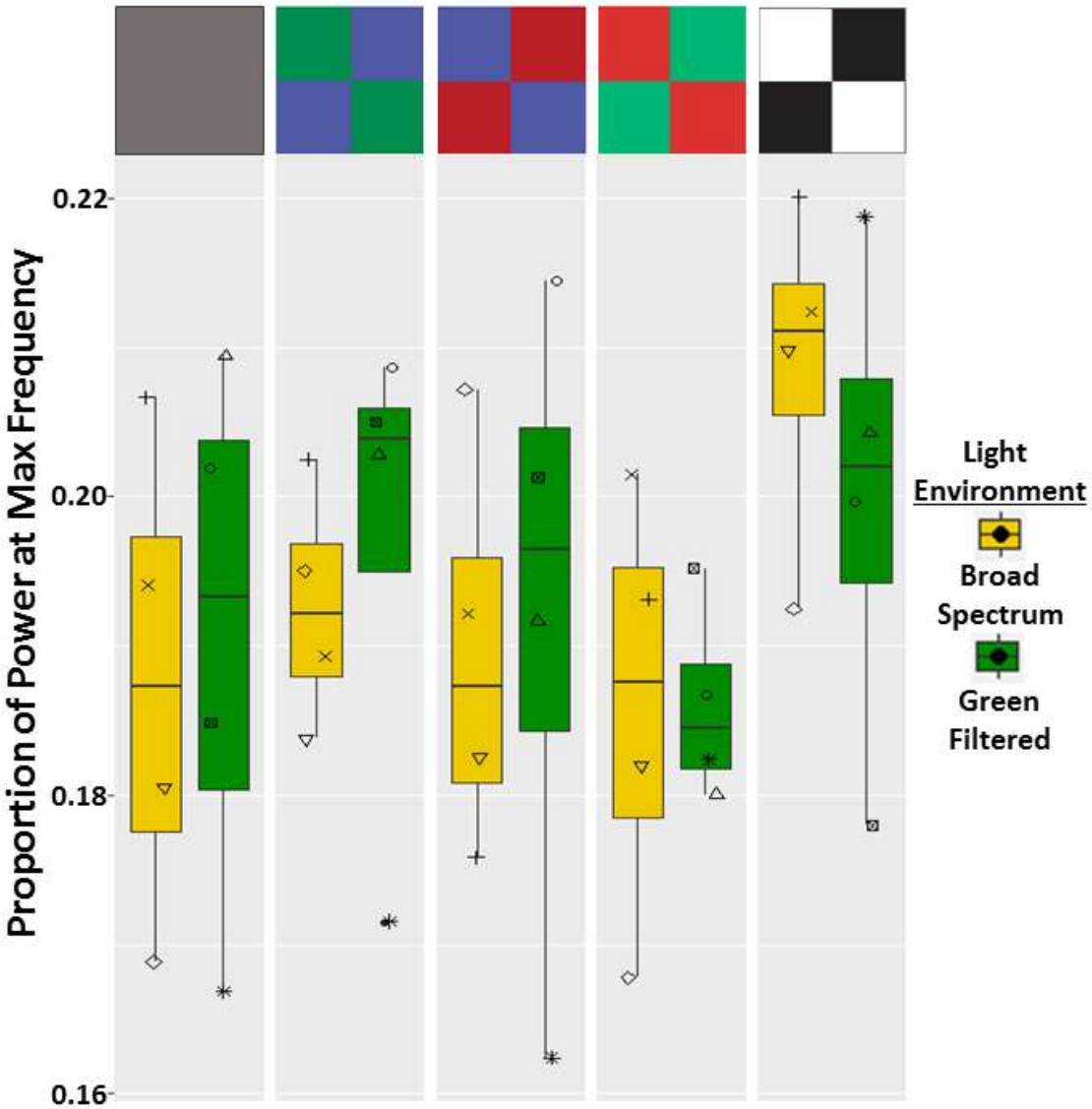

Figure 23: The proportion of power at the maximum spatial frequency band (granularity analysis) of starry flounder (n = 8, shapes represent individuals) camouflaging in response to five different checkerboards (top of each panel). Fish were held in either a broad-spectrum (yellow bars) or green-filtered light (green bars) environment for seven weeks.

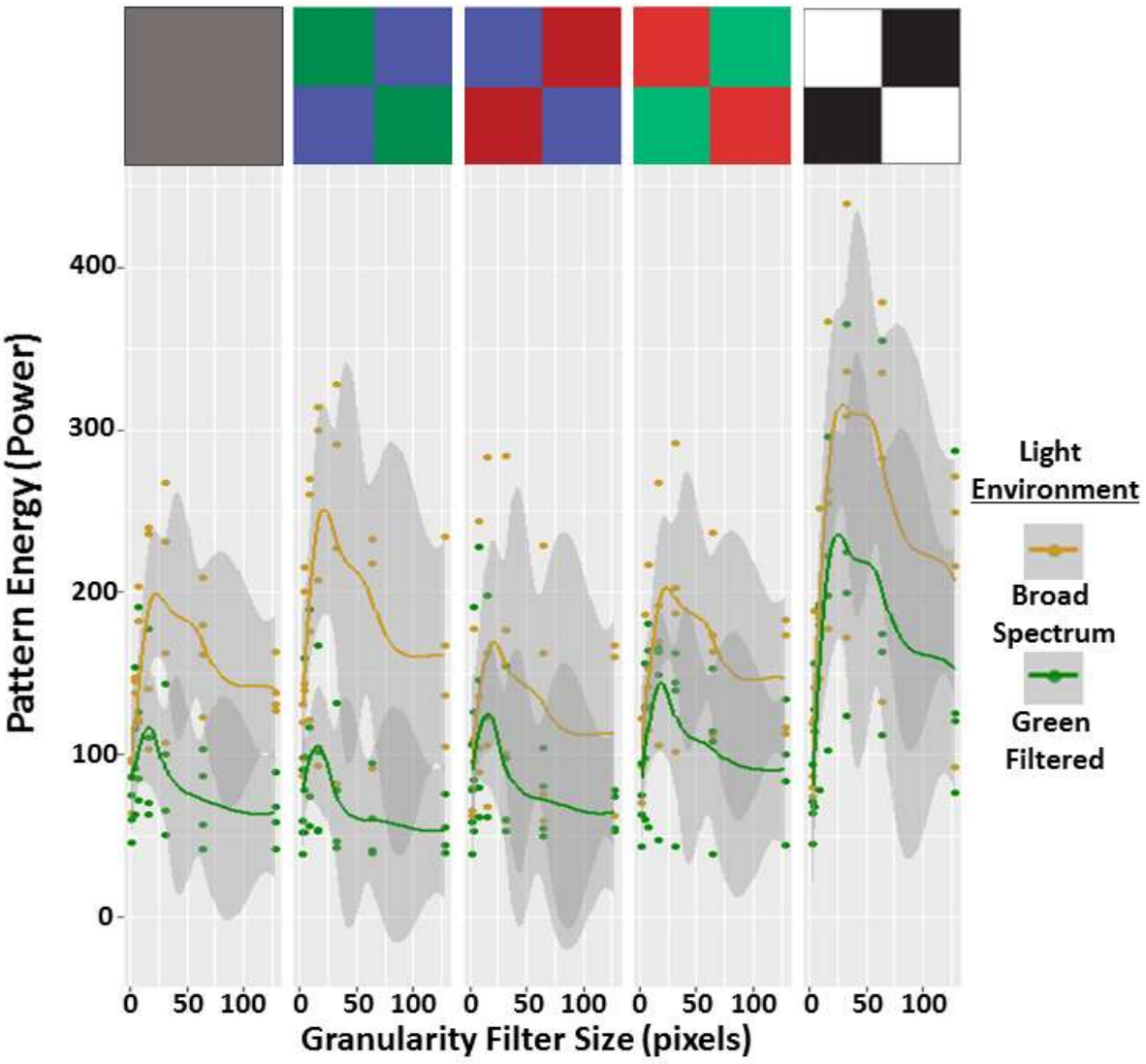

Figure 24: Granularity analysis of starry flounder camouflage held for seven weeks in either broad spectrum sunlight (yellow line) or green-filtered sunlight (green line). Each panel represents a different checkerboard substrate. The y-axis is the energy that passes through each granularity band, or filter, along the x-axis.

Digital-PCR

Fish from the seven-week broad spectrum and seven-week green filtered treatments that were transferred to the behavioural arena and exposed to white LED light for three hours (i.e., the duration of the behavioural assay) had no statistical difference in expression (Figure 25). Fish that were immediately euthanized after being removed from these treatments (the 'baseline fish') had significantly different opsin expression; individuals held in green-filtered light had lower expression of UV sensitive (*Sws1*) and short-wavelength sensitive (*Sws2B*) opsins compared to those exposed to broad spectrum light (student's t-test, $t = 3.9414$, $p = 0.01121$ and $t = 1.1458$, $p = 0.004792$, respectively) (Figure 25, Figure 26).

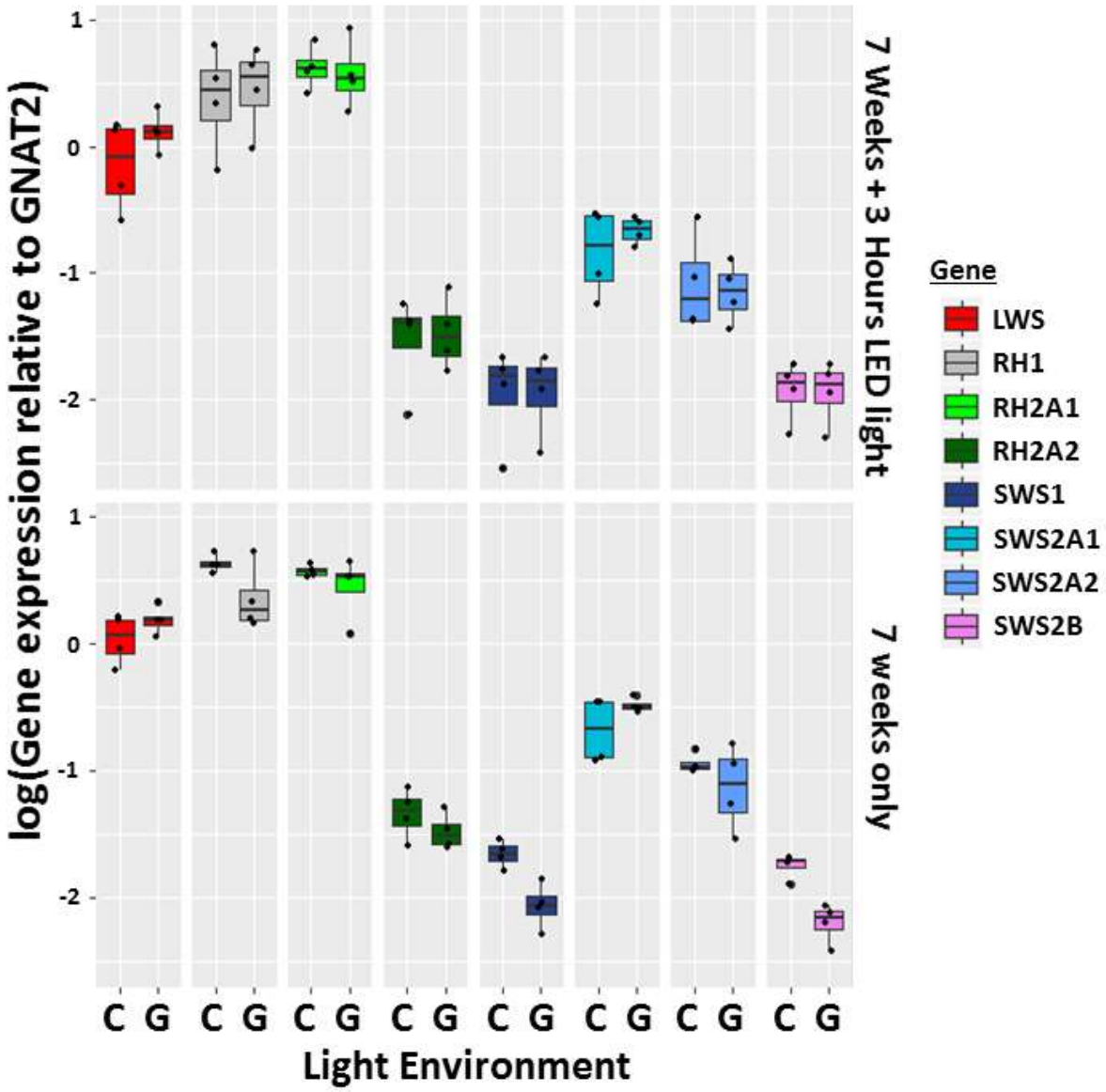

Figure 25: *Gnat2* normalized opsin expression of starry flounder held in either broad spectrum sunlight (x-axis, C) or green-filtered sunlight (x-axis, G) for seven weeks. Fish (n=4) were euthanized immediately after being removed from the light environments (the "Baseline" panel, bottom) or 3 hours after being transferred to the behavioural arena (the "3 Hour" panel, top) illuminated with four white LED lights (n=4).

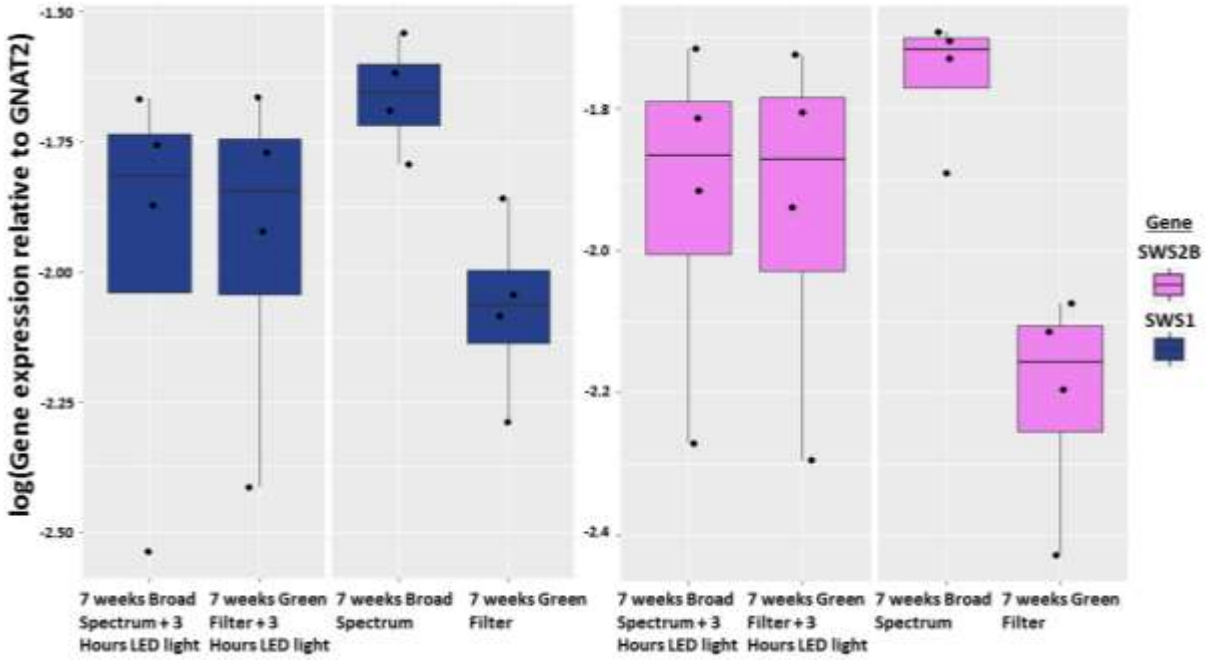

Figure 26: *Gnat2* normalized opsin expression (blue = *Sws1*, purple = *Sws2B*) of starry flounder held in either broad spectrum sunlight or green-filtered sunlight for seven weeks. Fish (n=4) were euthanized immediately after being removed from the light environments (the "Baseline" panels) or 3 hours after being transferred to the behavioural arena (the "3 Hours" panels) illuminated with four white LED lights (n=4).

Discussion

Opsin expression plasticity in response to light environment

Opsin expression in the starry flounder retina changed in response to the seven week broad spectrum and green light treatments, and then changed again within three hours. Killifish opsin expression responded to varying light conditions within one to three days (Fuller and Claricoates, 2011). Killifish reared in clear water had higher *Sws1* and *Sws2B* expression compared to red-stained water, and those changes matched the *in situ* light availability (Fuller et al., 2003; Fuller and Claricoates, 2011). The present study found evidence for a more rapid response. *Sws1* and *Sws2B* expression was significantly lower in fish exposed to green-filtered light compared to those in broad spectrum light. *Sws1* and *Sws2B* wavelengths of maximum absorbance correlate with the light available in the tanks. The green-filter excluded light at wavelengths lower than 450 nm; *Sws1* and *Sws2B* are maximally sensitive to 369 nm and 415 nm, respectively. The six other visual pigments have wavelengths of maximum absorbance within the light available in the green-filtered tank, and were expressed at the same level in both light environments. The difference, apparently induced by the absence of short-wavelength light, was lost after only three hours of exposure to the four white LEDs in the camouflage trials. Although the white LEDs do not emit UV light, they do emit near-UV and blue light, which is enough to induce higher expression of *Sws1* and *Sws2B* opsins. Size can play a role in UV expression. Salmonids lose UV sensitivity as they develop (Cheng et al., 2006).

However, the differences observed here are not due to ontogeny. *Sws1* and *Sws2B* expression was not correlated with size.

The rapid plasticity of opsins has implications for the visual ecology of starry flounder. The changes could function as a way of tuning the retina to varying light conditions. Increasing populations of photoreceptors sensitive to the light in the environment could improve visual sensitivity and confer benefits for predator avoidance and prey capture. Future studies should investigate whether plasticity is a persistent phenomenon throughout starry flounder ontogeny, or if the retina is plastic at certain stages of development. Starry flounder are found at depths of more than 200 meters, but occasionally migrate kilometers up river (Love, 2011). These two environments are spectrally dramatically different, and a tunable retina even at later ontogenetic stages could be adaptive.

Varying light environments, driven by water depth or season, affects opsin expression in several species of damselfish, whereas other species appear to have more stable expression patterns (Stieb et al., 2016). In stickleback, opsin expression is shifted toward longer wavelengths in freshwater populations relative to marine populations, and these shifts correlate with differences in the light available (Rennison et al., 2016). Furthermore, there is evidence for local adaption to light among benthic and limnetic ecotypes within a lake. Based on laboratory rearing experiments, stickleback opsin expression is primarily under genetic control, a result of standing genetic variation (Rennison et al., 2016), rather than environmental influences. Rennison et al. (2016)'s observations are consistent with Novales Flamarique et al. (2013). Why some species

appear to possess plastic opsin expression while others do not warrants further investigation.

A change in opsin expression may not immediately reflect the opsin proteins present in the outer segment of a cell (Young, 1967; Hagstrom et al., 1998). Photoreceptors are terminally differentiated; they are long lived, and the cellular components must be regularly turned over to prevent a loss of function (Williams, 2002). Outer segment shedding renews the components of outer segment. In mouse, rat, and frog, radioactively labelled amino acids accumulated at the base of the outer segment within 24 hours. In rods, the labelled amino acids proceeded as a "reaction band" to the distal point of the outer segment in approximately ten days (Young, 1967). Similar observations were observed in rhesus monkey and cat cone cells (Anderson et al., 1978). The changes in expression observed in the present study are occurring in differentiated cells, and are not a result of new photoreceptor cell production; the changes in expression are unlikely to result in changes at the protein level within three hours. Bream reared under yellow light and sampled as larvae (days 0 – 40), post-settlement (days 41 – 100), juvenile (days 101 – 210) and adult (days > 1 year) increased expression of *Rh2* and *Lws* and those changes were reflected in microspectrophotometric measurements (Shand et al., 2008). Similarly, ontogenetic shifts in opsin expression in coho salmon resulted in opsin protein-level shifts as measured by MSP (Temple, 2008). The starry flounder used in the behavioural assay are better represented by the baseline expression data than the data collected from their retinas after three hours under a white LED light. If the *Sws1* and *Sws2B* expression patterns were consistent with the baseline over seven weeks, then we predict that the opsin protein populations in the retina would reflect those changes. However, it would be

valuable to complement future behavioural assays with immunohistochemistry, or a survey of the retina using microspectrophotometry to confirm our prediction.

Empirical evidence for active camouflage in starry flounder

The behavioural assay presented here provides empirical evidence that starry flounder actively camouflage. The fish tested showed noticeable changes within 10 seconds, and the body pattern was stable within minutes, indicating direct neural input, rather than slow, hormonal changes mediating the response. Camouflage in fish is the aggregate response of millions of chromatophores in the skin. Unlike cephalopod molluscs, whose camouflage has been thoroughly investigated (see: Messenger, 2001; Hanlon, 2007), fish camouflage involves the physical movement of pigment, rather than muscular contraction and expansion of the cell itself (Fujii, 2000). Therefore, it is not surprising that fish camouflage is relatively slow compared to the remarkably fast change observed in cephalopods, which in some cases can occur in as little as two seconds (Allen et al., 2009).

Colourful camouflage or achromatically driven?

Although not statistically significant, we found tantalizing evidence of light environment affecting the neuronal camouflage response is observed in the standard deviation of luminance of fish measured on the blue-green checkerboard (Figure 21). Higher standard deviation of luminance equates to more light-and-dark contrasting patterns (i.e., disruptive or mottle camouflage), whereas low values equate to low pattern contrast (i.e., uniform camouflage). A fish camouflaging as mottle or disruptive would

indicate that the fish can see a difference between the blue and green checkers. The broad spectrum fish deployed more mottle camouflage compared to green-filtered fish, and must therefore detect a greater difference between the blue and green checkers. Differential visual performance on the blue and green substrate is supported by the gene expression, with broad spectrum fish expressing more UV- and blue-sensitive opsins, possibly conferring greater visual sensitivity to short-wavelength light. These data suggest a positive correlation with the *Sws1* and *Sws2B* opsin expression and an ability to detect a noticeable difference between blue and green hues.

Apart from the one intriguing result on the blue and green checkerboard, there was no statistically significant relationship between light environment and the neural camouflage. The camouflage signal may have been reduced by the noise generated by hormonal camouflage. The fish exhibited different colours based on light environment. The green-filtered light environment resulted in fish that were substantially darker, potentially masking the predominant neural response (i.e., dark melanophores and white leukophores). An alternative explanation is that the *Sws1* and *Sws2B* opsins are not main drivers of the camouflage response. If opsins do play a role, perhaps the UV and blue single cones are not involved in the camouflage response. Double cones are hypothesized to contribute chiefly to luminance vision, motion detection (Boehlert, 1978), and polarization vision (Hawryshyn et al., 2003). More precisely, the long-wavelength outer segment in goldfish double cones is used for motion detection (Schaerer and Neumeyer, 1996). Similar specializations could be contributing to the camouflage response in starry flounder. Future studies using different filters attempting to change opsin expression in different photoreceptors (e.g, M and L cones) would be informative. The preponderance

of unequal double cones in the dorsal retina, which receives reflected light from the substrates, may be functionally important for the camouflage response. In cichlid, the pattern of expression in double cones was reversed dorso-ventrally in response to red light illumination from below (Dalton et al., 2015). If similar bottom-up illumination of starry flounder "flips" the double cone opsin expression dorso-ventrally, we could test whether the unequal double cones play an important role in camouflage.

Camouflage may be visually mediated through achromatic channels (e.g., cuttlefish have only one visual pigment). The most pronounced pattern changes were observed on the black and white checkerboard. That is not to say colour vision is unimportant to camouflage behaviour. Gulf flounder (*Paralichthys albiguttata*) and ocellated flounder (*Ancylopsetta ommata*) of family Paralichthydae preferred to settled on blue and green substrates after being adapted to the same colour (Mast, 1914). Mäthger et al. (2006) created a series of checkerboards that were white and green, with the white checker position getting progressively darker until the final substrate was black and green. At some point the green checker matched the luminance of the grey checker, and cuttlefish deployed a uniform camouflage pattern when place on top. Thus, cuttlefish camouflage is achromatic. A similar design would be useful to confirm whether starry flounder camouflage is driven by luminance, colour, or both.

Improvements to the camouflage experiment

Printing a substrate that reduces the light signal to hue, and only hue, is remarkably difficult. The printed colours are a mix of a cyan, magenta, yellow, and black (Appendix

C, Figure 32), and the result is a colour with a broad wavelength distribution. The sensitivity of starry flounder photoreceptors affect how the checkers are seen. Photoreceptors with longer outer segments are more sensitive, and if certain pigments are more sensitive to light, contrast could be perceived from two colors with the same light intensity. The image analysis toolbox can calculate the "just noticeable difference" of two colours modelled to starry flounder vision. That would require UV photography, but it would aid in selecting colours that match intensity based on photon catch estimates modelled using the pigment absorbance data from chapter 2. Alternatively, one could use substrates similar to Ishihara plates, those used to test for colour blindness in humans (Ishihara, 1918). Ishihara plates have a pattern of randomly sized dots, and make no attempt to control for intensity. Rather, the intensity of two colours varies, and the pattern contained within the substrate is only visible using colour vision. Another alternative would be to use a LED lights or lasers projected below the fish. Lasers can generate light with very narrow bandwidths, enabling precise control of the wavelength of light. Using fibre optics guiding the light into spectrally flat materials (e.g., PTFE plastic) one could illuminate the substrate from below, creating a highly controlled colourful substrate.

The sample size of this experiment was small. Equipped with the knowledge that opsin expression is rapidly plastic, future experiments will be run with subsamples of fish providing the opsin expression, and a larger sample size of fish run through the behavioural assay. The behavioural assay is non-invasive and could feasibly be run under sunlight at the beach, with catch-and-release facilitating many more fishes run through the assay. Power analysis indicated a sample size of 20 fish per treatment would permit

the detection of significant differences if the data presented here are representative of the population.

More pronounced differences may not have been observed because algae growth in the tanks resulted in the broad spectrum light environment being slightly green-shifted. Future lab experiments should include regular water changes to keep the algae growth down.

The experiment did not control for the difference in overall light intensity between the two environments. The green-filtered environment allows approximately 12% sunlight through compared to 88% in the broad spectrum environment. Although it is possible the differences in opsin expression could be due to light intensity, the evidence contrary to that point is two-fold. One, the opsins that were expressed significantly lower correspond to the wavelengths of light completely omitted by the filters. Two, the other opsins were not noticeably affected by the significantly lower light intensities in the green-filtered tank. Our rational behind selecting the green filter was that is approximates the light environments starry flounder encounter at depths in the turbid, coastal waters around Vancouver Island. With that said, follow-up studies that match light intensity, but vary colour, would enhance the present study.

Concluding remarks

The goal of this thesis from the outset was to use molecular tools to inform aspects of an animal's behaviour and ecology. To that end we characterized how many opsins the starry flounder has. We found eight opsins all of which are expressed and translated into

proteins in photoreceptors of the retina. Those eight opsins utilize vitamin A1 to form pigments that are maximally sensitive to light at eight different maxima, ranging between ultra-violet and red wavelengths. We measured regional variations within the retina, and found adaptations consistent with our understanding of starry flounder's demersal life history. We were struck by the relative paucity of evidence for variation in opsin expression affecting visual performance. Previous studies have found that light affects opsin expression, and we aimed to replicate those affects in the starry flounder by holding them in different filtered light environments. We found significant differences in UV and blue opsin expression after seven weeks in either broad spectrum light of green-filtered light. Surprisingly, that change was lost after three hours under white LED light, indicating a high degree of plasticity in opsin expression. By exploiting starry flounder's visually-mediated adaptive camouflage, we were able to quantify visual performance on a variety of substrates. Although we did not find statistically significant differences between fish from different light environments, fish with higher UV- and blue-sensitive opsins camouflaged with more contrasting patterns on blue-green checkerboards. This suggests that possessing greater populations of UV and blue opsins results in improved performance when discriminate between blue and green wavelengths. Follow-up studies in the Taylor lab will take place to confirm and expand upon these results.

Bibliography

Ahnelt, P. K., Kolb, H., & Pflug, R. (1987). Identification of a subtype of cone photoreceptor, likely to be blue sensitive, in the human retina. Journal of Comparative Neurology, 255(1), 18-34.

Allen, J. J., Mäthger, L. M., Barbosa, A., & Hanlon, R. T. (2009). Cuttlefish use visual cues to control three-dimensional skin papillae for camouflage. Journal of Comparative Physiology A, 195(6), 547-555.

Anderson, D. H., Fisher, S. K., & Steinberg, R. H. (1978). Mammalian cones: disc shedding, phagocytosis, and renewal. Investigative Ophthalmology & Visual Science, 17(2), 117-133.

Applebury, M. L., Antoch, M. P., Baxter, L. C., Chun, L. L. Y., Falk, J. D., Farhangfar, F., Kage, K., Krzystolik, M. G., Lyass, L. A., & Robbins, J. T. (2000). The murine cone photoreceptor: a single cone type expresses both S and M opsins with retinal spatial patterning. Neuron, 27(3), 513-523.

Bao B., Ke Z., Xing J., Peatman E., Liu Z., Xie C., Xu B., Gai J., Gong X., Yang G., Jiang Y., Tang W., & Ren D. (2011). Proliferating cells in suborbital tissue drive eye migration in flatfish. Developmental Biology, 351: 200-207.

Barbosa, A., Mäthger, L. M., Buresch, K. C., Kelly, J., Chubb, C., Chiao, C. C., & Hanlon, R. T. (2008). Cuttlefish camouflage: the effects of substrate contrast and size in evoking uniform, mottle or disruptive body patterns. Vision research, 48(10), 1242-1253.

Barnard, J. L., Thomas, J. D., & Sandved, K. B. (1988). Behavior of gammaridean Amphipoda: Corophium, Grandidierella, Podocerus, and Gibberosus (American Megaluropus) in Florida. Crustaceana. Supplement, 234-244.

Bates, H. W. (1862). XXXII. Contributions to an Insect Fauna of the Amazon Valley. Lepidoptera: Heliconidæ. Transactions of the Linnean Society of London, 23(3), 495-566.

Beaudry, F. E. G., Iwanicki, T., Mariluz, B. R. Z., Darnetand, S., Schneider, P., & Taylor, J. S. (*submitted*). 18 non-visual opsins in the ancestor of vertebrates, astonishing duplication in ray-finned fish, and loss in Amniota. Molecular Phylogenetics and Evolution.

Beckmann, H., Hering, L., Henze, M. J., Kelber, A., Stevenson, P. A., & Mayer, G. (2015). Spectral sensitivity in Onychophora (velvet worms) revealed by electroretinograms, phototactic behaviour and opsin gene expression. The Journal of Experimental Biology, 218(6), 915-922.

Bergstrom, C.A. (2007). Morphological evidence of correlational selection and ecological segregation between dextral and sinistral forms in a polymorphic flatfish, *Platichthys stellatus*. Journal of Evolutionary Biology, 20(3), 1104-1114.

Bergstrom, C.A., & Palmer, A.R. (2007). Which way to turn? Effect of direction of body asymmetry on turning and prey strike orientation in Starry flounder *Platichthys stellatus* (Pallas)(Pleuronectidae). Journal of Fish Biology, 71(3), 737-748.

Boehlert, G. W. (1978). Intraspecific evidence for the function of single and double cones in the teleost retina. Science, 202(4365), 309-311.

Chang, B. S., Crandall, K. A., Carulli, J. P., & Hartl, D. L. (1995). Opsin phylogeny and evolution: a model for blue shifts in wavelength regulation. Molecular phylogenetics and evolution, 4(1), 31-43.

Chapman, B. B., Morrell, L. J., Tosh, C. R., & Krause, J. (2010). Behavioural consequences of sensory plasticity in guppies. Proceedings of the Royal Society of London B: Biological Sciences, 277(1686), 1395-1401.

Cheng, C. L., & Flamarique, I. N. (2007). Chromatic organization of cone photoreceptors in the retina of rainbow trout: single cones irreversibly switch from UV (SWS1) to blue (SWS2) light sensitive opsin during natural development. Journal of Experimental Biology, 210(23), 4123-4135.

Cheng C.L., Novales Flamarique I., Hárosi F.I., Rickers-Haunerland J., & Haunerland N.H. (2006). Photoreceptor layer of salmonid fishes: transformation and loss of single cones in juvenile fish. Journal of Comparative Neurology, 495: 213-235.

Cortesi, F., Musilová, Z., Stieb, S. M., Hart, N. S., Siebeck, U. E., Malmstrøm, M., Tørresen, O.K., Jentoft, S., Cheney, K.L., Marshall, N.J., Carleton, K.L., & Salzburger, W. (2014). Ancestral duplications and highly dynamic opsin gene evolution in percomorph fishes. Proceedings of the National Academy of Sciences, 201417803.

Cott, H. B. (1940). Adaptive coloration in animals.

Dalton, B. E., Lu, J., Leips, J., Cronin, T. W., & Carleton, K. L. (2015). Variable light environments induce plastic spectral tuning by regional opsin coexpression in the African cichlid fish, Metriaclima zebra. Molecular Ecology, 24(16), 4193-4204.

Darwin, C. (1859). On the origin of species by means of natural selection. Murray, London.

Davies, W. I., Tamai, T. K., Zheng, L., Fu, J. K., Rihel, J., Foster, R. G., Whitmore, D. & Hankins, M. W., (2015). An extended family of novel vertebrate photopigments is widely expressed and displays a diversity of function. Genome research, 25(11), 1666-1679.

Engström K., & Ahlbert I-B. (1963). Cone types and cone arrangements in the retina of some flatfishes. Acta Zoologica, 44: 119-129.

Evans, B. I., & Fernald, R. D. (1990). Metamorphosis and fish vision. Journal of Neurobiology, 21(7), 1037-1052.

Evans, B. I., & Fernald, R. D. (1993). Retinal transformation at metamorphosis in the winter flounder (Pseudopleuronectes americanus). Visual Neuroscience, 10(06), 1055-1064.

Evans B.I., Hárosi F.I., & Fernald R.D. (1993). Photoreceptor spectral absorbance in larval and adult winter flounder. Visual Neuroscience, 10: 1065-1071.

Felsenstein, J. (1981). Evolutionary trees from DNA sequences: a maximum likelihood approach. Journal of Molecular Evolution, 17(6), 368-376.

Felsenstein J. (1985). Confidence limits on phylogenies: An approach using the bootstrap. Evolution 39:783-791.

Fujii, R. (2000). The regulation of motile activity in fish chromatophores. Pigment Cell Research, 13(5), 300-319.

Fuller, R. C., Fleishman, L. J., Leal, M., Travis, J., & Loew, E. (2003). Intraspecific variation in retinal cone distribution in the bluefin killifish, Lucania goodei. Journal of Comparative Physiology A, 189(8), 609-616.

Fuller, R. C., Carleton, K. L., Fadool, J. M., Spady, T. C., & Travis, J. (2005). Genetic and environmental variation in the visual properties of bluefin killifish, Lucania goodei. Journal of Evolutionary Biology, 18(3), 516-523.

Fuller, R. C., & Claricoates, K. M. (2011). Rapid light-induced shifts in opsin expression: finding new opsins, discerning mechanisms of change, and implications for visual sensitivity. Molecular Ecology, 20(16), 3321-3335.

Fujimoto M., Arimoto T., Morishita F., & Naitoh T. (1991). The background adaptation of the flatfish, Paralichthys olivaceus. Physiology & Behavior, 50: 185-188.

Frisch, K. V. (1950). Bees: Their Vision. Chemical Senses, and Language. Cornell University Press, Ithaca, New York, USA.

Gegenfurtner, K. R., & Sharpe, L. T. (2001). Color vision: From genes to perception. Cambridge University Press.

Gur, D., Leshem, B., Pierantoni, M., Farstey, V., Oron, D., Weiner, S., & Addadi, L. (2015). Structural Basis for the Brilliant Colors of the Sapphirinid Copepods. Journal of the American Chemical Society, 137(26), 8408-8411.

Hagstrom, S. A., Neitz, J., & Neitz, M. (1998). Variations in cone populations for red–green color vision examined by analysis of mRNA. NeuroReport, 9(9), 1963-1967.

Hanlon, R. (2007). Cephalopod dynamic camouflage. Current Biology, 17(11), R400-R404.

Hárosi F.I. (1987). Cynomolgus and rhesus monkey visual pigments. Application of Fourier transform smoothing and statistical techniques to the determination of spectral parameters. The Journal of General Physiology, 89: 717-743.

Hárosi F.I. (1994). An analysis of two spectral properties of vertebrate visual pigments. Vision Research, 34: 1359-1367.

Hárosi F.I., & Novales Flamarique I. (2012). Functional significance of the taper of vertebrate cone photoreceptors. The Journal of General Physiology, 139: 159-187.

Hasegawa, E. I. (2005). Changes in rhodopsin–porphyropsin ratio of chum and pink salmon. Fisheries Science, 71(5), 1091-1097.

Hawryshyn, C. W. (2000). Ultraviolet polarization vision in fishes: possible mechanisms for coding e–vector. Philosophical Transactions of the Royal Society B: Biological Sciences, 355(1401), 1187-1190.

Hawryshyn, C. W., Moyer, H. D., Allison, W. T., Haimberger, T. J., & McFarland, W. N. (2003). Multidimensional polarization sensitivity in damselfishes. Journal of Comparative Physiology A, 189(3), 213-220.

Helvik J.V., Drivennes Ø., Naess T.H., Fjose A., & Seo H-C. (2001a). Molecular cloning and characterization of five opsin genes from the marine flatfish Atlantic halibut (Hippoglossus hippoglossus). Visual Neuroscience, 18: 767-780.

Helvik, J. V., Drivenes, Ø., Harboe, T., & Seo, H-C. (2001b). Topography of different photoreceptor cell types in the larval retina of Atlantic halibut (Hippoglossus hippoglossus). Journal of Experimental Biology, 204(14), 2553-2559.Hoke K.L., Evans B.I. Fernald R.D. (2006). Remodeling of the cone photoreceptor mosaic during metamorphosis of flounder (Pseudopleuronectes americanus). Brain, Behavior and Evolution, 68: 241-254.

Hurvich, L. M., & Jameson, D. (1957). An opponent-process theory of color vision. Psychological review, 64(6p1), 384.

Isayama T. & Makino C.L. (2012). Pigment mixtures and other determinants of spectral sensitivity of vertebrate retinal photoreceptors. In: Akutagawa E, Ozaki K, editors. Photoreceptors: physiology, type and abnormalities. Hauppauge, NY: Nova Science Publishers. p 1-32.

Ishihara, S. (1918). Tests for Color Blindness. American Journal of Ophthalmology, 1(5), 376.

Jacobs, G. H., Fenwick, J. C., Calderone, J. B., & Deeb, S. S. (1999). Human cone pigment expressed in transgenic mice yields altered vision. The Journal of Neuroscience, 19(8), 3258-3265.

Jacobs, G. H., Williams, G. A., Cahill, H., & Nathans, J. (2007). Emergence of novel color vision in mice engineered to express a human cone photopigment. Science, 315(5819), 1723-1725.

Jacobs, G. H. (2009). Evolution of colour vision in mammals. Philosophical Transactions of the Royal Society B: Biological Sciences, 364(1531), 2957-2967.

Jacobs, G. H. (2013). Losses of functional opsin genes, short-wavelength cone photopigments, and color vision—a significant trend in the evolution of mammalian vision. Visual Neuroscience, 30(1-2), 39-53.

Kasagi, S., Mizusawa, K., Murakami, N., Andoh, T., Furufuji, S., Kawamura, S., & Takahashi, A. (2015). Molecular and functional characterization of opsins in barfin flounder (Verasper moseri). Gene, 556(2), 182-191.

Kelman, E. J., Tiptus, P., & Osorio, D. (2006). Juvenile plaice (Pleuronectes platessa) produce camouflage by flexibly combining two separate patterns. Journal of Experimental Biology, 209(17), 3288-3292.

Kim, H. J., Son, E. D., Jung, J. Y., Choi, H., Lee, T. R., & Shin, D. W. (2013). Violet light down-regulates the expression of specific differentiation markers through rhodopsin in normal human epidermal keratinocytes. PloS one, 8(9), e73678.

Kimura, M. (1980). A simple method for estimating evolutionary rates of base substitutions through comparative studies of nucleotide sequences. Journal of molecular evolution, 16(2), 111-120.

Kondrashev, S. L., Miyazaki, T., Lamash, N. E., & Tsuchiya, T. (2013). Three cone opsin genes determine the properties of the visual spectra in the Japanese anchovy, Engraulis japonicus (Engraulidae, Teleostei). The Journal of Experimental Biology, 216(6), 1041-1052.

Lee, S.M., Lee, J.H. & Kim, K.D., (2003). Effect of dietary essential fatty acids on growth, body composition and blood chemistry of juvenile starry flounder (*Platichthys stellatus*). Aquaculture, 225(1), 269-281.

Leech, D. M., & Johnsen, S. (2006). Ultraviolet vision and foraging in juvenile bluegill (Lepomis macrochirus). Canadian Journal of Fisheries and Aquatic Sciences, 63(10), 2183-2190.

Levine, J. S., MacNichol, E. F., Kraft, T., & Collins, B. A. (1979). Intraretinal distribution of cone pigments in certain teleost fishes. Science, 204(4392), 523-526.

Love, M.J. (2011). Certainly more than you want to know about the fishes of the Pacific coast. Really Big Press: Santa Barbara, California.

Lythgoe, J. N. (1979). Ecology of vision. Clarendon Press; Oxford University Press.

Mancuso, K., Hauswirth, W.W., Li, Q., Connor, T.B., Kuchenbecker, J.A., Mauck, M.C., Neitz, J. & Neitz, M. 2009. Gene therapy for red–green colour blindness in adult primates. Nature 461(7265):784-787.

Melin, A. D., Fedigan, L. M., Hiramatsu, C., Hiwatashi, T., Parr, N., & Kawamura, S. (2009). Fig foraging by dichromatic and trichromatic Cebus capucinus in a tropical dry forest. International Journal of Primatology, 30(6), 753-775.

Nathans, J., & Hogness, D. S. (1983). Isolation, sequence analysis, and intron-exon arrangement of the gene encoding bovine rhodopsin. Cell, 34(3), 807-814.

Nathans, J., & Hogness, D. S. (1984). Isolation and nucleotide sequence of the gene encoding human rhodopsin. Proceedings of the National Academy of Sciences, 81(15), 4851-4855.

Nathans, J., Thomas, D., & Hogness, D. S. (1986). Molecular genetics of human color vision: the genes encoding blue, green, and red pigments. Science, 232(4747), 193-202.

Nei M. & Kumar S. (2000). Molecular Evolution and Phylogenetics. Oxford University Press, New York.

Newton, I. (1704). Opticks, or, a treatise of the reflections, refractions, inflections & colours of light.

Novales Flamarique, I., & Hárosi, F. I. (2002). Visual pigments and dichroism of anchovy cones: a model system for polarization detection. Visual neuroscience, 19(04), 467-473.

Novales Flamarique I. (2011). Unique photoreceptor arrangements in a fish with polarized light discrimination. The Journal of Comparative Neurology, 51: 714-737.

Novales Flamarique I. (2013). Opsin switch reveals function of the ultraviolet cone in fish foraging. Proceedings of the Royal Society of London B, 280: 20122490.

Novales Flamarique I. & Browman H.I. (2001). Foraging and prey search behaviour of small juvenile rainbow trout (Oncorhynchus mykiss) under polarized light. The Journal of Experimental Biology, 204: 2415-2422.

Novales Flamarique, I., & Hawryshyn, C. W. (1993). Spectral characteristics of salmonid migratory routes from southern Vancouver Island (British Columbia). Canadian Journal of Fisheries and Aquatic Sciences, 50(8), 1706-1716.

Novales Flamarique I. & Hawryshyn C.W. (1997). Is the use of underwater polarized light by fish restricted to crepuscular time periods? Vision Research. 37: 975-989.

Novales Flamarique I. & Hárosi F.I. (2000). Photoreceptors, visual pigments, and ellipsosomes in the mummicho killifish, Fundulus heteroclitus: a microspectrophotometric and histological study. Visual Neuroscience 17: 403-420.

Novales Flamarique, I., Cheng, C. L., Bergstrom, C., & Reimchen, T. E. (2013). Pronounced heritable variation and limited phenotypic plasticity in visual pigments and opsin expression of threespine stickleback photoreceptors. Journal of Experimental Biology, 216(4), 656-667.

Novales Flamarique I. & Wachowiak M. (2015). Functional segregation of retinal ganglion cell projections to the opstic tectum of rainbow trout. Journal of Neurophysiology, 114: 2703-2717.

Novales Flamarique I., Hawryshyn C.W., & Hárosi F.I. (1998). Double cone internal reflection as a basis for polarization detection in fish. The Journal of the Optical Society of America A, 15: 349-358.

Mast, S. O. (1916). Changes in shade, color, and pattern in fishes, and their bearing on the problems of adaptation and behavior, with especial reference to the flounders Paralichthys and Ancylopsetta (No. 821). Government Printing Office.

Melin, A.D., Fedigan, L.M., Hiramatsu, C., Hiwatashi, T., Parr, N., & Kawamura, S. (2009) Fig Foraging by Dichromatic and Trichromatic Cebus capucinus in a Tropical Dry Forest, International Journal of Primatology, 30, pp. 753-775.

Messenger, J. B. (2001). Cephalopod chromatophores: neurobiology and natural history. Biological Reviews of the Cambridge Philosophical Society, 76(04), 473-528.

Morris, E. (2013). Opsin gene repertoire and expression in flatish. Bachelor of Science, Honours Thesis, Department of Biology, University of Victoria. Supervisor: Taylor, J.S.

Müller, F. (1878). Ueber die vortheile der mimicry bei schmetterlingen.

Olsson, P., Lind, O., & Kelber, A. (2015). Bird colour vision: behavioural thresholds reveal receptor noise. The Journal of experimental biology, 218(2), 184-193.

Orcutt, H. G. (1950). The Life History of the Starry Flounder: *Platichthys stellatus* (Pallas) (No. 78). California State Print. Office.

Owens, G. L., Rennison, D. J., Allison, W. T., & Taylor, J. S. (2012). In the four-eyed fish (*Anableps anableps*), the regions of the retina exposed to aquatic and aerial light do not express the same set of opsin genes. Biology letters, 8(1), 86-89.

Parry, J.W.L., Carleton, K.L., Spady, T., Carboo, A., Hunt, D.M., & Bowmaker, J.K. (2005) Mix and Match Color Vision: Tuning Spectral Sensitivity by Differential Opsin Gene Expression in Lake Malawi Cichlids, Current Biology, 15, pp. 1734-1739.

Phillips, G. A., Carleton, K. L., & Marshall, N. J. (2015). Multiple genetic mechanisms contribute to visual sensitivity variation in the Labridae. Molecular biology and evolution, msv213.

Pokorny, J., & Smith, V. C. (1970). Wavelength discrimination in the presence of added chromatic fields. Journal of the Optical Society of America, 60(4), 562-569.

Ramachandran, V. S., Tyler, C. W., Gregory, R. L., Rogers-Ramachandran, D., Duensing, S., Pillsbury, C., & Ramachandran, C. (1996). Rapid adaptive camouflage in tropical flounders. Nature, 379, 815 – 818

Rayleigh, J. W. S. B. (1871). On the scattering of light by small particles.

Rennison, D. J., Owens, G. L., Allison, W. T., & Taylor, J. S. (2011). Intra-retinal variation of opsin gene expression in the guppy (Poecilia reticulata). The Journal of Experimental Biology, 214(19), 3248-3254.

Rennison, D. J., Owens, G. L., & Taylor, J. S. (2012). Opsin gene duplication and divergence in ray-finned fish. Molecular Phylogenetics and Evolution, 62(3), 986-1008.

Saitou N. & Nei M. (1987). The neighbor-joining method: A new method for reconstructing phylogenetic trees. Molecular Biology and Evolution 4:406-425.

Sakai, Y., Ohtsuki, H., Kasagi, S., Kawamura, S., & Kawata, M. (2016). Effects of light environment during growth on the expression of cone opsin genes and behavioral spectral sensitivities in guppies (Poecilia reticulata). BMC Evolutionary Biology, 16(1), 1.

Sandkam, B., Young, C. M., & Breden, F. (2015). Beauty in the eyes of the beholders: colour vision is tuned to mate preference in the Trinidadian guppy (Poecilia reticulata). Molecular ecology, 24(3), 596-609.

Seehausen, O., Terai, Y., Magalhaes, I. S., Carleton, K. L., Mrosso, H. D., Miyagi, R., van der Sluijs, I., Schneider, M. V., Maan, M. E., Tachida, H. & Imai, H., (2008). Speciation through sensory drive in cichlid fish. Nature, 455(7213), 620-626.

Schaerer, S., & Neumeyer, C. (1996). Motion detection in goldfish investigated with the optomotor response is “color blind”. Vision research, 36(24), 4025-4034.

Shand, J., Davies, W. L., Thomas, N., Balmer, L., Cowing, J. A., Pointer, M., Carvalho, L.S., Trezise, A.E.O., Collin, S.P., Beazley, L.D., & Hunt, D. M. (2008). The influence of ontogeny and light environment on the expression of visual pigment opsins in the retina of the black bream, Acanthopagrus butcheri. Journal of Experimental Biology, 211(9), 1495-1503.

Smith, A. R., D’Annunzio, L., Smith, A. E., Sharma, A., Hofmann, C. M., Marshall, N. J., & Carleton, K. L. (2011). Intraspecific cone opsin expression variation in the cichlids of Lake Malawi. Molecular ecology, 20(2), 299-310.

Smith, A.R., Ma, K., Soares, D., & Carleton, K.L. (2012) Relative LWS cone opsin expression determines optomotor threshold in Malawi cichlid fish, Genes, Brain, and Behavior, 11, 185-192

Spottiswoode, C. N., & Stevens, M. (2010). Visual modeling shows that avian host parents use multiple visual cues in rejecting parasitic eggs. Proceedings of the National Academy of Sciences, 107(19), 8672-8676.

Stieb, S. M., Carleton, K. L., Cortesi, F., Marshall, N.J., Salzburger, W. (2016). Depth dependent plasticity in opsin expression varies between damselfish (Pomacentridae) species. Molecular Ecology, *accepted manuscript*

Stevens, M. (2013). Sensory ecology, behaviour, and evolution. OUP Oxford.

Stevens, M., & Merilaita, S. (2009). Animal camouflage: current issues and new perspectives. Philosophical Transactions of the Royal Society of London B: Biological Sciences, 364(1516), 423-427.

Stuart-Fox, D., & Moussalli, A. (2009). Camouflage, communication and thermoregulation: lessons from colour changing organisms. Philosophical Transactions of the Royal Society of London B: Biological Sciences, 364(1516), 463-470.

Sumner, F. B. (1911). The adjustment of flatfishes to various backgrounds: A study of adaptive color change. Journal of Experimental Zoology, 10(4), 409-506.

Tamura K., Stecher G., Peterson D., Filipski A., & Kumar S. (2013). MEGA6: Molecular Evolutionary Genetics Analysis version 6.0. Molecular Biology and Evolution, 30: 2725-2729.

Temple, S. E. (2011). Why different regions of the retina have different spectral sensitivities: a review of mechanisms and functional significance of intraretinal variability in spectral sensitivity in vertebrates. Visual Neuroscience, 28(04), 281-293.

Terai, Y., Seehausen, O., Sasaki, T., Takahashi, K., Mizoiri, S., Sugawara, T., Sato, T., Watanabe, M., Konijnendijk, N., Mrosso, H. D. & Tachida, H. (2006). Divergent selection on opsins drives incipient speciation in Lake Victoria cichlids. PLoS Biol, 4(12), e433.

Thayer, G. H., & Thayer, A. H. (1909). Concealing-coloration in the animal kingdom. Macmillan Company.

Thoen, H. H., How, M. J., Chiou, T. H., & Marshall, J. (2014). A different form of color vision in mantis shrimp. Science, 343(6169), 411-413.

Troscianko, J., & Stevens, M. (2015). Image Calibration and Analysis Toolbox–a free software suite for objectively measuring reflectance, colour and pattern. Methods in Ecology and Evolution.

Tsutsumi, M., Ikeyama, K., Denda, S., Nakanishi, J., Fuziwara, S., Aoki, H., & Denda, M. (2009). Expressions of rod and cone photoreceptor-like proteins in human epidermis. Experimental Dermatology, 18(6), 567-570.

Williams, D. S. (2002). Transport to the photoreceptor outer segment by myosin VIIa and kinesin II. Vision research, 42(4), 455-462.

Woese, C. R. (2004). A new biology for a new century. Microbiology and molecular biology reviews, 68(2), 173-186.

Yokoyama, S., & Yokoyama, R. (1996). Adaptive evolution of photoreceptors and visual pigments in vertebrates. Annual Review of Ecology and Systematics, 543-567.

Yokoyama, S. (1997) Molecular genetic basis of adaptive selection: examples from color vision in vertebrates. Annual Review of Genetics, 31, 315-336.

Yokoyama, S. (2000). Molecular evolution of vertebrate visual pigments. Progress in retinal and eye research, 19(4), 385-419.

Yokoyama, S. (2008). Evolution of dim-light and color vision pigments. Annual Review of Genomics and Human Genetics, 9, 259-282.

Yokoyama, S., & Radlwimmer, F. B. (1998). The" five-sites" rule and the evolution of red and green color vision in mammals. Molecular Biology and Evolution, 15(5), 560-567.

Young, R. W. (1967). The renewal of photoreceptor cell outer segments. The Journal of cell biology, 33(1), 61-72.

Zhaoping, L., Geisler, W. S., & May, K. A. (2011). Human wavelength discrimination of monochromatic light explained by optimal wavelength decoding of light of unknown intensity. PloS One, 6(5), e19248.

Appendix

Appendix A – Starry flounder visual opsin full length coding sequences

>*Platichthys stellatus* RH1
ATGAACGGCACAGAGGGACCATATTTTTATGTCCCCATGCAAAATACTACCGGCATT
GTCCGGAGTCCTTATGAGTACCCTCAGTATTACCTTGTCAACCCAGCAGCTTATGCTG
CCCTGGGTGCCTATATGTTCCTGCTCATCCTCGTTGGTTTTCCCGTCAACTTCCTCACT
CTCTACGTTACCCTCGAACACAAGAAGCTGCGAACCCCTCTAAACTACATCCTGCTG
AACCTTGCGGTGGCTGACCTCTTCATGGTGTTTGGAGGATTCACCACAACGATGTAC
ACCTCTATGCATGGCTACTTCGTTCTAGGTCGTCTTGGCTGCAACCTAGAAGGATTCT
TTGCAACCCTCGGAGGTGAAATTTCCCTGTGGTCACTTGTTGTTCTGGCTGTTGAAAG
GTGGATGGTTGTCTGCAAGCCAATCAGCAACTTTCGCTTTGGAGAAAACCATGCCAT
CATGGGTTTGGCCTTCACCTGGTTTGCAGCCTCTGCTTGCGCTGTACCCCCTCTTGTTG
GCTGGTCTCGTTACATCCCTGAGGGCATGCAGTGCTCATGTGGAGTGGACTACTACA
CACGTGCAGAAGGTTTCAACAATGAATCCTTTGTGATCTACATGTTCATCTGCCACTT
CCTCATTCCAATGGCTATTGTGTTTTTTTGCTATGGCCGTCTGCTCTGTGCTGTCAAAG
AGGCTGCTGCTGCCCAGCAGGAGTCAGAGTCCACCCAAAGGGCTGAGAGGGAAGTC
ACCCGCATGGTTGTGATCATGGTTATTGGTTACCTGGTATGCTGGTGTCCCTATGCAG
GTGTGGCCTGGTATATCTTCCTAAATCAGGGCTCTGAGTTCGGACCTCTTTTTATGAC
CGTCCCCGCCTTCTTTGCCAAGAGCTCTGCCATCTACAACCCATTGATCTACATCTGC
ATGAACAAACAGTTCCGTCACTGCATGATCACCACCTTGTGCTGTGGGAAGAATCCC
TTCGAGGAGGAGGAGGGAGCGTCCAGTACCAAGACCGAGGCCTCTTCTGCCTCCTCT
AGCTCTGTCTCACCAGCATAA

>*Platichthys stellatus* RH2A1
ATGGCTTGGGACGGCGGAATCGAGCCCAATGGCACAGAGGGCAAGAACTTCTACAT
CCCCATGTCCAACAGGACTGGGATCGTTAGAAGTCCTTTTGAATACCCTCAGTATTAC
ATGGTGGATTCCATGATGTACAAAGTTCTAGCTTTCTACATGTTTTTCCTGATCTGCA
CTGGAACCCCCATCAACGGTCTGACGTTGTTCGTCACGGCTCAGAACAAGAAACTCA
GGCAACCCCTGAACTACATCCTGGTCAACCTGGCCGTGGCCGGGCTCATCATGTGCG
CTTTCGGATTCACCATCACCATCACCTCTGCTTTTAACGGCTACTTCATTCTGGGAGC
CACTTTCTGCCAAATTGAGGGATTCATGGCCACACTCGGAGGTGAAGTCGCTCTCTG
GTCTCTGGTCGTCCTGGCTGTTGAGCGATACATCGTCGTCTGCAAACCCATGGGAAG
CTTCAAGTTCAGCGGAACTCATGCAGGAATCGGAGTCCTCTTCACCTGGATCATGGC
TTTCGCATGCGCTGGCCCCCCACTGTTCGGCTGGTCCAGGTACCTACCCGAGGGCAT
GCAGTGCTCATGCGGACCAGACTACTACACTCTGGCCCCCGGCTACAACAACGAATC
ATACGTCATCTACATGTTTGTCGTCCACTTCTTCCTTCCAGTCTTTGTGATTTTCTTCA
CCTATGGAAGCCTGGTGCTGACAGTCAAAGCTGCTGCAGCCCAGCAGCAGGAGTCA
GAGTCCACCCAGAAGGCTGAGAGGGAGGTGACACGCATGTGCGTCCTGATGGTCTTT
GGCTTCCTGGTAGCTTGGGTGCCATATGCCAGTTTCGCTGGCTGGATCTTCTTGAACA
AGGGAGCTGCCTTCACCGCCATGACTGCATCCATCCCTGCCTTCTTTGCTAAGAGCTC
AGCTCTCTACAACCCTGTGATCTACGTGCTGTTCAACAAACAGTTCCGTAACTGCATG
CTGAGCGCTATTGGAATGGGAGGCATGGTGGAGGATGAAACCTCAGTGTCTGCCAGC
AAAACAGAAGTGTCCTCAGTCTCTTAA

>*Platichthys stellatus* RH2A2
ATGACCTGGGACGGAGGAATCGAGCCCAATGGCACCGAGGGCAAGAACTTCTACAT
CCCCATGTCCAACAGGAGTGGGGTCGTCAGAAGTCCCTTTGAGTACCCTCAGTATTA
TTTGGCGGATCCCATCATGTACAAGCTTCTCGCCGTCTACATGCTCTTCCTGATCTGC
ACTGGAACCCCCATCAATTGTCTGACGCTGCTGGTCACGGCTCGGAACAAGAAGCTC
AGACAACCTCTCAACTACATCCTGGTCAACCTGGCCGTGGCCGGACTCATCATGTGC
TGTTTCGGATTCACCATCACCTTCATCACTGCCATCAATGGTTACTTCGTCCTCGGGG
TCACTGCCTGTGCTTTGGAAGGATTATTGGCCACCCTTGGCGGTCAGGTTTCTCTCTG
GTCTCTGGTCGTCCTGGCTGTTGAGAGATACATCGTCATCTGCAAACCCATGGGGAG
CTTCAAGTTCACCGGAAGTCACGCGGCAGCTGGAGTCATTTTCACCTGGATCATGGC
TTTTGCTTGTGCTACGCCACCTCTTTTTGGCTGGTCCAGGTACATCCCCGAGGGCATG
CAGTGCTCCTGCGGCCCCGACTACTACACTCTGGCCCCCGGCTTCAACAATGAATCA
TACGTCGTCTACTTGTTTGTCGTCCACTTCACGGCTCCTGTCTTCACAATTTTCTTTAC
TTATGGAAGCCTCATTCTGACAGTCAAAGCCGCTGCAGGCCAGCAGCAGGATTCAGA
GTCCACTCAGAAGGCTGAGAAGGAGGTGACACGCATGTGCTTCCTGATGGTCATTGG
CTTCCTGGTAGCTTGGGTACCATATGCCACTTTCGCAGCCTGGATCTTCATAAACAAG
GGGGCCACCTTTACTGCCCTGACCGCAACCATCCCCGCCTTCTTCGCTAAGAGCTCAG
CCTTGTACAACCCCGTGATCTACGTGCTGATGAACAAACAGTTCCGTAGCTGCATGC
TGAGCAGTATTGGAATGGGCGGCATGGTGGAGGATGAGGCATCAGTGTCTGCCAGC
AAGACAGAGGTGTCCTCTGTGTCTTAA

>*Platichthys stellatus* SWS1
ATGGGGAAACACTTCCACCTGTATGAGAACGTTTCTAATGTGAGTCCTTTTGATGGG
CCCCAGTATTACCTGGCACCTCAATGGGCTTTTCACCTGCAGACGATCTTCATGGGCT
GCGTCCTGCTCGCTGGCACTCCTTTAAACTTTGTGGTTCTTCTTGTGGCACTCAAGTA
CAAGAAGCTCCGAGTCCCTCTCAATTACATCCTCGTCAACATCTGCTTCGCAGGATTA
ATCTTTGTGGTGTTCTCAGTGAGCCAGGTGTTTGTCTCCACCATGAGGGGTTACTACT
TCCTGGGTCCCACACTGTGTGCACTGGAATCTGCCATGGGCTCGATAGCAGGTTTGG
TCACGGCGTGGTCTTTGGCTGTTCTCTCTTTTGAAAGATACCTGGTCATCTGTAAACC
ATTCGGAGCCTTCAAGTTTGGCAGGAATCAGGCCGCCGGTGCTGTGGCCTTCACCTG
GTTCATGGGGATCAGCTGTGCCATCCCACCTTTCTTTGGATGGAGCAGGTACATCCCT
GAAGGTCTGGGCTGCTCGTGTGGTCCTGATTGGTACACGCACAACGAGGAGTTTCAC
TGCAGCAGCTACACAAACTTCTTGATGGTGACGTGCTTCATCCTTCCGCTCAGCGTCA
TCATCTTCTCCTACTCTCAGCTGCTGAGCTCCCTGAGAGCTGTCGCAGCTCAGCAGAC
GGAGTCAGTCTCGACTCAGAAGGCAGAGAAGGAAGTGTCGAGGATGATTATCGTGA
TGGTCGGTTCCTTCCTCACCTGTTACGGTCCATATGCCCTCGCTGCTCTTTACTTCGCT
CACTCTTCAGACACAAACAAAGACTACCGACTCGTCACCATCCCGGCATTCTTCTCC
AAGAGCTCCTGCGTCTACAACCCGTTGATCTACGTCTTCATGAACAAACAGTTTCAA
GCCTGTATCATGGAAACTGTGTTTGGAAAGAAAATGGACGAATCATCTGAAGTTTCT
TCAAAAACTGAGGCATCTTCAGTTTCCACAGTTAATTAATGT

>*Platichthys stellatus* SWS2A1
ATGAAGCACGGTCGACCCATGGAGCTTCCAGAGGATTTCTGGATCCCCATCCCTTTG
GATACAAACAACATCACGACTCTCAGCCCCTTCCTCGTCCCCCAGGACCATCTAGCA
AGCTCATCCACCTTCTACGCCATGGCCATATTCATGTTTTTTGTTTTTGTTATGGGCAC
TAGCATCAATACACTCACCATCCTGTGCACGGTGAAATACAAGAAGCTCCGGTCCCA
CCTCAACTACATCCTGCTGAACTTGGCTCTGGGGAACCTTCTCGTGTCCTGTGTGGGC
TCCTTTGTTGGCTTCGGCGCATTTTCAGCCAGATACTTCATTTTTGGAGCGCTTGCAT
GCAAGATTGAAGGTTTCATGGTGACACTTGGTGGGATGGTCAGCTTGTGGTCTCTGG
CTGTGATAGCTTTTGAAAGATGGCTTGTCATCTGCAAGCCATTAGGTAACTTTATTTT
CAAGCCTGACCATGCTATAGCTTGCTGCGTATTCACCTGGGTGTTTGGACTTATTGCC
TCAACTCCACCTCTGTTCGGATGGAGCAGATACATCCCGGAGGGTCTGCAGTGCTCC
TGTGGACCAGACTGGTACACCACAAACAACAAATACAACAATGAATCCTACGTGAT
GTTCCTTTTCTGCTTCTGCTTTGCTGTTCCCCTCACCACCATCATCTTCTGCTACTCAC
AGCTGCTCATTACTATGAAAATGGCCGCAAAGGCTCAAGCGGAGTCTGCCTCCACCC
AGAAGGCAGAGAAGGAGGTGACCAGGATGGTGGTGGTCATGGTGATGGGCTTCTTG
GTGTGCTGGTTGCCCTACACCACCTTTGCTCTGTGGGTCGTGAACCATCGTGGGCAAA
CATTCGACCTGAGGTTTGCTACTATGCCAGCTGTCTTCTCCAAATCCTCTGCGGTCTA
CAACCCTATCATCTATGTTTTACTCAACAAACAGTTCCGTTCATGCATGATGAAGATG
GTGGGAATGGGTGGAGGTGATGATGACGAATCTTCAACATCATCAACCTCAGTCACC
GAAGTCTCCAAAGTTGGGCCTGCTTAA

>*Platichthys stellatus* SWS2A2
ATGAAGTCAAATCGTGGTGAGGAGCTGCCAGAGGACTTCTGGATACCCGTCCCTCTG
GACACCAACAACATCACAGCACTCAGCCCTTTCCTTGTTCCCCAGGATCACTTGGGG
AGCCCGGGCATCTTCTACGCAATGGCAGGATTTATGTTTTTCGTATTTGTGGTGGGCA
CCAGCATCAACACCCTGACCATTGCATGCACCGTCAAATACAAAAAGCTGCGGTCCC
ACCTTAACTACATCCTGGTGAATTTGGCTGTGGCGAACCTTCTTGTATCCTGTGTGGG
CTCCTTCACGGCCTGCTGCTCCTTTTCAACCAGATATTTCATTTTTGGAGCTCTAGCAT
GCAAGATTGAAGGTTTTATGGCAACACTCGGAGGTATGGTCAGCTTGTGGTCTCTGG
CTGTGATAGCTTTTGAAAGATGGCTGGTTATCTGCAAGCCACTTGGTAACTTTATTTT
CAAGCCTGACCATGCTATAGCTTGCTGCGTATTCACCTGGGTGTTTGCACTTATTGCC
TCACTCCCTCCTCTGTTTGGATGGAGCAGGTACATCCCAGAGGGTCTGCAGTGCTCCT
GTGGACCAGACTGGTACACCACAAACAACAAATACAACAATGAATCCTACGTGATG
TTCCTTTTCGGCTTCTGCTTTGCTGTTCCCTTTACCACCATCATCTTTTGCTACTCACA
GCTGCTCATCACACTGAAAATGGCAGCAAAGGCTCAAGCGGAGTCTGTCTCCACCCA
GAAGGCAGAGAGGGAGGTGACCAGGATGGTGGTTCTCATGGTGATGGGCTTCCTGG
TGTGCTGGTTGCCCTACACTAGCTTTGCCCTTTGGGTGGTGAACAACCGAGGGCAAT
CGTTCGACCTGAGACTGGCCACCATACCCTCCTGCTTCTCAAAGGCCTCTGCAGTCTA
TAACCCTGTCATCTACGTCCTGTTCAATAAACAGTTTCGTTCATGCATGATGACGATG
CTGGGGATGGGAGGAGATGAGGAGGAGTCATCAACAACACAGTCAGTTACTGAAGT
CTCCAAAGTTGGGCCTGCTTAA

>*Platichthys stellatus* SWS2B
ATGAGGGGAAATCGCGTTGTGGAGTTCCCAGATGACTTTTGGATCCCGGTCCCTCTG
GACACCGACAACATCACGTCCCTCAGCCCCTACCTGGTACCGCAGGATCACCTAGGA
AGCAAAGGACTCTTTTATTTCATGTCAGCTTTTATGTTTCTCCTGTTTGTGGCTGGCAC
AGCCATCAACACGCTGACCATTGCGTGCACCATCCAATACAAGAAGCTCCGGTCTCA
TCTGAACTACATCCTGGTGAACCTGTCGGTTGCAAACCTCCTCGTCTCATCCGTGGGC
TCTTTCACCTGCTTCTACTGCTTTGCCTTCAGATACATGATTCTTGGTCCACTTGGGTG
CAAGATTGAAGGATTTACAGCGACTGTTGGTGGAATGGTCAGCCTGTGGTCTCTGGC
TGTGATAGCCTTTGAAAGATGGATTGTTGTCTGCAAGCCAGTAGGAAACTTCTCCTTC
AAATCCAGCCATGCCATAGCTTGCTGTGCTCTAACGTGGGTCTTTGCTTTGATGGCTG
CGATTCCTCCTCTGGTTGGATGGAGTAGGTACATCCCTGAGGGTATGCAGTGCTCCTG
TGGACCAGACTGGTACACAACTGACAACAAGTTCAACAACGAGTCCTATGTGATGTT
CCTCTTCTGCTTCTGCTTCTCTGTCCCCTTCTTCACCATCGTTTTCTGCTACTCACAGCT
GCTCTTCACGCTGAAATCGGCAGCAAAGGCTCAAGCGGAGTCTTCCTCCACCCAAAA
GGCGGAGAGGGAGGTGACCAGGATGGTGGTTCTCATGGTGATTGGCTTCCTGGTGTG
CTGGATGCCCTACGCTTCCTTTGCTCTCTGGATTATAAACAACCGAGGGCAACCGTTC
GACCTGAGACTGGCCACCATACCCTCCTGTCTCTCTAAAGCCTCCACAGTCTACAACC
CTGTTATTTACATCTTCCTCAATAAACAGTTCCGCTCATGCATAAGGAAGATGTTGGG
GATGAGTGGAGGTGATGACGAGGAGTCATCGACAAGTCAATCGGTTACTGAAGTCTC
TAAAGTTGGACCTGCTTAG

>*Platichthys stellatus* LWS
ATGGCAGAAGAGTGGGGAAAACAGGCGTTTGCTGCCAGGCGGTACAATGAAGACAC
GACAAGGGGATCTGTTTTTGTATATACAAACAGCAATCATACCAGAGATCCCTTTGA
GGGGCCCAATTACCACATTGCTCCTCGATGGGTTTACAACTTGGCAACCCTCTGGAT
GTTTTTTGTGGTCGTTGCATCAGTTTTCACAAATGGTCTCGTCATTGTGGCCACAGCT
AAGTTCAAGAAACTCCGTCACCCACTGAACTGGATCTTGGTCAATCTTGCAGTCGCT
GATCTTGGAGAAACAGTTTTTGCCAGCACCATTAGTGTATGCAACCAGTTTTTTGGTT
ACTTCATTCTGGGACACCCGATGTGCATCTTTGAGGGCTATGTTGTCTCAGTGTGTGG
AATTGCTGGTCTCTGGTCCCTGTCCATCATCTCCTGGGAGAGATGGATAGTTGTGTGC
AAACCTTTTGGAAACGTCAAGTTTGATGCCAAATGGGCCACAGGTGGAATTCTGTTC
TCCTGGATCTGGCCAGCAGTGTGGTGTGCTCCCCCAATCTTTGGCTGGAGCAGGTACT
GGCCTCATGGACTGAAGACCTCCTGTGGACCTGACGTATTTAGTGGAAGTGAAGACC
CTGGAGTTCAGTCCTTCATGATTGTTCTTATGCTGACATGTTGCATACTTCCCCTGGG
TGTTATCATCTTGTGCTACCTGGCCGTCTGGTGGGCCATCCATTCTGTTGCGATGCAG
CAGAAGGAATCGGAGTCAACCCAGAAAGCTGAGAGAGAAGTGTCCAGAATGGTCGT
TGTCATGATCTTGGCATATTGTGTCTGCTGGGGACCTTATACAGGCTTTGCCTGCTTC
GCTGCGGCCAACCCTGGATATTCCTTCCACCCTCTGGCTGCTGCCATGCCTGCATACT
TTGCTAAGAGCGCCACCATTTACAACCCTATCATCTATGTATTCATGAACCGACAGTT
CCGCACATGCATCATGCAACTCTTTGGCAAAGAAGTGGAAGATGCTTCTGAAGTATC
CTCATCAAAGACAGAGGTCTCATCTGTGGCTCCTGCATAA

Appendix B – Starry flounder opsin amino acid sequences

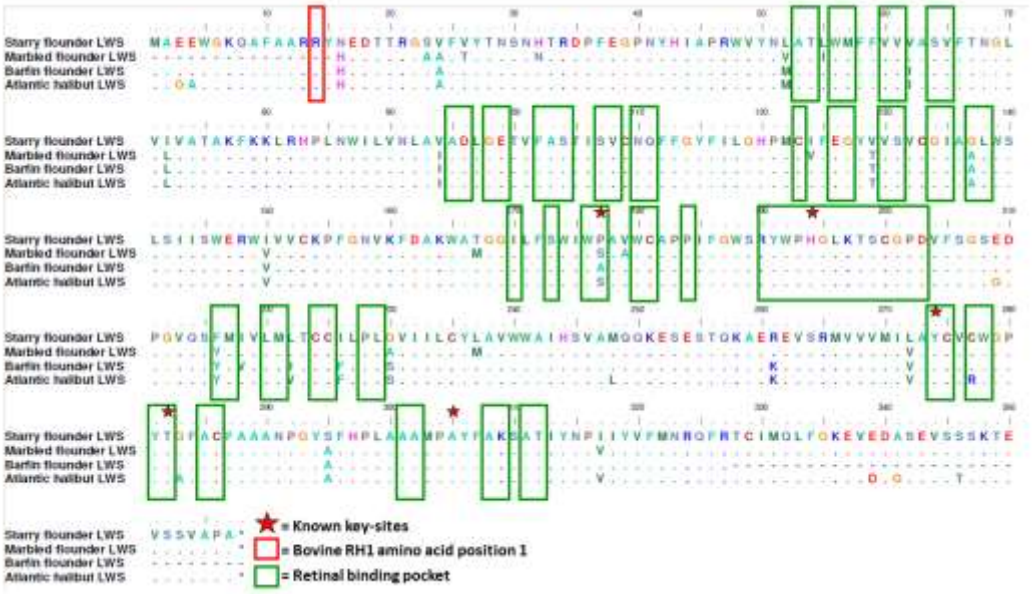

Figure 27: Starry flounder, marbled flounder, barfin flounder, and Atlantic halibut LWS amino acid sequences aligned to bovine rhodopsin (position 1 = red box) with the amino acid position pertaining to the retinal binding pocket highlighted (green box). Starry flounder differs from barfin flounder in the retinal binding pocket at several positions (136, 177, 216) and at known key-sites (red stars) (Chang et al., 1995; Yokohama, 2008; Phillips et al., 2015).

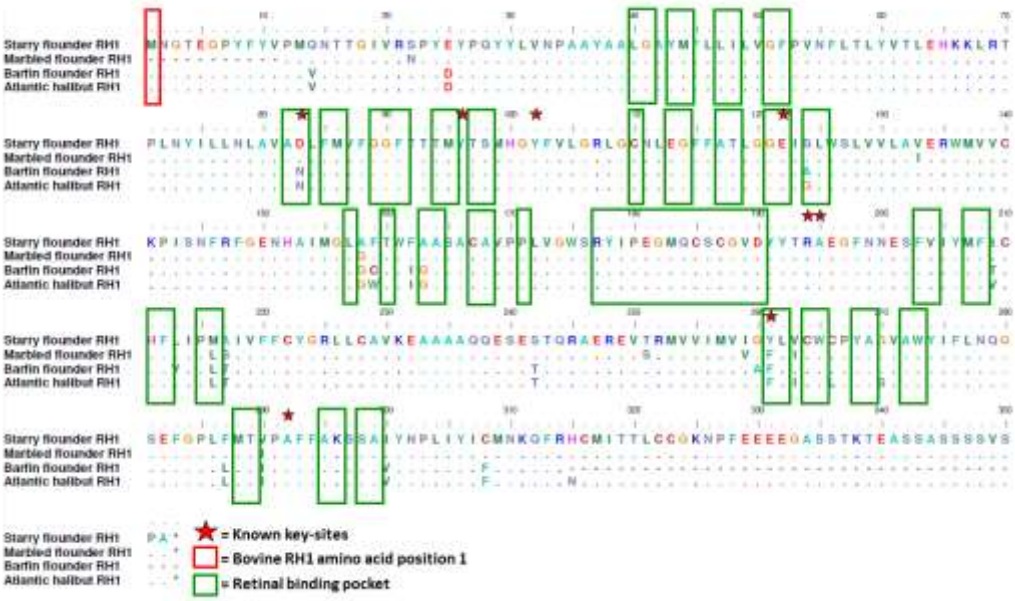

Figure 28: Starry flounder, marbled flounder, barfin flounder, and Atlantic halibut RH1 amino acid sequences aligned to bovine rhodopsin (position 1 = red box) with the amino acid position pertaining to the retinal binding pocket highlighted (green box). Starry flounder differs from barfin flounder in the retinal binding pocket at several positions (83, 124, 163, 216, 261) and at known key-sites (red stars) (Chang et al., 1995; Yokohama, 2008; Phillips et al., 2015).

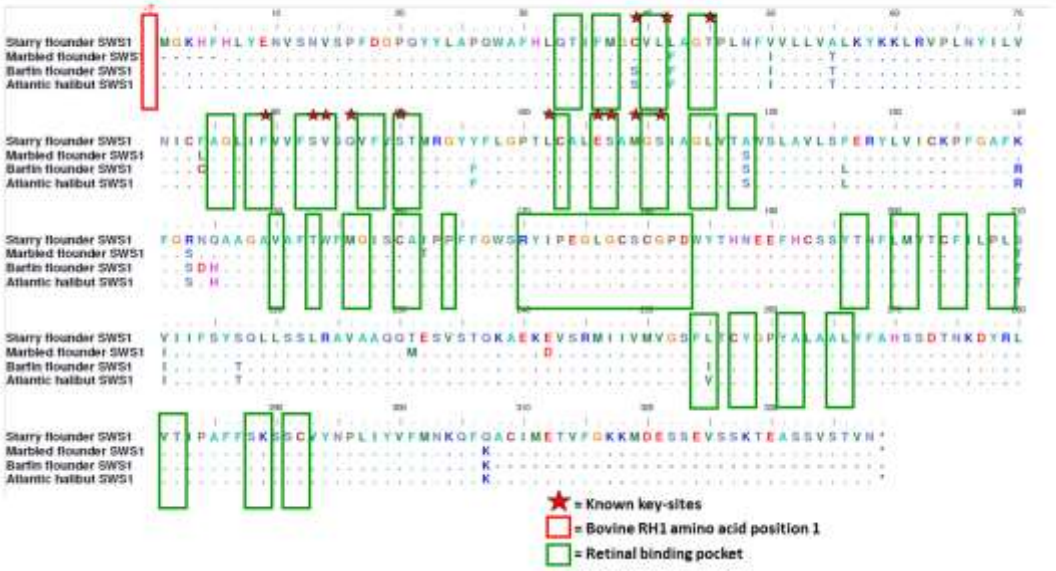

Figure 29: Starry flounder, marbled flounder, barfin flounder, and Atlantic halibut SWS1 amino acid sequences aligned to bovine rhodopsin (position 1 = red box) with the amino acid position pertaining to the retinal binding pocket highlighted (green box). Starry flounder differs from barfin flounder in the retinal binding pocket at several positions (118, 255) and at known key-sites (red stars) (Chang et al., 1995; Yokohama, 2008; Phillips et al., 2015).

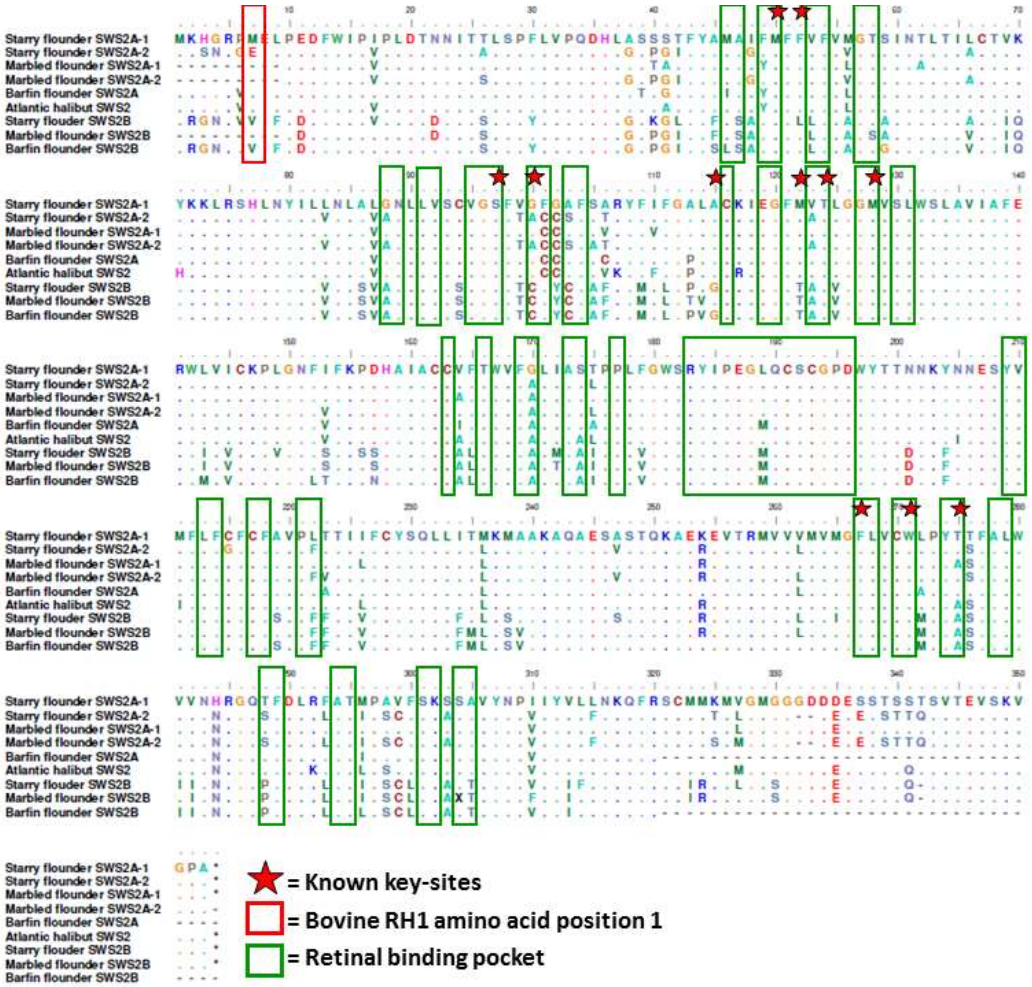

Figure 30: Starry flounder, marbled flounder, barfin flounder, and Atlantic halibut SWS2 amino acid sequences aligned to bovine rhodopsin (position 1 = red box) with the amino acid position pertaining to the retinal binding pocket highlighted (green box). Starry flounder SWS2 paralogs differ from barfin flounder in the retinal binding pocket at several positions (SWS2A*: 46, 170, 189; SWS2B: 46) and at known key-sites (red stars) (Chang et al., 1995; Yokohama, 2008; Phillips et al., 2015). *SWS2A in barfin flounder is orthologous to starry flounder SWS2A1.

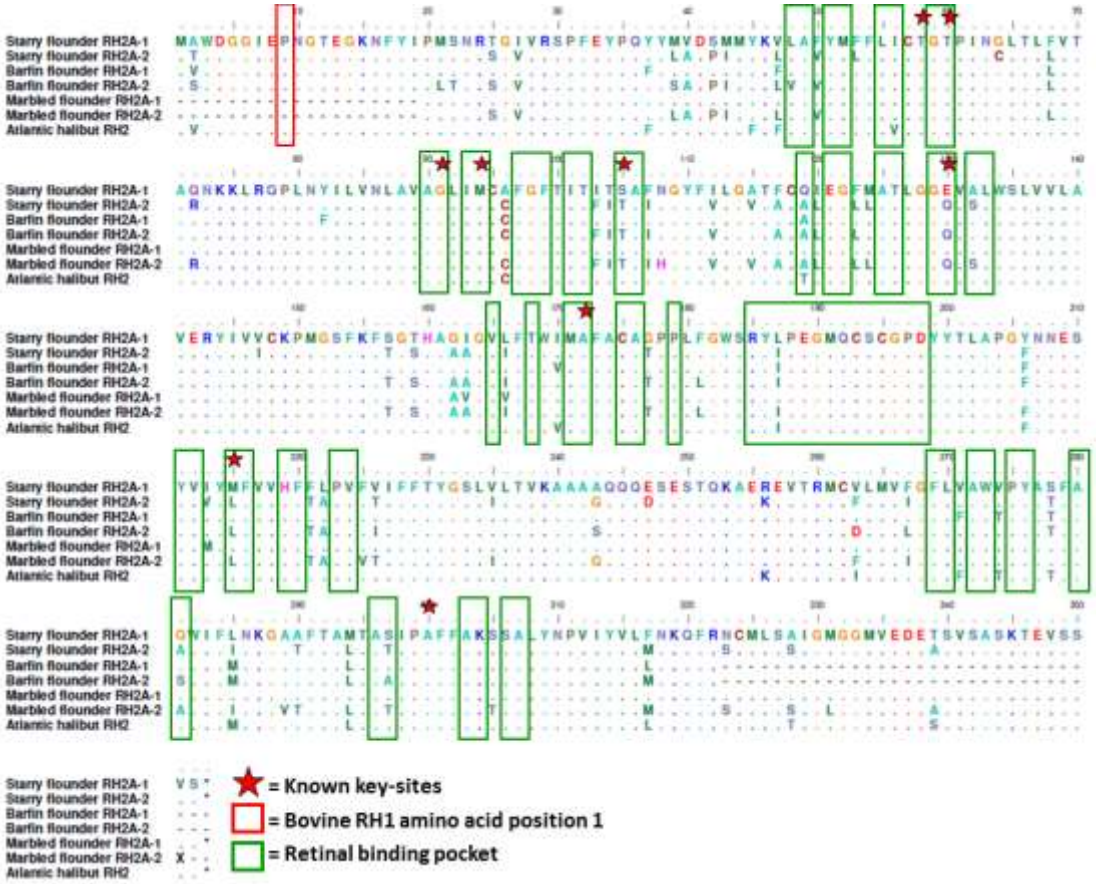

Figure 31: Starry flounder, marbled flounder, barfin flounder, and Atlantic halibut RH2 amino acid sequences aligned to bovine rhodopsin (position 1 = red box) with the amino acid position pertaining to the retinal binding pocket highlighted (green box). Starry flounder ortholog differs from barfin flounder in the retinal binding pocket at several positions (RH2A1: 119, 187; RH2A2: 48, 281, 297) and at known key-sites (red stars) (Chang et al., 1995; Yokohama, 2008; Phillips et al., 2015).

Appendix C – Specifications for camouflage experiment substrates

	Lab Colour Values	Hue, Saturation and Brightness values
blue L40:	L40 a13 b-43	H233 S52 B65
green L50:	L51 a-45 b23	H154 S100 B55
blue L40:	L40 a13 b-43	H233 S52 B65
red L40:	L41 a60 b49	H358 S83 B73
red L50:	L50 a65 b44	H0 S78 B86
green L65:	L65 a-52 b22	H159 S100 B71
black L12:	L12 a2 b0	H316 S11 B14

(These values send 100% Photo Black ink to the printer with no additional pigment)

Figure 32: Final colour combinations for the printed substrates used in the behavioural assay. Printed checkerboard size = 1 cm^2.

Appendix D – R code for plotting and analysing camouflage patterns

```
  camo5=read.csv("C:/Users/Tom Iwanicki/Dropbox/MSc Project/Fish Colour and
Vision/Experiments/Behaviour/Flatfish Behaviour/Data/Image Analysis Results
None.csv")
  head(camo5)
  str(camo5)
  library(nlme)    ## for lme()
  library(multcomp)          ## for multiple comparisons eg Tukey
  library(ggplot2)           ## for plotting

  #     REORDER THE CHECKER FACTOR LEVELS SO GREY IS THE
INTERCEPT
```

```
	print(levels(camo5$checker))
	camo5$checker=factor(camo5$checker,levels(camo5$checker)[c(4,1,2,5,3)])
	print(levels(camo5$checker))

camopowerSD<-aggregate(powerSD~sample+checker+treatment, data=camo5, mean)
head(camopowerSD)

ggplot(camopowerSD, aes(treatment, powerSD, fill=treatment)) +
	geom_boxplot() + facet_grid(.~checker) +
	scale_fill_manual(values = c("gold2","green4"),
		name="Light\nEnvironment",
			labels=c("Broad Spectrum","Green")) +
	ylab("Power Standard Deviation") +
	geom_jitter(aes(shape = sample), width=0.5, size = 2) +
	scale_shape_manual(values=c(1,2,3,4,5,6,7,8),
		guide=FALSE) +
	scale_x_discrete(breaks = 1,
		labels=c("")) +
	xlab(NULL)

	#
	# MIXED EFFECTS MODEL FOR POWER SD - RANDOM EFF = SAMPLE
	# TO CONTROL FOR WITHIN INDIVIDUAL VARIATION
	#

	powerSD.mod <- lme(powerSD ~ treatment*checker,
		 random = ~1 | sample, data = camopowerSD)

	anova(powerSD.mod)
	summary(powerSD.mod)

	#TUKEY MULTICOMPARISON

	camopowerSD$treatmentchecker <- interaction(camopowerSD$treatment,
		camopowerSD$checker)	## create an interaction term

	powerSD.multicomp <- lme(powerSD ~ treatmentchecker,
		 random = ~1 | sample, data = camopowerSD)
	summary(glht(powerSD.multicomp, linfct=mcp(treatmentchecker="Tukey")))

	######################

camomaxFreq<-aggregate(maxFreq~sample+checker+treatment, data=camo5, mean)
head(camomaxFreq)

ggplot(camomaxFreq, aes(treatment, log10(maxFreq), fill=treatment)) +
```

```
        geom_boxplot() + facet_grid(.~checker) +
        scale_fill_manual(values = c("gold2","green4"),
                name="Light\nEnvironment",
                        labels=c("Broad Spectrum","Green")) +
        ylab("log(Maximum Frequency)") +
        geom_jitter(aes(shape = sample), width=0.5, size = 2) +
        scale_shape_manual(values=c(1,2,3,4,5,6,7,8),
                guide=FALSE) +
        scale_x_discrete(breaks = 1,
                labels=c("")) +
        xlab(NULL)

        #IF ANYONE ON MY COMMITTEE NOTICES THIS DURING MY
        #DEFENSE, I WILL BUY THEM A BEER AT THE GRAD LOUNGE
        #AFTERWARD
        #
        # MIXED EFFECTS MODEL FOR MAXFREQ - RANDOM EFF = SAMPLE
        # TO CONTROL FOR WITHIN INDIVIDUAL VARIATION
        #

        maxFreq.mod <- lme(maxFreq~ treatment*checker,
                 random = ~1 | sample, data = camomaxFreq)

        anova(maxFreq.mod)

        summary(maxFreq.mod)

        #TUKEY MULTICOMPARISON

        camomaxFreq$treatmentchecker <- interaction(camomaxFreq$treatment,
                camomaxFreq$checker)         ## create an interaction term

        maxFreq.multicomp <- lme(maxFreq~ treatmentchecker,
                 random = ~1 | sample, data = camomaxFreq)
        summary(glht(maxFreq.multicomp, linfct=mcp(treatmentchecker="Tukey")))

        ######################

   camopropPower<-aggregate(propPower~sample+checker+treatment, data=camo5,
mean)
   head(camopropPower)

   ggplot(camopropPower, aes(treatment, propPower, fill=treatment)) +
        geom_boxplot() + facet_grid(.~checker) +
        scale_fill_manual(values = c("gold2","green4"),
                name="Light\nEnvironment",
```

```
                labels=c("Broad Spectrum","Green")) +
    ylab("Proportion Power") +
    geom_jitter(aes(shape = sample), width=0.5, size = 2) +
    scale_shape_manual(values=c(1,2,3,4,5,6,7,8),
            guide=FALSE) +
    scale_x_discrete(breaks = 1,
            labels=c("")) +
    xlab(NULL)


    #
    # MIXED EFFECTS MODEL FOR MAXFREQ - RANDOM EFF = SAMPLE
    # TO CONTROL FOR WITHIN INDIVIDUAL VARIATION
    #

    propPower.mod <- lme(propPower~ treatment*checker,
             random = ~1 | sample, data = camopropPower)

    anova(propPower.mod)

    summary(propPower.mod)

    #TUKEY MULTICOMPARISON

    camopropPower$treatmentchecker <- interaction(camopropPower$treatment,
            camopropPower$checker)      ## create an interaction term

    propPower.multicomp <- lme(propPower ~ treatmentchecker,
             random = ~1 | sample, data = camopropPower)
    summary(glht(propPower.multicomp, linfct=mcp(treatmentchecker="Tukey")))

    ######################


camolumSD<-aggregate(lumSD~sample+checker+treatment, data=camo5, mean)
head(camolumSD)

ggplot(camolumSD, aes(treatment, lumSD, fill=treatment)) +
    geom_boxplot() + facet_grid(.~checker) +
    scale_fill_manual(values = c("gold2","green4"),
            name="Light\nEnvironment",
                labels=c("Broad Spectrum","Green")) +
    ylab("Luminance Standard Deviation") +
    geom_jitter(aes(shape = sample), width=0.5, size = 2) +
    scale_shape_manual(values=c(1,2,3,4,5,6,7,8),
            guide=FALSE) +
```

```
scale_x_discrete(breaks = 1,
          labels=c("")) +
xlab(NULL)


#
# MIXED EFFECTS MODEL FOR MAXFREQ - RANDOM EFF = SAMPLE
# TO CONTROL FOR WITHIN INDIVIDUAL VARIATION
#

lumSD.mod <- lme(lumSD~ treatment*checker,
           random = ~1 | sample, data = camolumSD)

anova(lumSD.mod)

summary(lumSD.mod)

#TUKEY MULTICOMPARISON

camolumSD$treatmentchecker <- interaction(camolumSD$treatment,
          camolumSD$checker)## create an interaction term

lumSD.multicomp <- lme(lumSD~ treatmentchecker,
           random = ~1 | sample, data = camolumSD)
summary(glht(lumSD.multicomp, linfct=mcp(treatmentchecker="Tukey")))

######################
```